ABSTRACT

Title of Document: CHARACTERIZATON OF HUMAN HOLOCARBOXYLASE SYNTHETASE ACTIVITY AND SPECIFICITY

Maria del Mar Ingaramo, Doctor of Philosophy, 2011

Directed By: Dr. Dorothy Beckett, Department of Chemistry and Biochemistry

Human Holocarboxylase Synthetase (HCS) transfers the vitamin biotin to the biotin carboxyl carrier protein (BCCP) domains of five biotin-dependent carboxylases. There are two major forms of HCS present in mammalian cells, which differ by 57 amino acids at their N-terminus. Both variants catalyze biotinylation through a two step reaction in which an activated intermediate, bio-5'-AMP, is first synthesized from biotin and ATP. In the second step, the biotin moiety is covalently attached to a specific lysine residue on the carboxylase. The mammalian carboxylases comprise the cytosolic acetyl-CoA carboxylase 1 (ACC1), the outer mitochondrial membrane bound acetyl-CoA carboxylase 2 (ACC2), and the three mitochondrial carboxylases pyruvate carboxylase (PC), 3-methylcrotonyl-CoA carboxylase (MCC) and propionyl-CoA carboxylase (PCC).

In order to investigate the HCS reaction mechanism and specificity, both isoforms were recombinantly expressed, purified, and biochemically characterized. The basic mechanistic features of the two HCS variants were investigated using steady state and pre-steady state kinetic methods. The latter methods allow the determination of the rates of bio-5'-AMP synthesis and biotin transfer independent of each other. Both isoforms catalyze the overall reaction similarly and synthesize bio-5'-AMP with a rate of $0.1s^{-1}$. Biotin transfer to the BCCP domain fragments of ACC1 and ACC2 carboxylases, to which HCS has continuous access from the cytosol, is slow and saturable. In contrast, biotin transfer to the BCCP domain fragments from the mitochondrial carboxylases PC, PCC and MCC is characterized by rates that are significantly faster and limited by the collision of enzyme and acceptor substrate. The same pre-steady state methods were applied to two biotin ligases from archaea and prokarya, and showed that this collision limited biotin transfer mechanism is widespread among evolutionary domains.

The observation of a collision limited reaction emphasizes the role of protein substrate recognition in the biotinylation reaction, and provides a mechanism for establishing a hierarchy among carboxylases that favors mitochondrial substrates. This default hierarchy can be overridden according to cellular demands by modifying the carboxylases' expression. The results support the idea that in the cell one of the mechanisms of biotin-related metabolism regulation relies on HCS specificity to control biotin distribution among carboxylases.

CHARACTERIZATON OF HUMAN HOLOCARBOXYLASE SYNTHETASE ACTIVITY AND SPECIFICITY.

By

Maria del Mar Ingaramo

Dissertation submitted to the Faculty of the Graduate School of the
University of Maryland, College Park, in partial fulfillment
of the requirements for the degree of
Doctor of Philosophy
2011

Advisory Committee:
Professor Dorothy Beckett, Chair
Professor Iqbal Hamza
Professor George Lorimer
Associate Professor Richard Stewart
Professor Sergei Sukharev

Acknowledgements

I would like thank my advisor, committee members, professors and co-workers for their support, guidance and help. I thank Dr. Roy Gravel for providing the plasmid containing the 58-HCS coding sequence and the overexpression plasmid for p67, the RIKEN group for supplying the expression plasmids for *Ph*BPL and *Ph*BCCP, Dr. Chrisopher Lima for the plasmid used for purification of SUMO protease, Yishan Zhou and Joy Zhao for the purification of PhBCCP, Kyle Daniels for the purification of *Ph*BPL, and Emily Streaker for the purification of *Ec*BPL.

This work was supported, in whole or in part, by National Institutes of Health Grants R01-GM46511 and S10-RR15899 to Dr. Beckett. In addition, I am thankful for support from the University of Maryland summer research fellowships and the Bailey graduate student fellowship.

Table of Contents

List of Tables

List of Figures

List of Abbreviations

58-HCS	protein product of translation initiation at methionine 58 of the full-length protein
ACC	acetyl-CoA carboxylase
BC	biotin carboxylase domain
BCCP	biotin carboxyl carrier protein
bio-5'-AMP	biotinyl 5'-adenylate
BPL	biotin protein ligase
BSA	bovine serum albumin
CT	carboxyl transferase domain
Ec	*Escherichia coli*
HCS	holocarboxylase synthetase
Hs	*Homo sapiens*
IPTG	isopropyl β-D-thiogalactoside
FL-HCS	full-length holocarboxylase synthetase
MALDI-TOF	matrix-assisted laser desorption ionization time-of-flight
MCC	methylcrotonyl-CoA carboxylase
MCD	multiple carboxylase deficiency
p67	carboxyl-terminal fragment of the propionyl-CoA-carboxylase α subunit containing a his_6 tag
PC	pyruvate carboxylase
PCC	propionyl-CoA carboxylase
Ph	*Pyrococcus horikoshii*
PKG	protein kinase G
PPi	pyrophosphate
SUMO protein	small ubiquitin-like modifier protein
TC	transcarboxylase domain
TCA	tricarboxylic acid cycle
Tricine	N-[2-hydroxy-1,1-bis(hydroxymethyl)ethyl]glycine
Tris	2-amino-2-hydroxymethyl-propane-1,3-diol
SUMO protein	small ubiquitin-like modifier protein

Chapter 1: Background and introduction

1.1 Introduction

Cells adjust the flux of their metabolic processes in a constant effort to maintain homeostasis. This is a natural response to stress that aids in cell survival and adaptability. Central to this response is the ability to control and regulate processes such as enzymatic activity, transcription and translation as a function of nutritional needs. This work lays the foundation to understand the biochemical basis of those processes that determine the metabolic fate of the nutrient biotin in mammalian cells. In particular, it focuses on expanding our understanding of human holocarboxylase synthetase (HCS), a key enzyme in biotin related metabolism and regulation.

1.1.1 Biotin

Biotin, also known as vitamin B7 or vitamin H, is an essential nutrient required by most organisms for viability. The only organisms that do not require biotin are the Lyme disease causing agent *Borrelia burgdorferi*, the endocellular symbiont *Buchnera sp*., mycoplasmas and thermoplasmas (1). Most prokaryotes, plants and some fungi can synthesize biotin (2). In contrast, most higher eukaryotes, including all animals, depend on their diet as a source of the vitamin. Alternatively, it is been suggested that the bacterial community of the intestinal flora may also function as a biotin source for higher organisms (3).

Biotin was originally discovered by Margaret Boas in 1927 when she recognized that there was a component in certain foods that protected mice against ‘egg white injury’ (4). She named this component ‘protective factor X’. Today, the

'egg white injury', a condition characterized by severe dermatitis, loss of hair, and lack of muscular coordination, is known to arise from the presence of the protein avidin in the egg white (Fig. 1A). Avidin, which binds biotin with one of the tightest binding affinities known to date, prevents biotin absorption by the mice. In 1940, Paul Gyorgy realized that the vitamin H that he had extracted from liver in 1931, as well as the coenzyme R from Rhizobium discovered by Allison in 1933, and the biotin isolated from egg yolk by Kogl and Tonnis in 1935, were all one and the same (5). Subsequently, the structure of biotin was solved by DU Vigneaud in 1942 (6), after recognition that biotin is composed of a ureido ring fused with a tetrahydrothiophene ring and a carboxyl group on an n-valeric acid side chain (Fig. 1B). Only one of the eight possible stereoisomers, d-(+)-biotin, is biologically active (7).

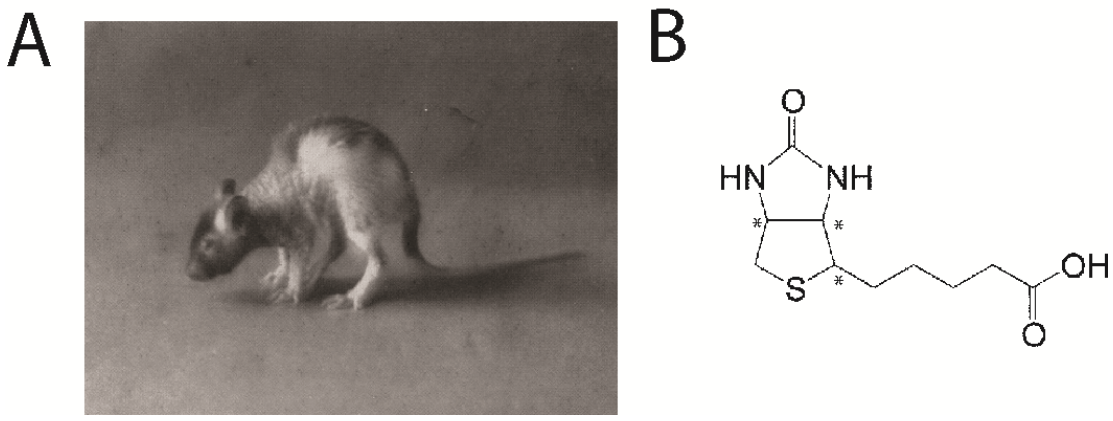

Figure 1. Biotin and the egg white injury. A. Picture of a mouse displaying egg white injury. The symptoms are observed after depriving mice from biotin by feeding them egg white (reprinted from (4)) B. Structure of biotin.

1.1.2 Biotin as a cofactor

The importance of biotin derives from its function as a cofactor for biotin-dependent carboxylases. In the carboxylation reaction, a carboxyl group is added to one molecule, for example, acetyl-CoA, to produce another metabolite that has been extended by one carboxyl group, like malonyl-CoA. Biotin acts as an intermediate carrier of the carboxyl group, which is originally taken up from a bicarbonate donor and eventually handed to the metabolic acceptor molecule (Fig. 2A). The reaction is complex, and is catalyzed in distinct spacio-temporal steps that occur in different carboxylase domains ((8), Fig. 2B). Biotin performs its carrier function while covalently attached to a specific lysine of the BCCP (biotin carboxyl carrier protein) domain. This domain works as a swinging arm, able to reach TC and BC domains more than 60Å away (9). The BCCP domain interacts first with the BC domain (biotin carboxylase), where ATP is used to activate bicarbonate by producing a carboxyphosphate intermediate. This reaction also requires divalent ions. After the N-1 position of biotin is carboxylated, the BCCP domain brings the biotin to the TC (transcarboxylase) domain, where the carboxyl group is indirectly transferred to the acceptor metabolite through intermediate CO_2 formation(10).

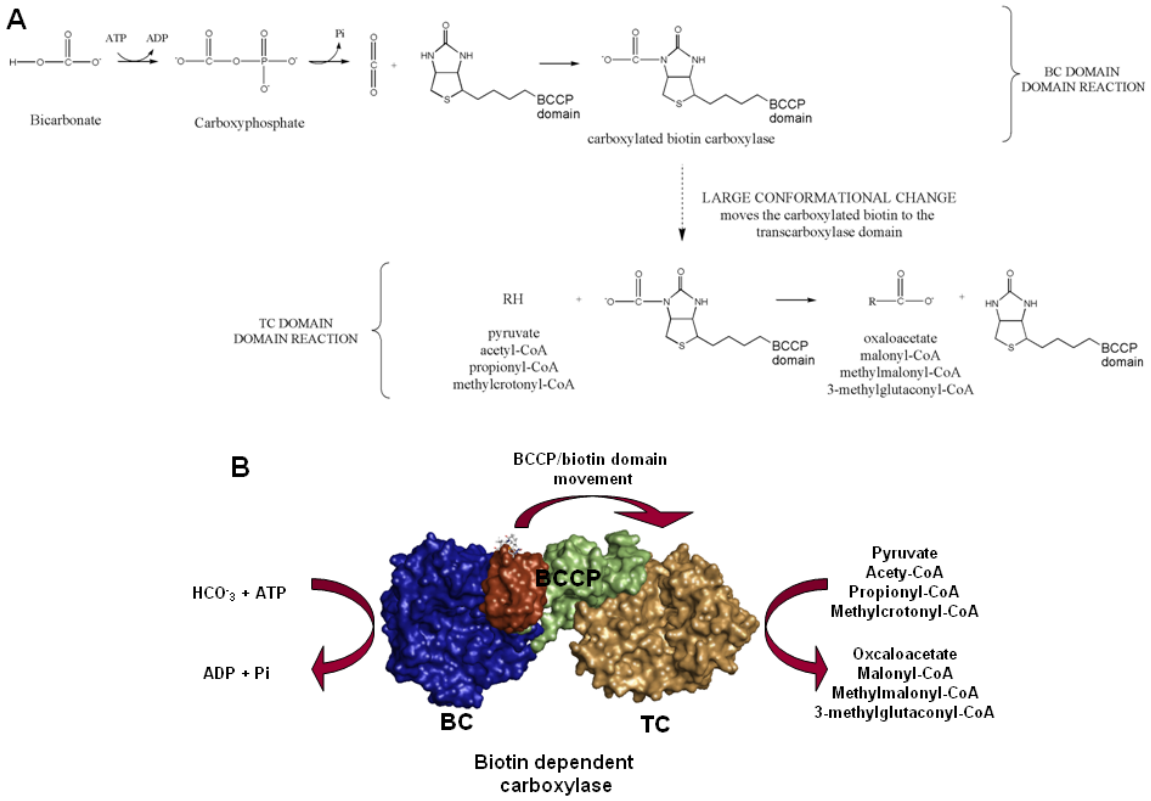

Figure 2. Biotin dependent carboxylases reaction and domain structure. A. The carboxylase reaction involves taking bicarbonate and ATP to transiently transfer a carboxyl group to biotin. The carboxyl group is subsequently added to either pyruvate, acetyl-CoA, propionyl-CoA or methycrotonyl-CoA, depending on the identity of the carboxylase(8,11). B. Carboxylases are composed of repeating units of the BC, BCCP and CT domain. The flexible linker (green) of the BCCP domain (red) moves the biotin moiety between the BC (blue) and TC domain (gold), where the two parts of the carboxylation reaction occur.

1.1.3 Biotin dependent carboxylases

Biotin dependent carboxylases are involved in a variety of metabolic processes, some of which are essential for cell viability. Most organisms, as is the case in the widely studied *E. coli*, possess at least one such carboxylase, namely acetyl-CoA carboxylase (ACC). This carboxylase catalyzes the conversion of acetyl-CoA to malonyl-CoA, and as a result, is of fundamental importance for fatty acid anabolism. Indeed, this chemical step is the first committed step of fatty acid synthesis. In *E. coli*, the enzyme consists of four polypeptides, BC, BCCP, TC-α and TC-β (12). However, the overall stoichiometry of subunits is still a matter of debate.

Mammalian cells have five biotin dependent carboxylases involved in various metabolic processes (Fig. 3A,B). Like the bacterial ACC, cytosolic acetyl-CoA carboxylase 1 (ACC1) is involved in fatty acid synthesis by catalyzing the conversion of acetyl-CoA to malonyl-CoA. Because this carboxylase has been linked to obesity and diabetes, it has been the topic of much research. The BC, BCCP and TC domains of the mammalian enzyme lie on a single polypeptide whose regulation has been found to be multi-level and complex. The expression pattern varies depending on the tissue, with the highest levels occurring in adipose tissue (13). In addition, the mRNA can be alternatively spliced to produce different variants. The expression levels are responsive to glucose, insulin, thyroid hormone and leptin (14). Citrate and glutamate are among the currently identified allosteric regulators of ACC1, and citrate is known to activate ACC1 by inducing homopolymerization of the enzyme (15). ACC1 activity can be inhibited by hormone responsive phosphorylation of several residues. This extensive regulation at multiple levels and the fact that an ACC1 knock-out

mutation in mice is embryonic lethal (16) are in accord with a central role of ACC1 in metabolism.

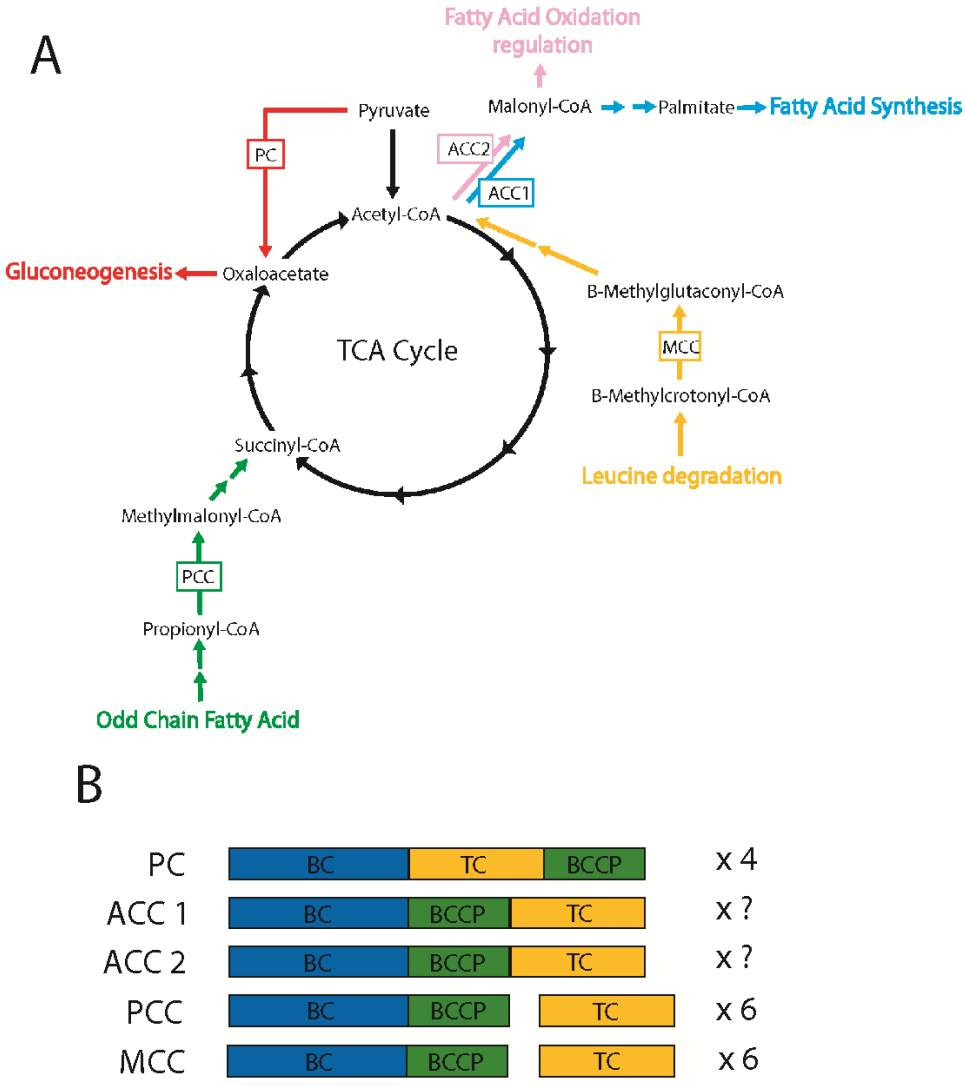

Figure 3. Mammalian biotin dependent carboxylases associated metabolic pathways and assembly states. A. Mammalian cells have five different biotin dependent carboxylases that are involved in a variety of metabolic pathways. B. Mammalian biotin dependent carboxylases are large multimeric complexes. The domain architecture is highlighted by the different colors. The number of times that the domains are repeated in an active complex is shown on the right. Biotin is attached to the BCCP subunit (adapted from (11)).

Acetyl-CoA carboxylase 2 (ACC2) is the product of a different gene than that coding for ACC1, although the two enzymes maintain 70% similarity (11). It catalyzes the same reaction as ACC1, but is involved in regulation of fatty acid oxidation. Even though the two ACCs catalyze the same reaction the two are not interchangeable and have different functions. This is evidenced by the very different results obtained with ACC2 mice knockouts, which aside from a few phenotypic traits, mature normally (17). A publication by Soo Choi *et al.* indicating that the ACC2 knockout mice displayed increased insulin sensitivity and continuous fat oxidation led to much interest to use this enzyme as a target to treat diabetes and obesity (18). However, a more recent paper suggests that the phenotypes are not as pronounced as originally thought (17). An N-terminal leader sequence is responsible for its localization and anchoring to the cytoplasmic side of the outer mitochondrial membrane (19). ACC2 displays differential tissue expression, with increased expression in muscle, and there are also different splice variants (14). It also contains several phosphorylation sites that may be involved in its regulation (14). Therefore, ACC2 is also subject to extensive regulation.

Propionyl-CoA carboxylase (PCC) catalyzes the conversion of propionyl-CoA to S-methylmalonyl-CoA. It is part of the odd-chain fatty acid synthesis pathway and is also involved in isoleucine, threonine, methionine and valine catabolism. The enzyme localizes to the mitochondrial matrix. It is a $\alpha_6\beta_6$ heterododecamer, with the alpha subunit carrying the biotin moiety (11). PCC has also been established as an essential gene product, since knock-out mice die hours after birth (20).

Pyruvate carboxylase (PC) carboxylates pyruvate to produce oxaloacetate. The enzyme is a mitochondrial homotetramer involved in gluconeogenesis and fatty acid synthesis. There are at least two mRNAs that arise from differential splicing of the 5'UTR. These variants have different tissue-dependent expression resulting from the control of two different promoters (21). In rats, the expression from these promoters display different transcriptional response to hormones and metabolites induced upon fasting or by diabetes. PC is allosterically activated by acetyl-CoA, but no phosphorylation-dependent regulation has been identified.

Methycrotonoyl-CoA carboxylase (MCC) converts 3-methylcrotonoyl-CoA to 3-methylglutaconyl-CoA. It is a heterododecameric mitochondrial enzyme involved in the degradation of the amino acid leucine. Its oligomeric structure is of the $(\alpha\beta)_6$ form, and the biotin is attached to the alpha subunit. The enzyme is mainly expressed in kidney and liver tissue. It has been reported that, in plants, a mechanism for regulating its activity among different plant organs is based on the extent of biotinylation (22).

1.1.4 Biotin protein ligases

Biotin protein ligases (BPLs) catalyze attachment of biotin to the specific lysine on the carboxylases BCCP domain, and understanding this class of enzymes has been the main focus of our efforts. The biotin transfer reaction occurs in two steps. In the first step an activated intermediate, bio-5'-AMP, is synthesized from biotin and ATP, with the release of pyrophosphate. This occurs through the formation of an anhydride bond between the biotin carboxyl group and the ATP alpha phosphate (23). The second step involves covalent attachment of the biotin moiety to

a carboxylase acceptor lysine residue. The products of this second half reaction are the biotinylated carboxylase and AMP (Fig. 4).

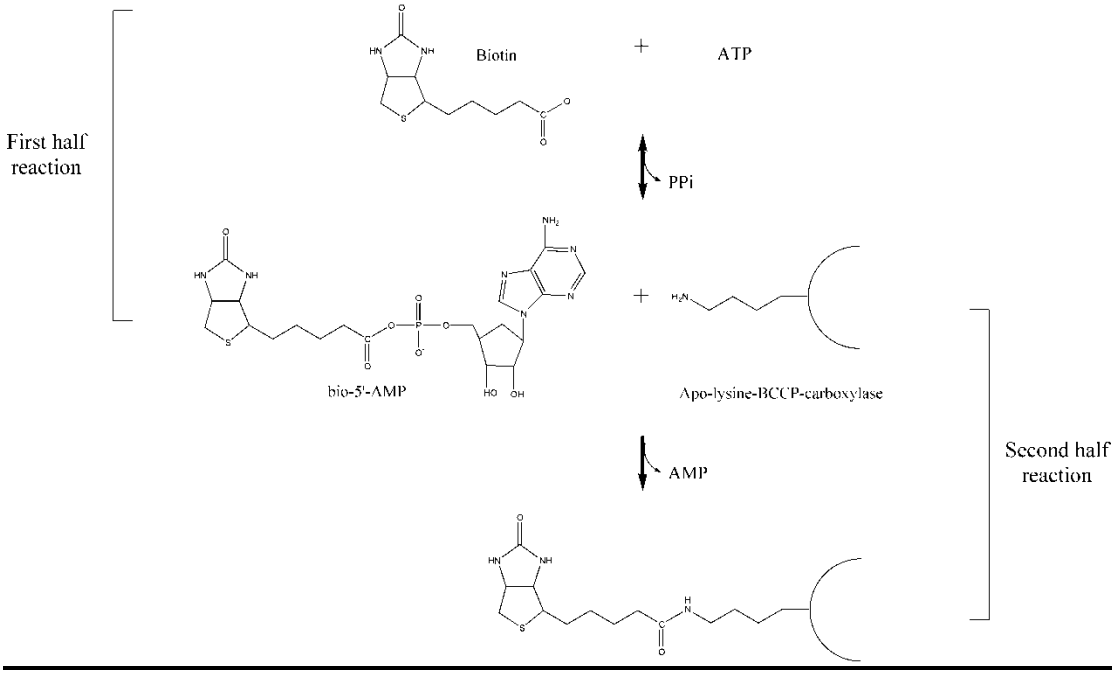

Figure 4. Biotin protein ligase reaction. The reaction occurs in two steps. First, an activated bio-5'-AMP intermediate is formed from biotin and ATP. Then, the biotin moiety is transferred to a specific lysine on the BCCP domain of carboxylases, with the release of AMP as a product.

1.1.5 BirA and other ligases

The majority of the knowledge on ligases originates from studies performed with the *E. coli* enzyme, which is also known as BirA. This protein is a 35kDa metabolic enzyme and transcriptional repressor. Its N-terminal domain contains a DNA binding motif, while the C-teminus contains the catalytic residues involved in

bio-5'-AMP synthesis and biotin transfer (24). BirA is central to the sensing and maintenance of biotin homeostasis in *E. coli,* by virtue of its ability to function as a repressor and a biotin ligase (25). After bio-5'-AMP synthesis, BirA can either transfer biotin to the BCCP domain of ACC, or it can homodimerize (Fig. 5). BirA dimers can act as transcriptional repressors by directly binding to a DNA regulatory sequence and inhibiting the expression of the biotin biosynthetic operon (26). As a result, BirA function will depend on biotin concentration and levels of unbiotinylated BCCP (27). When the concentration of biotinylated carboxylase is high, BirA will homodimerize and bind to the operator. On the other hand, when most of the carboxylases are unbiotinylated, BirA will heterodimerize with the carboxylase and biotinylate the BCCP subunits. Because the dimerization reactions utilize the same surface on BirA, they are mutually exclusive, and their dominance will determine if biotin is channeled towards metabolism or transcriptional repression. Mechanistically, hetero- and homo- dimerization events are isoenergetic, and this switch is kinetically controlled. Since heterodimerization is much faster than homodimerization, transcriptional repression will occur only after the pool of unbiotinylated BCCPs has been exhausted (28-29). BirA is, therefore, the key species through which biotin is partitioned between transcriptional repression and metabolism(30).

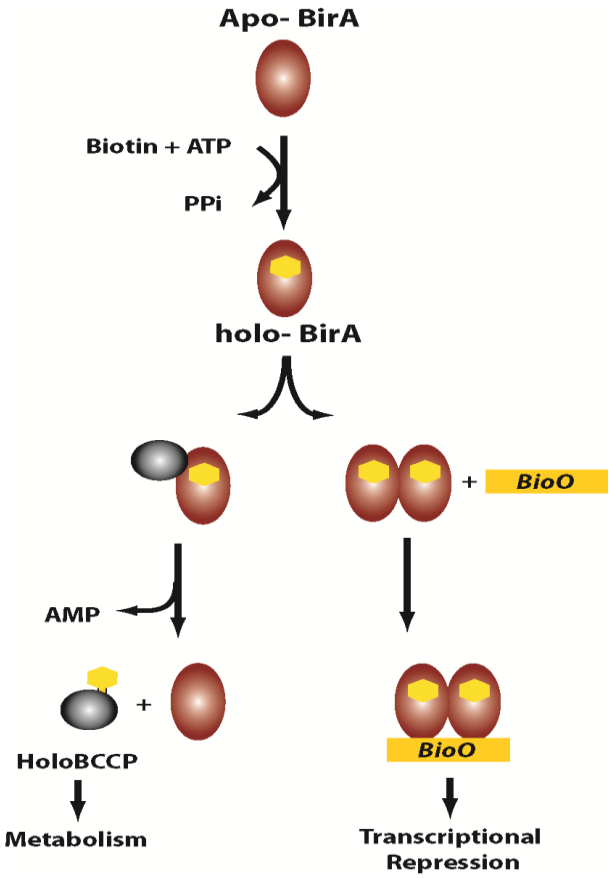

Figure 5. The biotin regulatory switch of *E. coli (30)*. Apo-BirA binds ATP and biotin to produce bio-5'AMP and form holo-BirA. Partitioning of holo-BirA function between metabolic activator and transcriptional repressor occurs through competition of hetero- and homo-dimerization. If BirA transiently heterodimerizes with a carboxylase, it will transfer the biotin moiety to the carboxylase BCCP domain, and activate metabolism. However, if holo-BirA homodimerizes it is now able to bind a specific sequence upstream of the biotin biosynthetic operon and repress expression.

Not all lower organism ligases are bi-functional (1). Monofunctional ligases catalyze biotin transfer to carboxylases, but do not regulate transcription in response to the vitamin. The monofunctional ligases characterized to date can be monomeric or constitutive dimers (31-33). Of particular interest has been the ligase from the

Pyrococcus horikoshii archeon due to the availability of crystal structures of a mutant enzyme bound to the BCCP fragment (34). It is noteworthy that this ligase does not homodimerize with the same surface that BirA uses, but both ligases use the same area to interact with BCCP. Several key residues were identified in the structure, many of which had been previously probed in BirA by alanine replacement. In addition, a large number of backbone contacts were identified. These backbone interactions are thought to be responsible for the ability of ligases to biotinylate BCCP from other species.

1.1.6 The mammalian biotin protein ligase, or human holocarboxylase synthetase

In contrast to the *E. coli* system, the mammalian biotin regulatory network is not as well understood. A link between biotin and transcriptional status of several genes has been known since the 1960s. However, the mechanism by which biotin affects transcription remains elusive. Studies in mammalian fibroblasts with mutant biotin ligase indicate that these cells are defective in biotin-responsive transcriptional response and suggest that the human ligase, like its *E. coli* counterpart, plays a role in biotin regulation (35). It has been proposed that the mechanism might involve direct biotinylation of nucleosomes (36), but the inability to detect endogenous biotinylated histones with methods other than antibodies has raised doubts about this hypothesis (37). Alternatively, a lack of biotin-transcriptional response in normal HepG2 upon inhibition of soluble guanylate cyclase suggested that regulation might occur through a signaling cascade involving the biotin ligase and PKG.

The human biotin ligase or human holocarboxylase synthetase (HCS or *Hs*BPL), is a 726 amino acid protein with a molecular weight of 81 kDa. The C-terminal domain encompasses the catalytic region and is 36% identical to BirA across a 126 amino acid region, while its N-terminal sequence bears no homology to any known protein except to the N-terminus of other higher organism ligases (38). Characterization of HCS mRNA indicated that of the many different spliced mRNAs, two code for proteins differing on the N-terminus (39). One variant is the full-length protein and the other is a 74 kDa form, 58-HCS, which lacks the first 57 amino acids at the N-terminus. An additional intermediate, 7-HCS, which lacks the first 6 amino acids, has been proposed to arise from skipping of the first initiation codon in the full length transcript (39-40).

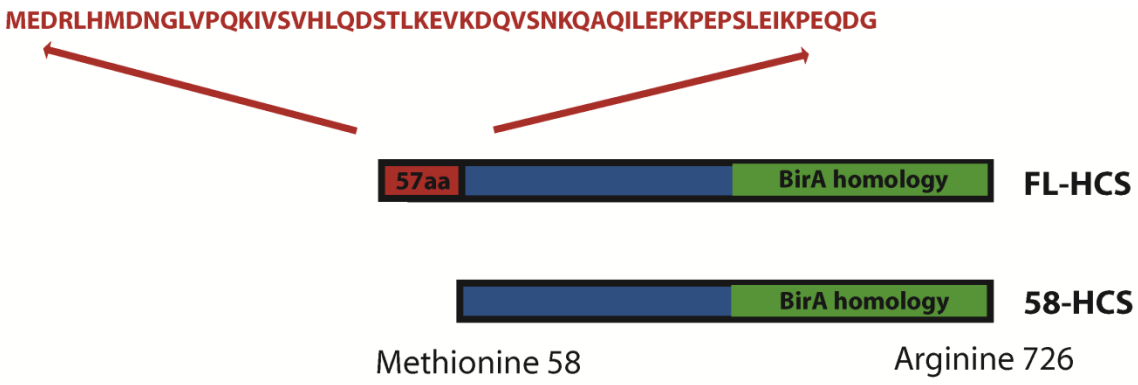

Figure 6. HCS isoforms. There are two main isoforms of HCS in human cells, FL-HCS and 58-HCS. The sequence of the additional 57 N-terminal residues that distinguishes between full length HCS and 58-HCS, the two isoforms found in mammalian cells is displayed in red. The BirA homologous region is highlighted in green

The HCS N-terminus appears to be involved in biotin acceptor substrate recognition. Studies that examined biotinylation of a truncated form of the BCCP domain of the mammalian PCC and of the bacterial BCCP substrate by different truncations of HCS in *E. coli* cell extracts determined that enzymes containing intermediate length N-terminal deletions interfered with biotin acceptor substrate recognition(41). In NMR studies performed with the BCCP domain of ACC2 and an N-terminal fragment of HCS consisting of residues 1-160, Lee *et al.* showed that the N-terminal domain affects the chemical shift of several residues of ACC2 BCCP (42). In addition, biotinylating activity was observed when adding the N-terminal HCS fragment and 160-HCS in trans, but it was compromised when catalyzed by the 160-HCS fragment alone.

Localization of HCS has been a matter of some debate. HCS displays no viable mitochondrial or nuclear localization signal (38). Narang et al found that HCS localized primarily to the nucleus (43). However, subsequent experiments with GFP-tagged HCS, as well as western blots, determined that FL-HCS localizes primarily to the cytoplasm (44). The same study determined that the majority of 58-HCS is also found in the cytoplasm, while a small fraction is present in the nucleus. Western blot analysis of isolated mitochondria was inconclusive regarding the presence or absence of HCS in this organelle. A different study of fresh placenta tissue by western blot showed that HCS was mainly in the cytoplasm. The mitochondrial fraction showed a band at 62 kDA that was proposed to be an isoform specific to the mitochondria (40).

A few studies have addressed the regulation of HCS. It was proposed that HCS was transcriptionally regulated as a function of biotin (35,45), but mRNA levels

of HCS do not always change with biotin concentration (46). Differential localization of the various isoforms in response to biotin is a plausible regulatory mechanism of carboxylase biotinylation. However, studies to determine the identity of the 62 kDa band observed in the mitochondria, and to assess distribution of HCS as a function of biotin have not been performed. In addition, a possible mechanism for regulation at the protein level emerged when a proteomic study identified threonine 146 and serine 147 as two likely phosphorylation sites on HCS (47). This finding, taken together with the activation of guanylate cyclase by biotin (48), raises the possibility that protein kinase G (PKG) is activated to phosphorylate transcription factors and, perhaps, HCS. The relevance of phosphorylation for HCS activity is also unknown, as are the kinases involved, but they suggest an additional level of regulation of biotin metabolism.

1.1.7 Biotin protein ligase-BCCP interaction

Although there are studies that provide information on structural and sequence elements important for BCCP recognition, a thorough understanding is still lacking. The crystal structure of the thermophillic *Pyrococcus horikoshii* ligase bound to the BCCP fragment is available(34). The ligase-BCCP interface is characterized by hydrogen bonds among backbone residues and extensive van der Waals contacts. However, not many of the interacting residues appear to be mediating specific contacts likely to be responsible for the protein-protein recognition specificity. In addition, screens have yielded peptides with amino acid sequences that do not resemble BCCP but can be biotinylated as efficiently, further highlighting the

challenge in the determination of the sequence/structural elements responsible for specificity(49).

The importance of several residues for the BCCP-ligase interaction has been obtained through mutational studies on both proteins. Studies on *E. coli* BCCP have identified, in addition to the target lysine, a glutamic acid at position 119 and several conserved glycine residues that affect biotinylation(50). Unexpectedly, mutation of the highly conserved methionine residues surrounding the target lysine in the MKM motif does not significantly affect biotinylation(51). In the *E. coli* ligase several surface loops are proposed to function in BCCP recognition and mutational analysis of these loops has identified R116 and R119 as important for interaction with BCCP(52). These residues are found in one of the conserved BirA loops, and are therefore likely to be important for the recognition of BCCP by ligases from all organisms.

1.1.8 Multiple carboxylase deficiency

Mutations on the HCS gene can lead to Multiple Carboxylase Deficiency (MCD), a disease characterized by ketoacidosis, organic aciduria and mental retardation (53-54). MCD presents a combination of the symptoms associated with deficiency of the individual carboxylases. There are no known naturally occurring HCS mutants that do not have at least some residual biotinylating activity, and null mutations are thought to be lethal in accord with HCS importance in biotin metabolism. MCD makes characterization of HCS and the effect of mutations even more pressing, although most MCD cases can be managed with pharmacological doses of biotin.

Information regarding the effect of certain amino acid changes on HCS activity can be obtained from the behavior of MCD associated variants. HCS catalytic activity in lysates obtained from MCD patients has been measured, usually using the bacterial carboxylase as a substrate. The variant enzymes display a wide range of defects that can affect both the catalytic activity and K_M for biotin(39,55-58). Some of the mutations affect positions in the catalytic domain of HCS. Others affect positions in the N-terminus and stress the importance of this domain to HCS function. Some broad correlations have been drawn regarding the effects of mutations and clinical symptoms responsiveness to biotin therapy. Those mutations altering the N-terminus tend to affect the k_{cat} (59), and to not respond as readily to biotin administration. Yet, a characterization regarding altered K_M for the acceptor substrates is rarely performed, despite its importance as it provides an explanation for poor biotin responsiveness.

1.2 The experimental problem

In spite of HCS importance for biotin metabolism, biochemical characterization of HCS function has been lacking. These studies have been hindered by the lack of a method to obtain sufficient amounts of pure protein. In chapter 2, we describe the recombinant expression of FL-HCS and 58-HCS in *E. coli* and their subsequent purification. In addition, chapter 2 includes the design of several assays to perform a steady state kinetic characterization of the effects of p67 or the minimal carboxylase acceptor substrate, ATP and biotin concentrations. Stopped flow studies of each of the two half reactions catalyzed by HCS showed that bio-5'-AMP

synthesis is the limiting step in the overall reaction. The two isoforms behaved similarly in all the assays, except for biotin transfer from the intermediate to the PCC biotin acceptor protein, where FL-HCS was twofold faster than 58-HCS. This led to the conclusion that HCS N-terminus is involved in biotin acceptor substrate recognition and highlighted the importance of protein-protein interaction as a source of substrate specificity.

Chapter 3 comprises a more detailed investigation of the biotin transfer reaction. The previous stopped flow experiments monitored the enzyme substrate disappearance and yielded information on the bimolecular rate of enzyme-substrate association. The same rates were obtained when monitoring product formation using tritium labeled biotin in a quench flow assay. This indicated that biotin transfer is limited by the bimolecular rate of enzyme-substrate association. Comparison to the results obtained with BirA, the *E. coli* enzyme, and PhBPL, an archaeal ligase, showed that this mechanistic aspect is conserved among evolutionary domains. In addition, the enzymes biotinylated the substrates from the other species with a wide range of rates, once again highlighting protein-protein interactions as the basis of selectivity in post-translational biotin addition.

Insight into HCS substrate specificity among the various endogenous human substrates is presented in Chapter 4. HCS associated with the biotin acceptor fragment of PC, PCC and MCC carboxylases with rates that range from 10000 to 35000 $M^{-1}s^{-1}$. ACC1 and ACC2 behaved differently, with the chemistry of biotin transfer becoming the rate limiting step. The different behavior correlated with the carboxylases localization, since ACC1 and ACC2 are present in the cytoplasm, while

the other carboxylases are transported into the mitochondria. A model consistent with these observations is that HCS biotinylates PC, PCC and MCC enzymes faster because mitochondrial enzymes are only transiently present in the cytoplasm and should be post-translationally modified before they reach their final destination. Conversely, HCS has continuous access to ACC1 and ACC2, so there has not been any evolutionary pressure to increase the biotinylation reaction speed. In addition, the data suggest a molecular mechanism for the establishment of a hierarchy that determines biotin distribution among carboxylases based on the rates of bimolecular association. Carboxylases will compete for the biotin, and those that have the highest apparent rate of association, which will depend on substrate concentration and inherent association rate, will be preferentially modified.

Chapter 2: Biochemical characterization of FL-HCS and 58-HCS

The work presented in this chapter was originally published in the Journal of Biological Chemistry: Maria Ingaramo and Dorothy Beckett. Distinct Amino Termini of Two Human HCS Isoforms Influence Biotin Acceptor Substrate Recognition. *Journal of Biological Chemistry*. 2009; 284, 30862-30870.

2.1 Abstract

The human holocarboxylase synthetase (HCS) catalyzes transfer of biotin to biotin-dependent carboxylases, and the enzyme is therefore of fundamental importance for many physiological processes, including fatty acid synthesis, gluconeogenesis, and amino acid catabolism. In addition, the enzyme functions in regulating transcription initiation at several genes that code for proteins involved in biotin metabolism. Two major forms of HCS exist in humans, which differ at the amino terminus by 57 amino acids. In this work, the two proteins were expressed in *Escherichia coli*, purified, and subjected to biochemical characterization. Equilibrium sedimentation indicates that the two proteins are monomers both in their apo-forms and when bound to the enzymatic intermediate biotinyl 5'-AMP. Steady state kinetic analyses as a function of biotin, ATP, or a minimal biotin-accepting substrate concentration indicate similar behaviors for both isoforms. However, pre-steady state analysis of biotin transfer reveals that the full-length HCS associates with the minimal

biotin acceptor substrate with a rate twice as fast as that of the truncated isoform. These results are consistent with a role for the HCS amino terminus in biotin acceptor substrate recognition.

2.2 Introduction

Biotin protein ligases are enzymes that are required for viability of all organisms. In metabolism these enzymes catalyze covalent linkage of biotin to biotin-dependent carboxylases as indicated in the following reactions,

$$E + biotin + ATP \longrightarrow E{\cdot}bio\text{-}5'\text{-}AMP + PPi$$
$$E{\cdot}bio\text{-}5'\text{-}AMP + apocarboxylase \rightleftharpoons E + holocarboxylase + AMP$$

in which the adenylated derivative of biotin, biotinyl 5'-AMP (bio-5'-AMP), is first synthesized from the substrates biotin and ATP (23). In the second step, the enzyme·adenylate complex interacts with the biotin acceptor domain or subunit of a carboxylase, and the biotin is covalently linked to the ε-amino group of a specific lysine residue on the acceptor. In humans the ligase is referred to as holocarboxylase synthetase (HCS).

Five biotin-dependent carboxylases, including acetyl-CoA carboxylases 1 and 2, 3-methylcrotonyl-CoA carboxylase, pyruvate carboxylase, and propionyl-CoA carboxylase, are the HCS substrates in humans. The biotin moiety serves as the transient carboxylate carrier as it is transferred from a donor to an acceptor in the reaction catalyzed by each enzyme. Biotin-dependent carboxylase-catalyzed reactions contribute to fatty acid synthesis and oxidation, gluconeogenesis, and amino acid catabolism. Mutations in the HCS gene cause multiple carboxylase deficiency, a

potentially fatal disease characterized by the concurrence of symptoms associated with each individual carboxylase deficiency (60-61).

In response to changes in biotin availability, HCS has been demonstrated to function in regulating transcription of the gene that encodes HCS itself as well as those that code for propionyl-CoA carboxylase, pyruvate carboxylase, acetyl-CoA carboxylase 1, and the sodium-dependent multivitamin transporter (48,62). This transcriptional regulatory process is associated with the soluble guanylyl cyclase signal transduction pathway (35). It has also been suggested that HCS exerts its transcriptional regulatory role by catalyzing biotin linkage to histones (36) (Fig. 7).

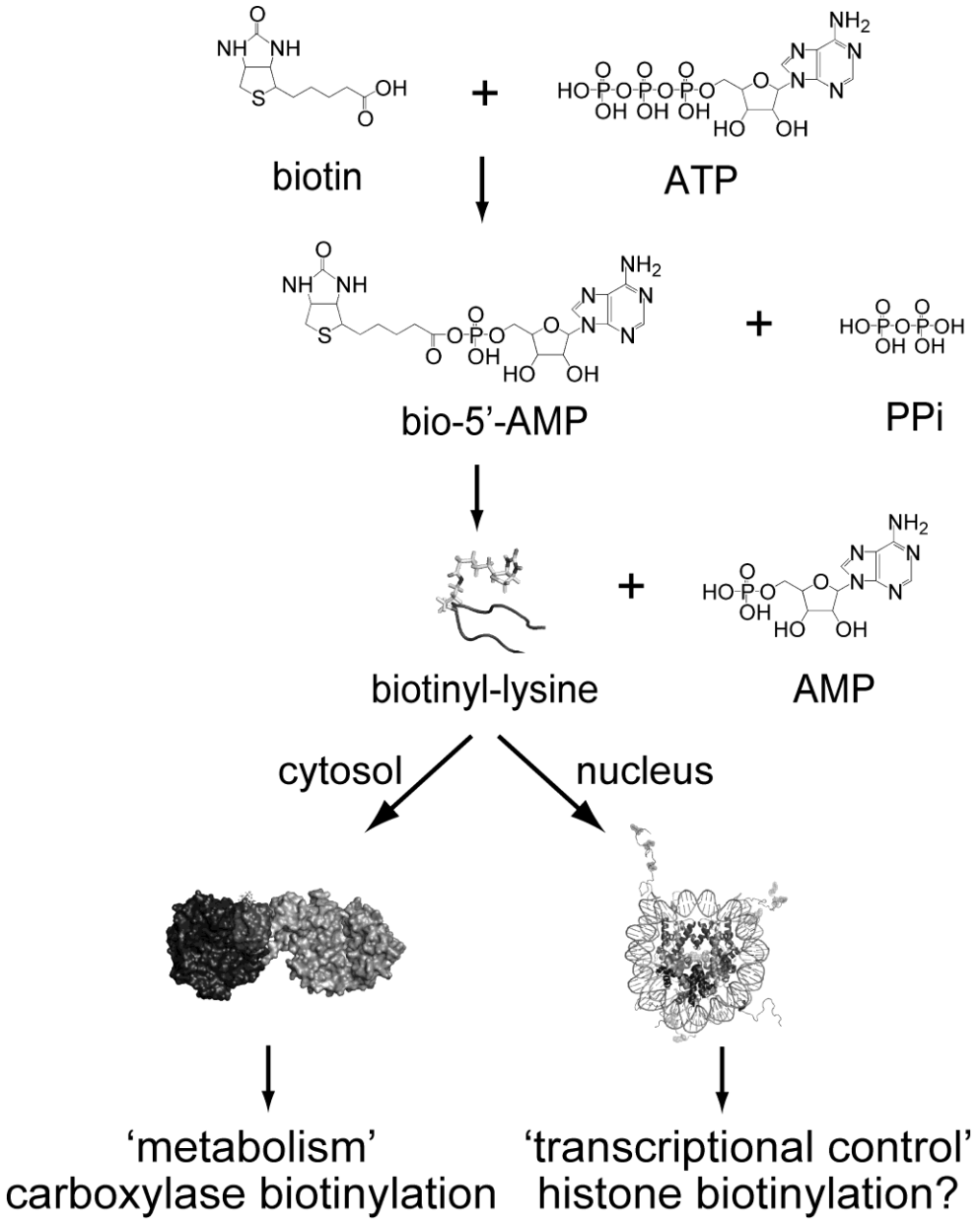

Figure 7. HCS function in metabolism and transcription regulation. The enzyme utilizes substrates biotin and ATP to catalyze synthesis of bio-5'-AMP. The HCS·intermediate complex interacts with carboxylases to transfer biotin or functions in transcription, perhaps through histone biotinylation.

Full-length HCS is a 726-amino acid polypeptide, characterized by a molecular mass of 81 kDa. Although residues 448–701 are homologous to the catalytic region of the *Escherichia coli* ligase, BirA (57), the sequence of the amino-terminal 447 residues of HCS bears homology only to the amino-terminal sequences of other mammalian holocarboxylase synthetases. Although only one copy of the HCS gene is present per haploid genome, analysis of the 5' termini of cDNAs (38), elucidation of the structure of the HCS gene (39), and purification of HCS from human tissue (40) indicate the existence of more than one form of the protein. Characterization of HCS cDNAs revealed an mRNA in which the initiator codon corresponds to methionine 58 in the full-length coding sequence(38). In addition, Western blot analysis of partially purified HCS from human placenta revealed three species that were assigned to the full-length HCS protein (FL-HCS) and species that initiated translation at methionine 7 or methionine 58 (58-HCS) (40).

The significance of these distinct HCS forms for functional biology is not known. It is possible that the two isoforms are characterized by different catalytic activities. Alternatively, the different forms may play distinct roles in the metabolic versus transcriptional functions of the enzyme. To investigate the enzymatic properties of the two isozymes, we have overexpressed and purified FL-HCS and 58-HCS to homogeneity. Sedimentation equilibrium measurements of the two proteins indicate that each is monomeric in both the unliganded state and when saturated with the intermediate in biotin transfer, biotinyl 5'-AMP. Steady state parameters governing the overall biotin transfer reaction using the model substrate p67, a fragment of propionyl-CoA carboxylase, show that they are very similar. However,

pre-steady state kinetic analysis of the second half-reaction revealed that FL-HCS associates with p67 at a faster rate than does 58-HCS. The results indicate that the two isoforms are functionally distinct and that the amino terminus influences the kinetics of interaction of the enzyme with the biotin acceptor protein.

2.3 Experimental procedures

2.3.1 Chemicals and Biochemicals

All chemicals used were at least reagent grade. The stock ATP solutions were prepared by dissolving ATP disodium salt (Sigma) into water and adjusting the pH to 7.5. The nucleotide concentration was determined by UV spectroscopy using an extinction coefficient at 259 nm of 15,400 M cm^{-1}. The D-[carbonyl-^{14}C]biotin (GE Healthcare) was stored desiccated under nitrogen at −20 °C. Biotin D-2,3,4,6-^{3}H was purchased from American Radiolabeled Chemicals, Inc., and stored at −20 °C. The bio-5'-AMP was synthesized and purified as described previously (23,63). Protein extinction coefficients were calculated according to Gill and von Hippel (64).

2.3.2 Expression Plasmid Construction

The strategy developed to overexpress FL-HCS and 58-HCS involved constructing plasmids that encode amino-terminal his_6-SUMO fusions of each protein using the linearized pSUMOpro (LifeSensors Inc.) expression vector (65). Primers containing an Esp3I restriction site were used to amplify the HCS coding sequences by PCR. The coding sequence for 58-HCS was amplified from a pGEX construct provided by Dr. Roy Gravel. The FL-HCS cDNA sequence (GenBankTM accession number NM_000411.4) was purchased from OriGene Technologies, Inc. After

digestion of the PCR product with Esp3I (Fermentas), the resulting two coding sequence fragments were ligated into the linearized pSUMO vector using T4 ligase (Roche Applied Science), and the ligation mixtures were transformed into the *E. coli* top10 strain. Plasmids were verified by sequencing the entire insert.

2.3.3 Purification of 58-HCS and FL-HCS

The plasmids encoding his_6-SUMO-FL-HCS and his_6-SUMO-58-HCS were transformed into *E. coli* RosettaTM(DE3). Once the culture had reached an A600 of 0.6, induction was achieved by the addition of lactose (Difco) to a final concentration of 0.5% (w/v) and allowed to proceed for 18–20 h at 25 °C. Cells were harvested, resuspended in 30 ml of lysis buffer/liter of culture (50 mM sodium phosphate buffer, pH 8, 500 mM sodium chloride, 1 mM 2-mercaptoethanol, 1 mM phenylmethylsulfonyl fluoride, and 5% (v/v) glycerol containing 10 mM imidazole), and lysed with three French press passes at 800–1000 p.s.i. The cellular debris was pelleted by centrifugation, and the supernatant was loaded onto a Ni^{2+}-Sepharose column (GE Healthcare). After washing extensively, 20 ml of lysis buffer containing 1 mM ATP, 0.5 mM magnesium chloride, and 1 μM of the biotin acceptor protein p67 was loaded on the column to remove residual biotin and bio-5'-AMP that was associated with the enzyme. After a wash step, the HCS protein was eluted with lysis buffer containing 400 mM imidazole. Sumo protease-1 (66) that was purified in this laboratory using an overexpression plasmid provided by Dr. C. Lima was added at a 1:100 (w/w) ratio to the HCS, and the mixture was dialyzed into buffer containing 10 mM sodium phosphate, pH 8.0, 60 mM NaCl, 5% (v/v) glycerol, 5 mM 2-mercaptoethanol. Following overnight incubation, the imidazole concentration was

adjusted to 40 mM, and the sample was loaded again onto Ni^{2+}-Sepharose resin to remove the his_6-SUMO tag and the his_6-tagged protease. The flow-through was collected and dialyzed against buffer containing 10 mM sodium phosphate, pH 8.0, 30 mM NaCl, 1 mM 2-mercaptoethanol, 5% glycerol. The resulting sample was loaded onto a Toyopearl anion exchange column (Tosoh Bioscience) and eluted with a linear gradient to 0.3 M NaCl. HCS was concentrated and stored in 10 mM Tris-HCl, pH 8, 200 mM sodium chloride, 10% glycerol at −80 °C. The yield was 2 mg of protein/liter of bacterial culture and the concentration of each protein was determined spectrophotometrically using an extinction coefficient at 280 nm of 56,610 M cm^{-1} (64). The proteins were at least 97% pure as judged by Coomassie Brilliant Blue staining of samples subjected to SDS-PAGE.

2.3.4 Purification of p67

The pDest17 plasmid coding for his_6-p67 was a generous gift from Dr. Roy Gravel. Purification of his_6-p67 was carried out as described previously (67), except for the use of an additional SP-Sepharose Fast Flow column (GE Healthcare). This column was run with a linear KCl gradient in 50 mM Tris-HCl, pH 7.5, at 4 °C, 5% glycerol, 1 mM 2-mercaptoethanol. The concentration was determined spectrophotometrically using an extinction coefficient at 276 nm of 4350 M cm^{-1}. The presence of biotinylated p67 in the preparations was undetectable, as determined by MALDI-TOF mass spectrometry using the α-cyano-4-hydroxycinnamic acid matrix (28). The same method was used to determine that all of the p67 preparation is active in accepting biotin.

2.3.5 Equilibrium Sedimentation Measurements

Equilibrium sedimentation measurements were carried out in a Beckman Optima XL-I analytical centrifuge equipped with a 4-hole An60-Ti rotor (Beckman Coulter). Double sector 12-mm path length cells with charcoal-filled Epon centerpieces and sapphire windows were used. Samples (V_{TOT} = 140 μl) were prepared at final concentrations ranging from 2 to 20 μM from protein that had been extensively dialyzed against reaction buffer (10 mM Tris-HCl, pH 7.50 ± 0.02 at 20.0 ± 0.1 °C, 200 mM KCl, 2.5 mM $MgCl_2$). Samples that contained HCS, FL- or 58-, and bio-5'-AMP were prepared with 1.5-fold molar excess of the ligand over the protein. Centrifugation was carried out at speeds ranging from 14,000 to 22,000 rpm for 12 h at each speed (68), and absorbance scans were acquired at 280 or 295 nm, if the bio-5'-AMP contribution needed to be avoided, with a step size of 0.001 cm and five averages per step. The data obtained for the samples run at the multiple speeds were subjected to a global single species analysis using the program WinNonLin (69), and the best fit value of σ obtained from the analysis was converted to molecular mass using the following equation,

$$\sigma = \frac{M(1-\bar{\upsilon}\rho)\omega^2}{RT}$$

in which M is the molecular mass; $\bar{v}$ is the partial specific volume of the protein, ρ is the buffer density; ω is the angular velocity; R is the gas constant; and T is the temperature. The value of ρ (1.007 g/ml) was determined pycnometrically (70), and $\bar{v}$ was calculated, based on the protein sequences, to be 0.7389 ml/g for 58-HCS or 0.7392 ml/g for FL-HCS using the program SedenTerp.

2.3.6 Steady State Kinetic Measurements

Kinetic measurements of the overall HCS-catalyzed reaction as a function of ATP or p67 concentration were performed by monitoring the incorporation of [^{14}C]biotin into p67. The reactions were carried out in reaction buffer at 37.0 ± 0.1 °C and initiated by the addition of enzyme to a final concentration between 50 and 150 nM. At designated time points, a 17-μl aliquot was quenched into a solution containing 5.1 μl of loading dye and 3.4 μl of 1% trifluoroacetic acid (in H_2O). The loading dye was composed of 50 mM Tris-HCl, pH 6.8, 4% SDS, 30% glycerol, 0.67 mg/ml Coomassie Brilliant Blue G-250, 735 mM 2-mercaptoethanol. Unincorporated [^{14}C]biotin was separated from the ^{14}C-biotinylated p67 by electrophoresis on a 16% acrylamide-SDS-Tricine gel (71). The gels were dried on Whatman 3MM paper and exposed to a phosphor screen (GE Healthcare) for 3 days. The phosphor screen image was scanned using a Storm PhosphorImager, and the volumes of the bands corresponding to [^{14}C]biotin-labeled p67 were quantified using the ImageQuant software (GE Healthcare). Initial velocities were obtained from the slope of counts versus time plot. The initial velocity versus substrate concentration data were subjected to nonlinear least squares analysis using the Michaelis-Menten equation with GraphPad Prism to obtain V_{max} and K_m. The V_{max} and k_{cat} values were converted from counts/min to micromolars of biotin using the relation between counts/min and micromolars obtained from a reaction containing 50 μM p67, 150 nM HCS, 10 μM biotin, and 1 mM ATP in standard reaction buffer incubated for 1 h to allow complete incorporation of the biotin into the acceptor protein. In experiments in which the Michaelis-Menten constants for p67 were determined, the [^{14}C]biotin and ATP

concentrations were set at saturating values of 10 μM and 1 mM, respectively. The K_m and k_{cat} values for ATP were determined in a similar fashion, with the exception that the reactions contained 50 μM p67, 10 μM [^{14}C]biotin, and variable ATP concentrations.

The biotin concentration dependences of the reactions catalyzed by FL- and 58-HCS were determined by quantitating the incorporation of [^{3}H]biotin into p67. Each reaction contained 16.67 nM [^{3}H]biotin and a supplement of unlabeled biotin to obtain the desired final total biotin concentration. The p67 and ATP concentrations were 150 μM and 1 mM, respectively. Reactions were initiated by addition of enzyme to 5 nM final concentration, and aliquots were quenched with trifluoroacetic acid added to a final concentration of 0.3% (v/v). Quenched reactions were filtered though BA 85 Protran nitrocellulose membranes (Whatman), and the retained radioactivity was quantified in ProteinReady^{+} scintillation fluid (Beckman) using a LS6500 Beckman counter. The measured disintegrations/min were converted to molar quantities of biotin incorporated by multiplying by total biotin concentration/dpm of unfiltered sample. The correction for filter retention was achieved by using the disintegrations/min associated with a filtered and unfiltered reaction in which 10 μM cold biotin and 16.67 nM [^{3}H]biotin were fully incorporated into p67.

2.3.7 Steady State Fluorescence Spectra

Steady state fluorescence spectra were acquired at 20 °C in reaction buffer using an ISS PC1 instrument. The excitation wavelength was 295 or 300 nm, and emission was monitored from 310 to 450 nm. The excitation slit width was set to 4 or

8 nm, and the emission slit width was 8 nm. Spectra were corrected for contributions from buffer and ligand and for dilution.

2.3.8 Initial Rate of Bio-5'-AMP Synthesis

The rate of bio-5'-AMP synthesis was measured at 20 °C by monitoring the intrinsic protein fluorescence decrease that accompanies synthesis of the intermediate. The experiments were performed in a Kintek 2001 stopped flow instrument using an excitation wavelength of 295 or 300 nm and monitoring the emission through a 340-nm cutoff filter (Corion Corp.). Several ATP solutions prepared at concentrations ranging from 25 to 800 μM were rapidly mixed in a 1:1 ratio with a solution of a fixed concentration of HCS containing 30 μM biotin. Initial HCS concentrations varied from 2 to 6 μM, and all solutions were prepared in degassed reaction buffer. A minimum of five traces that spanned at least eight half-lives of the process was collected at each ATP concentration. Transients were analyzed using a double exponential function with the Kintek software. The dependences of the apparent rates of the two phases on ATP concentration are discussed under "Results."

2.3.9 Measurement of the Bimolecular Association Rate Constant of HCS with p67

The bimolecular rate of association of HCS with p67 was obtained by monitoring the intrinsic fluorescence increase of HCS upon depletion of the bio-5'-AMP·HCS complex. The instrument and experimental setup were as described above, with the exception that one syringe contained varying concentrations of p67, and the second syringe contained a fixed concentration of the HCS·bio-5'-AMP complex. The HCS·bio-5'-AMP complex concentration before mixing ranged from 1 to 3 μM

in different experiments. This solution was prepared by combining HCS with biotin at half of the enzyme concentration and 100 μM ATP and incubating for 10 min to allow completion of bio-5'-AMP synthesis. This solution was rapidly mixed with p67, and the resulting time-dependent increase in intrinsic HCS fluorescence was monitored. At least five traces acquired at each [p67] were fit to single exponential to obtain apparent rates. The observed rates as a function of p67 concentration were subjected to further analysis as described under "Results."

2.4 Results

2.4.1 Purification of HCS Isoforms

The two HCS isoforms were expressed in *E. coli* as his_6-SUMO fusion proteins, and the purification protocol, which included three chromatography steps, yielded preparations that were >97% pure (Fig. 8). Because SUMO-protease-1 leaves no exogenous amino acids after cleavage, the final proteins correspond to native 58-HCS and FL-HCS. In the purification, it was necessary to incorporate steps to remove bio-5'-AMP from the preparations. This contamination was revealed by the ability to detect biotinylation of p67 in the absence of added biotin. Biotinylation was assayed as a shift in the mass of a fraction of the p67 using MALDI-TOF mass spectrometry. Both the *E. coli* and *Pyroccocus horikoshii* enzymes have been purified in this laboratory, and in contrast to the *Homo sapiens* enzyme, no contaminating substrate or intermediate has ever been detected in those preparations.

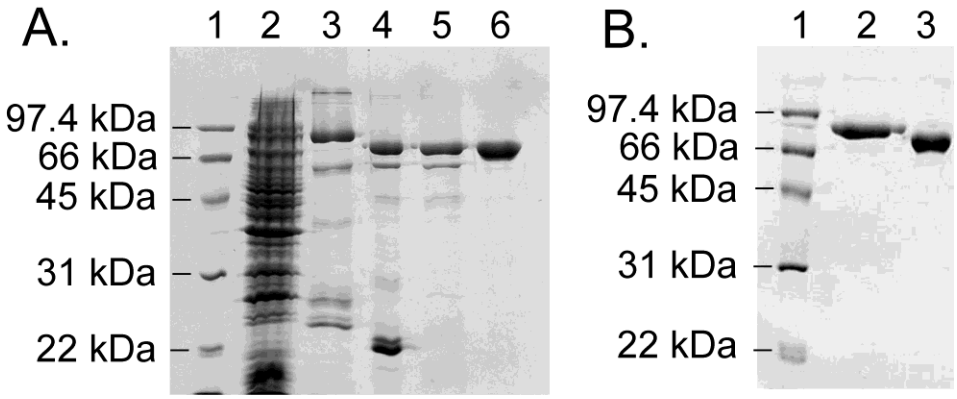

Figure 8. SDS-polyacrylamide gel of 58-HCS purification fractions. A, lane 1, low range molecular weight markers (Bio-Rad). Lane 2, crude extract after induction. Lane 3, sample obtained from the first Ni^{2+}-Sepharose column. Lane 4, sample after SUMO protease 1 cleavage. Lane 5, flow-through from the second $Ni2^{+}$-Sepharose column. Lane 6, material obtained after Toyopearl anion exchange column. B, 12% SDS-polyacrylamide gel of the pure proteins. Lane 1, low range molecular weight markers. Lane 2, FL-HCS; lane 3, 58-HCS.

2.4.2 Sedimentation Equilibrium Analysis of FL-HCS and 58-HCS Oligomeric State

Sedimentation equilibrium measurements were used to determine the oligomeric state of the two HCS enzymes in reaction buffer at 20 °C. Scans obtained for unliganded 58-HCS are shown in Fig. 9, along with the results of nonlinear least squares analysis of the data. Global analysis of data obtained for samples prepared at two protein concentrations and centrifuged at two rotor speeds using a single species model indicates a molecular weight consistent with the monomer. The experimentally determined molecular masses were 74 ± 4 and 83 ± 3 kDa for 58-HCS and FL-HCS, respectively. These values agree within error with the analytical molecular masses of 74 kDa for 58-HCS and 81 kDa for FL-HCS calculated from the amino acid sequence.

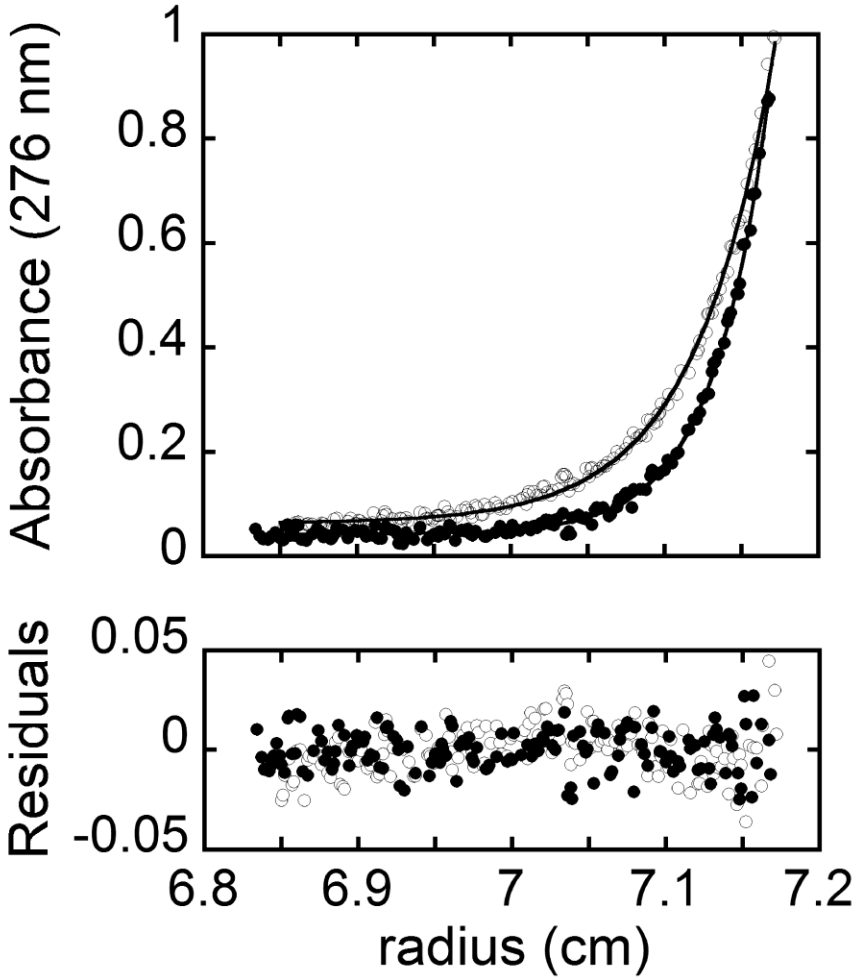

Figure 9. HCS analytical ultracentrifugation. Concentration distribution for 3.8 μM 58-HCS in reaction buffer at 20 °C. Absorbance versus radial position obtained at rotor speeds of 18,000 rpm (○) and 22,000 rpm (·). The solid lines represent the best fit of the data acquired at 3.8 and 1.9 μM 58-HCS and the two rotor speeds to a single species model. The residuals of the fit are provided in the bottom panel.

The *E. coli* biotin protein ligase undergoes a monomer-dimer transition that is dependent on bio-5'-AMP binding (70). To investigate the effect of the intermediate on the self-association of the two HCS enzymes, sedimentation equilibrium measurements were performed in the presence of excess bio-5'-AMP. The experimentally obtained molecular masses for the intermediate bound species were 79 ± 8 kDa for 58-HCS and 83 ± 7 kDa for FL-HCS, consistent with a monomeric species. Thus, both the unliganded and intermediate-bound forms of FL and 58-HCS are monomeric.

2.4.3 Kinetic Analysis of the Two-step HCS-catalyzed Reaction

In the HCS-catalyzed reaction, biotin is covalently linked to a specific lysine residue on the biotin carboxyl carrier protein domain of five distinct carboxylases. The physiologically relevant substrates contain multiple copies of this domain. To develop a simple assay for measuring the catalytic activity of the purified HCS enzymes, the p67 domain of propionyl-CoA carboxylase was employed as the model acceptor substrate. This protein corresponds to the carboxyl-terminal 67 residues of the α subunit of human propionyl-CoA carboxylase, which contains sufficient information for recognition by the human biotin protein ligase (72).

The two kinetic assays used in this work rely on measurements of incorporation of radiolabeled biotin into p67. In the first assay, [^{14}C]biotin incorporation into p67 was monitored. The [^{14}C]biotin-labeled p67 was separated from the unincorporated biotin by electrophoresis, and radioactivity in the bands corresponding to p67 was quantitated by phosphorimaging (Fig. 10A). The initial rate at several ATP concentrations and constant biotin and p67 concentrations exhibit the

expected increase in the rate of [^{14}C]biotin incorporation with increasing ATP concentration (Fig. 10B).

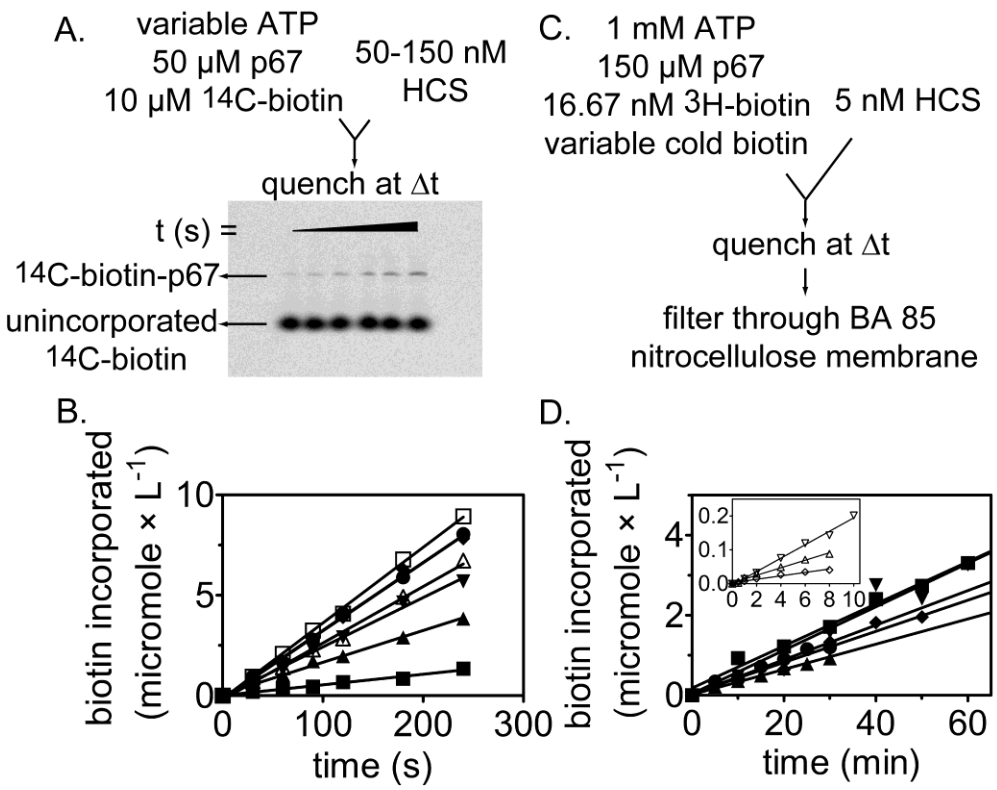

Figure 10. Kinetic assays used to determine Michaelis-Menten constants for HCS-catalyzed biotin transfer with respect to p67, biotin, and ATP. A, incorporation of [^{14}C]biotin into p67 was used to determine the kinetic constants with respect to p67 and ATP. The biotinylated p67 and free biotin are separated on a 16% acrylamide gel. B, biotin incorporation versus time at 150 nM 58-HCS, 50 μM p67, 10 μM [^{14}C]biotin, and a range of ATP concentrations as follows: (■, 5 μM; ▲, 30 μM; ▼, 90 μM; ♦, 250 μM; ·, 500 μM; □, 750 μM; and ▵, 1000 μM ATP. C, incorporation of [^{3}H]biotin into p67 used to determine the kinetic constants with respect to biotin. Biotinylated p67 is separated from unincorporated biotin by filtration through a nitrocellulose membrane. D, initial rates of biotin incorporated measured at 5 nM FL-HCS, 150 μM p67, 16.67 nM [^{3}H]biotin and variable unlabeled biotin concentrations as follows: ▼, 20 μM; ■, 10 μM; ♦, 7 μM; ·, 3 μM; and ▲, 1 μM biotin. The inset depicts the traces obtained for the following: ▽, 400 nM; Δ, 150 nM; and ◊, 50 nM total biotin. B and D, the lines were obtained from linear regression of the measured biotin incorporation versus time.

The second assay for HCS catalytic activity monitors [^{3}H]biotin incorporation into p67. The [^{3}H]biotin-labeled p67 was separated from the unincorporated biotin by filtration through nitrocellulose and quantitated by liquid scintillation counting (Fig. 10C). The relatively low Km value for biotin, the detection limit of the ^{14}C radiation using phosphorimaging, and a new lack of commercial availability of the [^{14}C]biotin motivated development of this second assay. Results of measurements of the initial rates of HCS-catalyzed [^{3}H]biotin incorporation at constant ATP and p67 concentrations and varying total biotin concentrations are shown in Fig. 10D. The time courses used for initial rate measurements at low biotin concentrations were carried out for a shorter time than those acquired at the higher biotin concentration. This is due to the higher specific activity of the substrate at the low cold biotin concentration, which allowed acquisition of data over shorter time periods.

To investigate if the amino-terminal 57-amino acid residues impact the basic catalytic properties of the human biotin protein ligase, the kinetic parameters associated with the process were measured for both FL-HCS and 58-HCS. Measurements of the initial rates of biotin transfer as a function of p67 concentration are shown in Fig. 11, A and B. The results indicate K_m values of 19 and 21 μM, respectively, for FL-HCS and 58-HCS (Table 1) and values of k_{cat} that are similar at 0.47 and 0.35 s^{-1}, respectively. The magnitudes of k_{cat}/K_m are, within error, identical.

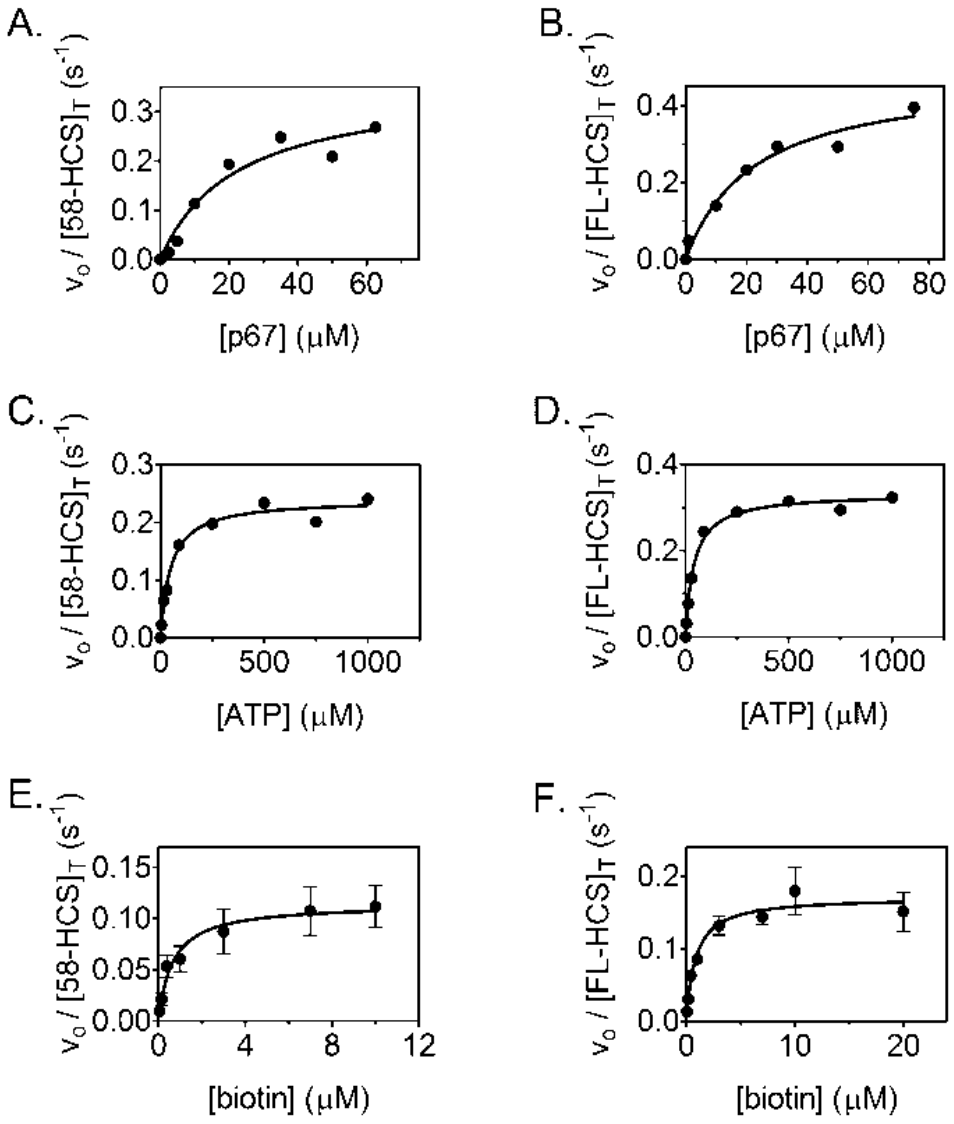

Figure 11. Steady state kinetic analysis of biotin incorporation into p67 catalyzed by 58-HCS and FL-HCS. Samples of steady state analysis of the reaction catalyzed by 58-HCS (A) and FL-HCS (B) as a function of p67 concentration are shown. Data were obtained as a function of ATP concentration for 58-HCS (C) and FL-HCS (D). E and F display results of steady state measurements for 58-HCS and FL-HCS as a function of biotin concentration. In these two panels each data point represents the average of the initial rate measured at each biotin concentration in three independent experiments. In E and F, the error bars represent the standard deviation of each three points. In each panel the solid line represents the best fit of the data to the Michaelis-Menten equation.

Table 1. Kinetic parameters for the overall HCS-catalyzed reaction.

HCS form	*Substrate*	K_M	k_{cat}	k_{cat}/K_M
		μM	s^{-1}	$x10^4\ M^{-1}\ s^{-1}$
58	p67	19 ± 4[a]	0.35 ± 0.02[a]	1.8 ± 0.4
	ATP	41 ± 10[a]	0.33 ± 0.02[a,b]	0.8 ± 0.2
			(0.24 ± 0.01)[a,c]	0.6 ± 0.1
	biotin	0.7 ± 0.3[d]	0.11 ± 0.01[d]	16 ± 7
FL	p67	21 ± 2[a]	0.47 ± 0.01[a]	2.2 ± 0.2
	ATP	47 ± 8[a]	0.45 ± 0.02[a,b]	1.0 ± 0.2
			(0.32 ± 0.01)[a,c]	0.7 ± 0.1
	biotin	0.8 ± 0.2[d]	0.17 ± 0.01[d]	21 ± 5

[a] The errors correspond to the standard deviation of two independent experiments.[b] The calculated value is based on the experimentally obtained k_{cat} at 50 μM p67.[c] Experimentally obtained k_{cat} was at 50 μM p67.[d] The error represents the standard error obtained from globally fitting data from three independent experiments.

A similar analysis as a function of ATP concentration (Fig. 11, B and D) provides K_m values for ATP of 41 and 47 μM for 58-HCS and FL-HCS, respectively. The magnitude of k_{cat} associated with ATP obtained from direct fitting of the data is lower than that obtained from measurements of the p67 concentration dependence of the reaction. This is attributable to the necessity, due to the appearance of a doublet for the labeled p67 at high concentrations, of using an acceptor protein concentration of 50 μM in the ATP concentration dependence measurements. Normalization of the resolved k_{cat} values obtained from analysis of the ATP concentration dependence of the reactions to those obtained from the measurements of the p67 concentration dependence reveals that they are identical (Table 1).

The FL-HCS and 58-HCS enzymes were subjected to Michaelis-Menten analysis of the biotin concentration dependence of the reaction using [^{3}H]biotin. The

results of measurements of the initial rates versus biotin concentration indicate that both FL- and 58-HCS-catalyzed reactions are well described by a Michaelis-Menten model (Fig. 11, E and F). The initial rate at each biotin concentration represents the average of at least three independent measurements. Results of nonlinear least squares analysis of the data indicate that the two enzymes are similar with respect to their rate versus biotin concentration profiles. The k_{cat} values resolved from the analysis are ~3-fold lower than those obtained from analysis of data obtained using SDS-PAGE to separate products from reactants. Because p67 and ATP concentrations used in the measurements were saturating, the differences in the values of k_{cat} reflect differences intrinsic to the two assays.

2.4.4 Pre-steady State Analysis of Bio-5'-AMP Synthesis

The overall reaction catalyzed by HCS can be classified as a ping-pong mechanism, which allows measurement of the two individual half-reactions. Upon bio-5'-AMP synthesis, decreases in intrinsic protein fluorescence of ~14% for FL-HCS and 23% for 58- HCS are observed (Fig. 12A). A stopped flow experiment was developed to investigate the first half-reaction, in which biotin-bound HCS was rapidly mixed with ATP. Measurement of the time dependence of the fluorescence decrease revealed that it was well described by a double exponential model (Fig. 12A, inset). A loss in amplitude with increasing ATP concentration was observed, which was attributed to the faster phase becoming increasingly fast and outside of the dead time of the stopped flow instrument. The apparent rates for the two phases were plotted as a function of ATP concentration (Fig. 12B). The observed linear

dependence of the faster phase on ATP concentration and the saturable slower phase are consistent with the following reaction,

$$HCS{\cdot}biotin + ATP \underset{k_{-1}}{\overset{k_1}{\rightleftharpoons}} HCS{\cdot}biotin{\cdot}ATP \xrightarrow{k_{cat}} HCS{\cdot}bio\text{-}5'\text{-}AMP + PPi$$

in which the slope of the linear dependence of the apparent rate of the fast phase on nucleotide concentration provides an estimate of the rate of association of ATP with the HCS·biotin complex, k_1 (Table 2). Nonlinear least squares analysis of the concentration dependence of the second phase using the Michaelis-Menten model yielded k_{cat} and K_m values for the reaction. The parameters obtained for 58-HCS and FL-HCS from these two analyses are similar in magnitude (Table 2).

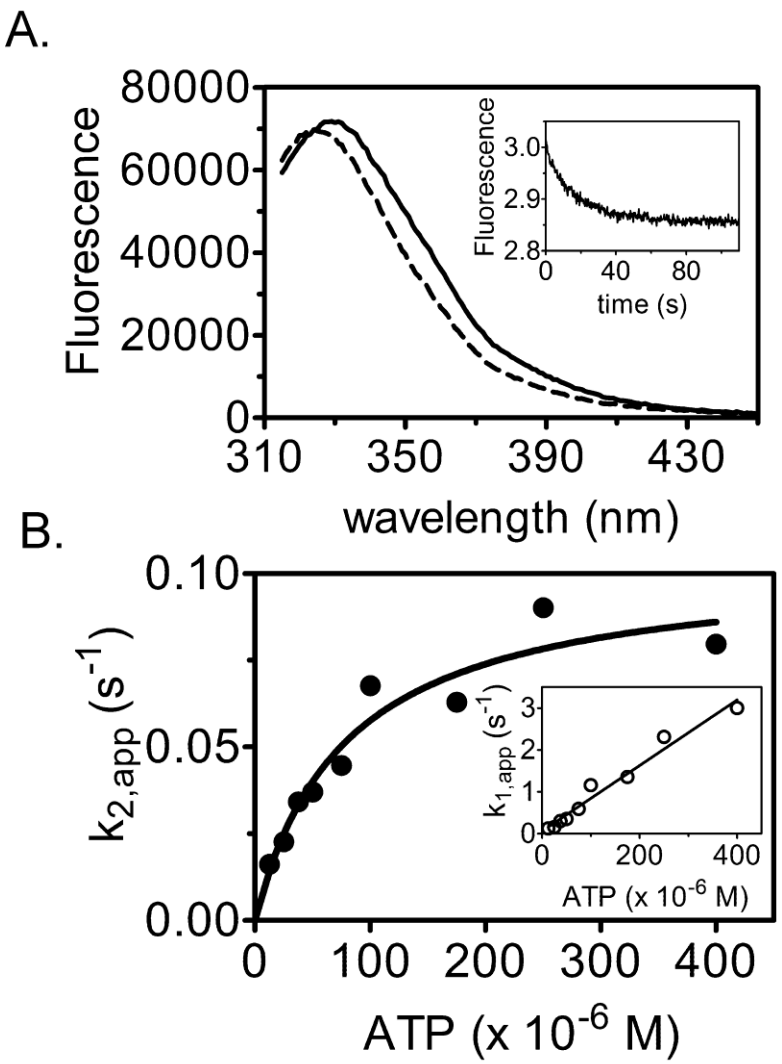

Figure 12. Pre-steady state analysis of bio-5'-AMP synthesis. A, fluorescence (arbitrary units) emission spectra of 1.5 μM HCS and 15 μM biotin before (solid line) and after (dashed line) addition of 100 μM ATP. Inset, representative stopped flow fluorescence (arbitrary units) trace obtained upon mixing 2 μM HCS and 30 μM biotin with 25 μM ATP. B, dependence of the apparent rate of bio-5'-AMP synthesis on ATP concentration. The line is the fit to the Michaelis-Menten equation. Inset, dependence of the apparent rate of ATP association with HCS-biotin on ATP concentration.

Table 2. Kinetic parameters for ATP dependence of bio-5'-AMP synthesis

HCS form	k_1	K_M	k_{cat}	k_{cat}/K_M
	$x10^3\ M^{-1}\ s^{-1}$	μM	s^{-1}	$x10^3\ M^{-1}\ s^{-1}$
58	4.9 ± 0.7[a]	50 ± 30[a]	0.12 ± 0.02[a]	2 ± 1
			(0.39 ± 0.06[b])	8 ± 5
FL	6 ± 1[c]	50 ± 20[c]	0.11 ± 0.02[c]	2 ± 1
			(0.36 ± 0.06[b])	7 ± 3

[a] The errors correspond to the standard deviation for two independent experiments.[b] The calculated k_{cat} values were obtained at 37 °C assuming that the rate doubles every 10 °C.[c] The errors correspond to the standard deviation for three independent experiments.

2.4.5 Single Turnover Analysis of the Biotin Transfer Reaction

The second half-reaction, transfer of biotin from bio-5'-AMP to p67, was also measured using stopped flow fluorescence. An increase in intrinsic protein fluorescence, which reports on depletion of the enzyme-intermediate species, occurs upon addition of p67 to the pre-formed HCS·bio-5'-AMP complex (Fig. 13A). In the measurements, HCS was first allowed to synthesize bio-5'-AMP from ATP and biotin. To ensure single turnover conditions, the biotin concentration used was half that of the HCS concentration. Moreover, because at micromolar protein concentrations HCS is at stoichiometric conditions with respect to bio-5'-AMP binding, virtually all of the intermediate is associated with HCS. The HCS·intermediate complex was rapidly mixed with varying concentrations of p67 under pseudo first-order conditions, and the resulting time-dependent increase in fluorescence was well described by a single exponential model (Fig. 13A, inset). The

amplitudes of the transients displayed no dependence on p67 concentration, indicating that the reaction goes to completion at all concentrations. Measurements performed over a large range of p67 concentrations up to 100 μM yield apparent rates that show no indication of leveling off (Fig. 13B). As a result, the fluorescent signal was interpreted as reporting on the initial p67 binding event that is governed by k_1 in the following reaction,

$$HCS{\cdot}bio\text{-}5'\text{-}AMP + p67 \underset{k_{-1}}{\overset{k_1}{\rightleftharpoons}} HCS{\cdot}bio\text{-}5'\text{-}AMP{\cdot}p67 \xrightarrow{k_{cat}} HCS + bio\text{-}p67 + AMP$$

The slope of the line relating the dependence of the apparent rate on p67 concentration provides a bimolecular rate constant for association of p67 with FL-HCS that is ~2-fold greater than for 58-HCS (Table 3).

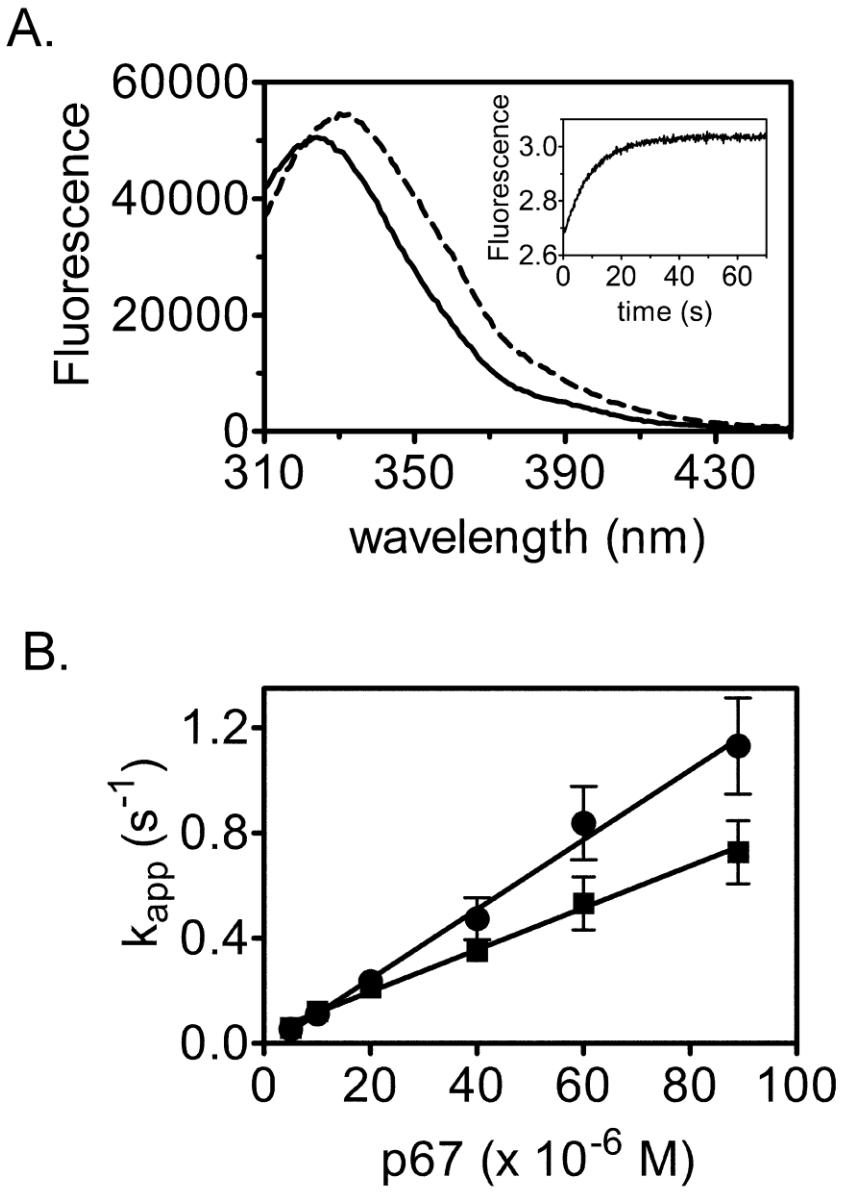

Figure 13. Single turnover measurements of biotin transfer from bio-5'-AMP to p67. A, fluorescence emission spectra (arbitrary units) of 1 μM 58-HCS, 0.5 μM biotin, and 100 μM ATP before (solid line) and after (dashed line) addition of 10 μM p67. Inset, representative stopped flow fluorescence trace (arbitrary units) obtained upon mixing 1 μM 58-HCS, 0.5 μM biotin, and 100 μM ATP with 20 μM p67. B, dependence of the apparent association rate of FL-HCS-bio-5-AMP (·) or 58-HCS-bio-5'-AMP (■) with p67 on acceptor protein concentration. Error bars represent the mean ± S.E. of at least five measurements performed at each [p67].

Table 3. Bimolecular association rate constants for HCS·bio-5'-AMP with p67.

HCS form	k_1
	$x10^3$ $M^{-1}s^{-1}$
58	7.6 ± 0.6[a]
FL	14 ± 1[a]

[a] The errors correspond to the standard deviation of two independent experiments.

2.5 Discussion

Elucidation of the biochemical details of human holocarboxylase synthetase function has implications for understanding the mechanism of the metabolic disorder, multiple carboxylase deficiency, as well as how this metabolic enzyme functions in transcription regulation. The significance of the existence of multiple forms of the enzyme for its distinct roles also merits further study. The results presented in this work indicate that although the two HCS isoforms catalyze the first of the two half-reactions in post-translational biotin addition with similar rates, they differ in the second half-reaction. Thus, the 57 amino-terminal residues appear to be involved in biotin acceptor protein recognition.

2.5.1 FL-HCS and 58-HCS Are Monomeric

Results of sedimentation equilibrium measurements indicate that in the micromolar concentration range both enzymes are monomeric regardless of ligation state. This result contrasts with that obtained for the *E. coli* enzyme, which homodimerizes in response to the adenylate binding (70). However, homodimerization of the *E. coli* enzyme is associated with the site-specific DNA binding function of the enzyme, a function that the human enzyme does not possess.

Studies of a number of simple monofunctional bacterial biotin protein ligases that do not possess a DNA binding domain indicate that they can exist as monomers or constitutive dimers. The structures of the dimeric enzymes, which utilize a surface distinct from that used by the *E. coli* enzyme to homodimerize, reinforce the idea that linkage of dimerization of the *E. coli* enzyme to bio-5'-AMP binding is idiosyncratic to its additional role in site-specific DNA binding.

Sedimentation analysis of the two HCS isoforms indicates that the HCS amino terminus plays no role in mediating homo-oligomerization of the protein. Several eukaryotic biotin protein ligases have been characterized at the sequence level. However, very few have been purified. Among these are the *Saccharomyces cerevisiae* and one of the two *Arabidopsis thaliana* enzymes. The chloroplastic *A. thaliana* enzyme has been overexpressed in and purified from *E. coli* and found to be monomeric in its native form (73). No characterization of the oligomeric state of the yeast enzyme was reported. Like the human enzyme, these eukaryotic enzymes are characterized at the primary structure level by a carboxyl terminus that is homologous to the monofunctional bacterial enzymes and the central and carboxyl-terminal domains of the bifunctional bacterial enzymes. Furthermore, they all possess amino-terminal segments of varying lengths. One potential role for these amino-terminal segments is in self-association of the protein. However, the characterization of the purified human and plant enzymes indicates that this is not the case.

2.5.2 Steady State Analysis of the Overall HCS-catalyzed Reaction

The FL- and 58-HCS isoforms exhibit similar kinetic properties in the overall biotin transfer reaction. However, the k_{cat} values for FL-HCS are consistently larger

than those measured for the truncated protein. For example, the k_{cat} values of 0.35 ± 0.02 and 0.47 ± 0.01 s^{-1} for 58-HCS versus FL-HCS, respectively, were resolved from measurements of the p67 concentration dependence of the reaction. Similarly modest differences in k_{cat} are observed in measurements of the dependence of the rate on ATP and biotin concentrations.

The values of the kinetic constants for two of the three substrates compare reasonably well with those reported previously for the human enzyme. However, the caveat to any comparison is that previous measurements were performed in fractionated cellular extracts. Previously reported values of the K_m for biotin range from 15 nM to 1 μM and thus are in the same range as the values of 700–800 nM reported in this work (74-77). The K_m values for ATP measured for FL-HCS and 58-HCS are ~40–50 μM, although previously reported values range from 190 to 250 μM (74-75). Finally, the Michaelis constants for p67 reported in this work cannot be compared with any other values because none exist in the literature.

2.5.3 Analysis of HCS Two Half-reactions

Transient state kinetic analysis can yield valuable insight into a reaction mechanism. This method relies on the use of high enzyme concentrations that allow the direct detection of intermediates. As a result, the analysis makes possible the determination of elementary rate constants(78). In this work, two transient state assays were used to obtain information on the two half reactions. The assay for bio-5'-AMP synthesis is based on rapidly mixing a large concentration of enzyme saturated with excess biotin with several ATP concentrations. Although the set up resembles an 'approach to steady state' experiment, the observed fluorescence change

indicates that on the examined timescale, a single turnover of bio-5'-AMP synthesis is observed. In the biotin transfer assay, a constant concentration of biotin is pre-incubated with twice as much enzyme and ATP to allow synthesis of bio-5'-AMP. This complex is rapidly mixed with p67 prepared at several concentrations. The excess enzyme allows for monitoring of only one reaction turnover.

Results of the pre-steady state measurements of the first half-reaction indicate that the two forms synthesize bio-5'-AMP with similar rates and K_m for ATP. Furthermore, the Michaelis constants for ATP for the half-reaction are the same as the values obtained for the overall reaction. Because the fluorescence signal at this temperature was more reliable, measurements of the half-reactions were performed at 20 °C. Assuming that the rate doubles every 10 °C, the values of k_{cat} for the first half-reaction at 37 °C are predicted to be $0.39 \pm 0.06\ s^{-1}$ for 58-HCS and $0.36 \pm 0.06\ s^{-1}$ for FL-HCS. These values agree with those obtained from measurements of the overall reaction and therefore indicate that bio-5'-AMP synthesis is the rate-limiting step in the two-step reaction.

Stopped-flow fluorescence measurements of second half-reaction, which report only on association of p67 with the enzyme·intermediate complex, indicate that FL-HCS associates with the acceptor protein at a rate twice that measured for 58-HCS. Furthermore, the absence of a leveling off of the rate as p67 concentration is increased is consistent with the conclusion that bio-5'-AMP synthesis is the rate-limiting step in the two-step reaction. Simulations of the kinetic time courses in the context of the model used for the analysis indicate a lower limit for the rate of biotin

transfer and product release of 1 s^{-1}, a value significantly greater than the k_{cat} value of 0.1 s^{-1} determined for the first half-reaction.

The distinct rates of association of FL- and 58-HCS with p67 are qualitatively consistent with the results of previous studies in which a series of truncation proteins of 58-HCS were characterized with respect to their abilities to catalyze biotin linkage to the biotin acceptor domain of the human propionyl-CoA carboxylase, p67, and the *E. coli* biotin carboxylase carrier protein fragment, BCCP87, of acetyl-CoA carboxylase (41). Those studies indicate that the amino-terminal region of the enzyme functions in dictating the relative specificity of the enzyme for the alternative acceptor protein substrates. However, in those studies, the physiologically relevant HCS forms, FL and 58, were not compared, and no time dependence was investigated.

2.5.4 Implications of the Distinct Rates of Association of 58-HCS and FL-HCS with p67

The most significant difference observed between FL-HCS and 58-HCS lies in the parameters describing their association with p67, with FL-HCS associating with the biotin acceptor substrate at a rate ~2-fold faster than 58-HCS. Although this difference is small, it may have consequences for the metabolic activities of carboxylases. The low biotin concentration in human tissue (nanomolar range) limits the supply of the HCS·bio-5'-AMP complex (79-80). Once the complex is formed, biotin utilization by the carboxylases depends, in part, on the efficiency with which it is transferred from the intermediate to the acceptor protein substrates. There are five biotin-dependent carboxylases present in mammalian cells that are involved in a

variety of distinct metabolic processes. A hierarchy of recognition of these carboxylases by HCS may exist, depending on how vital the reaction is to the survival of the cell. In addition, there is currently no information about the relative abundance of FL- and 58-HCS, each with its distinct rate of association with acceptor protein targets. Tissue-specific variation in the availability of the two isoforms could potentially provide a means of regulating activities of biotin-dependent carboxylases.

Other possible roles exist for distinct forms of the HCS. The function of HCS in transcription regulation is consistent with a nuclear role for the enzyme. Indeed, immunofluorescence studies indicate that the enzyme is localized to both the cytosol and the nucleus (43). The alternative HCS forms could be functionally distinct with regard to nuclear localization and, consequently, their relative significance for metabolism and transcription regulation.

In conclusion, the work presented here has established that two naturally occurring isoforms of HCS behave similarly in most respects, but they have distinct activities in biotin acceptor substrate binding, thus indicating a role for the amino-terminal amino acids in carboxylase recognition.

Chapter 3: The biotin transfer reaction across different species

The work presented in this chapter was originally published in the Journal of Biological Chemistry: Maria Ingaramo and Dorothy Beckett. Biotinylation: a post-translational modification controlled by the rate of protein:protein association. *Journal of Biological Chemistry*. 2011; 286, 13071-13078.

3.1 Abstract

Biotin protein ligases catalyze specific covalent linkage of the coenzyme biotin to biotin-dependent carboxylases. The reaction proceeds in two steps including synthesis of an adenylated intermediate followed by biotin transfer to the carboxylase substrate. In this work specificity in the transfer reaction was investigated using single turnover stopped-flow and quench-flow assays. Cognate and non-cognate reactions were measured using the enzymes and minimal biotin acceptor substrates from *E. coli*, *P. horikoshii* and *H. sapiens*. The kinetic analysis demonstrates that for all enzyme-substrate pairs the bimolecular rate of association of enzyme with substrate limits post-translational biotinylation. In addition, in noncognate reactions the three enzymes displayed a range of selectivities. These results highlight the importance of protein-protein binding kinetics for specific biotin addition to carboxylases and provide one mechanism for determining biotin distribution in metabolism.

3.2 Introduction

Post-translational protein modification is ubiquitous in biology and influences critical processes including metabolism, protein degradation and gene expression. The water soluble vitamin biotin, a required cofactor for biotin dependent carboxylases, functions as a transient carrier of carboxyl groups in their transfer from bicarbonate to small molecule metabolites, such as acetyl-CoA. The five mammalian biotin-dependent carboxylases function in gluconeogenesis, amino acid catabolism, and fatty acid synthesis and degradation (11). In its coenzyme function biotin must be covalently linked to a carboxylase in a highly specific post-translational modification reaction catalyzed by Biotin Protein Ligases (BPL). In this two-step reaction (figure 14A) an intermediate, bio-5'-AMP, is first formed from biotin and ATP substrates and the biotin is then linked via its carboxyl group to the ε amine of a specific lysine residue on the carboxylase (23). The target lysine residue is on the biotin carboxylase carrier protein (BCCP) domain of the carboxylase, an enzyme complex composed of multiple copies of BCCP, biotin carboxylase (BC), and carboxyl transferase (CT) moieties (11).

Previous studies of specificity in post-translational biotin addition are inconclusive. In any single organism, with few exceptions, only the specific target lysine on carboxylase substrates is biotinylated. Consistent with this specificity, the *Pyrococcus horikoshii* ligase:BCCP structure, in which BCCP refers to a minimal biotin accepting domain, is characterized by an extensive protein:protein interface (34). However, a lack of specificity is evident from numerous examples of interspecies biotinylation. For example, in vivo the *Escherichia coli* ligase

biotinylates BCCP domains from yeast (81), human (72), plant (82) and other bacteria (83), and the human p67, a commonly used substrate that includes propionyl-CoA carboxylase BCCP, can be biotinylated by partially purified BPLs from at least nine other organisms (38,84). This inter-species biotinylation may be attributable to the high degree of sequence conservation among ligases and BCCP domains. Alternatively, the qualitative nature of the methods used to measure inter-species reactivity may have precluded detection of selectivity in the reaction.

Comparison of BPL-BCCP pairs from *E.coli* (*Ec*), *Pyrococcus horikoshii* (*Ph*) and *Homo sapiens*, which represent three phylogenetic domains, illustrates the sequence and structural conservation among the enzymes and substrates. For example, the most disparate ligase catalytic domain sequences of *E. coli* and human (figure 14B) maintain 26 % sequence identity and 43 % similarity (85). Moreover, the structures of the catalytic domains of the *Ec* and *Ph* enzymes are nearly superimposable (24,86). Overlay of BCCP structures from the three organisms reveals that, with the exception of the "thumb" on the *E. coli* domain, they are identical (figure 15A). At the primary sequence level (figure 15B), the most disparate BCCP sequences from human and *E. coli* display 35 % identity and 54 % similarity (85).

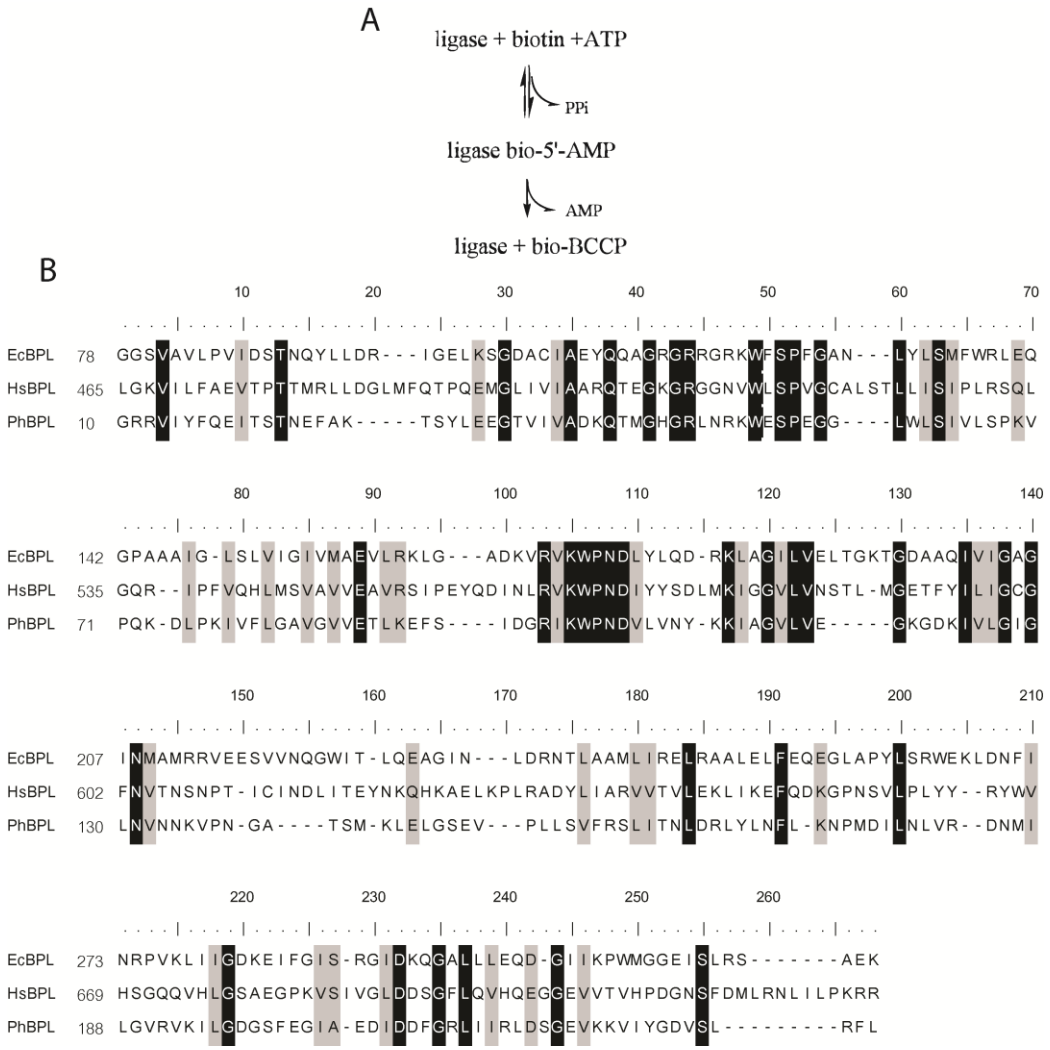

Figure 14. Ligases across evolutionary domains. A. Ligase catalyzed biotin transfer occurs in two steps in which an activated biotin intermediate is first synthesized from ATP and biotin with the release of pyrophosphate. In the second step, the biotin moiety of bio-5'-AMP is covalently attached to a specific lysine residue on BCCP. B. Alignment (87) of the *E. coli*, *H. sapiens* and *P. horikoshii* Biotin Protein Ligase catalytic domain sequences. The identities (black) and similarities (grey) are highlighted. The N-terminal domains of the *E. coli* and *H. sapiens* sequences are not shown.

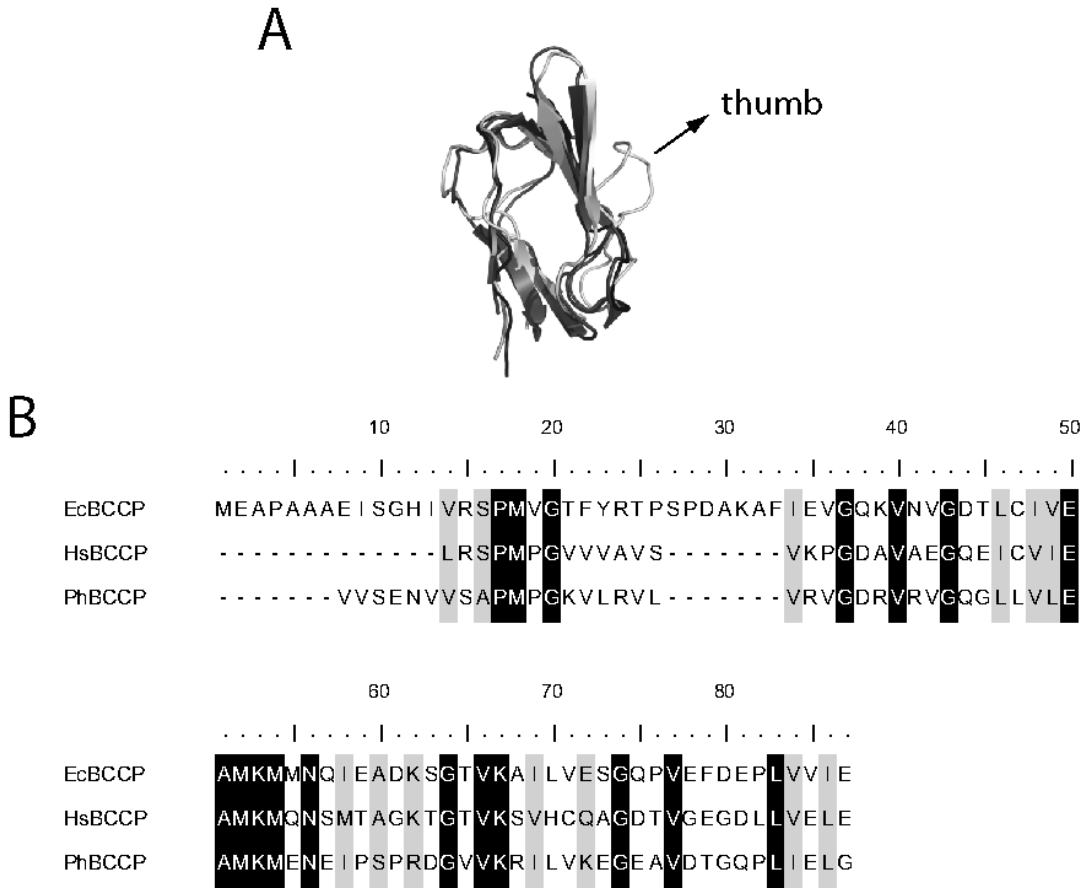

Figure 15. Alignment of structures and sequences of BCCP fragments. A. Superimposition of *Ph*BCCP (grey, 2EJG), *Hs*BCCP (dark grey, 2JKU) and *Ec*BCCP (light grey, 1A6X) structures generated with Pymol software (http://www.pymol.org). B. Sequence alignment of the three BCCPs, generated using Jalview(87-88). The working *Hs*BCCP sequence has an exogenous tyrosine residue at the N terminus, which was added in subcloning to allow for spectrophotometric protein concentration determination.

As indicated above, ligase-catalyzed biotinylation occurs in two steps and steady-state measurements with the human ligase revealed that bio-5'-AMP synthesis is the rate limiting step in the overall reaction. However, a single-turnover stopped-flow fluorescence assay in which the preformed enzyme intermediate complex is mixed with the BCCP substrate provides specific information about the ligase-acceptor protein interaction independent of the bio-5'-AMP synthesis step. Stopped-flow measurements of the *Hs*BPL catalyzed biotin transfer from the intermediate to a human BCCP substrate revealed a linear dependence of the apparent rate on substrate protein concentration with no evidence of saturation (28,32). The simplest interpretation of this kinetic behavior is that the assay reports on the bimolecular collision of the enzyme with substrate protein. However, it is not known if this is a general feature of the BPL-catalyzed reaction. Additionally, the stopped-flow measurements, which monitor the disappearance of the enzyme:intermediate complex, provide no information about product accumulation in the reaction, and, consequently, about which step limits turnover in the second half reaction.

In this work, the single turnover stopped flow and a quench flow assay that allows monitoring of product formation are applied to studies of the second step in BPL-catalyzed biotinylation. Measurements performed on three cognate enzyme-substrate pairs from *E. coli*, *P. horikoshii* and *H. sapiens* yield linear rate versus substrate concentration profiles in both assays. Furthermore, for each cognate enzyme.acceptor protein pair the bimolecular rates obtained using the stopped-flow and quench-flow assays are identical. Thus, bimolecular association of the enzyme-intermediate complex with BCCP substrate limits post-translational biotin transfer

from bio-5'-AMP to the acceptor protein. In addition, measurements performed on noncognate enzyme-substrate pairs reveal distinct levels of substrate selectivity by the three enzymes. The control of the biotin transfer rate by enzyme-substrate collision coupled with the discrimination in noncognate reactions stresses the importance of protein:protein recognition in post-translational biotin addition and has implications for control of biotin distribution in metabolism.

3.3 Experimental Procedures

3.3.1 Chemicals and Buffers

All chemicals used in buffer preparation were at least reagent grade. Bio-5'-AMP was synthesized and purified as previously described (23,63). Biotin d-[2,3,4,6-^{3}H] was purchased from American Radiolabeled Chemicals, Inc and stored under argon at -70^{o}C. Unlabeled d-biotin and ATP were obtained from Sigma-Aldrich. The ATP concentration in stock solutions, which were prepared by dissolving adenosine 5'-triphosphate disodium salt into water and adjusting the pH to 7.5, were determined by UV absorbance using an extinction coefficient at 259 nm of 15400 M cm^{-1}. Biotin solutions were prepared by dissolving the desired amount of powder in reaction buffer that had not been pH adjusted, adjusting the pH to 7.5, and bringing the solution to its final volume in a volumetric flask. The biotin stock was filtered, divided into 1 mL aliquots, and stored at -70 °C. The reaction buffer is composed of 10 mM Tris-HCl pH 7.50±0.02 at either 20 ^{o}C (*Ec*, *Hs*) or 40 ^{o}C (*Ph*), 2.5 mM $MgCl_2$, and 500 mM KCl (*Ph*) or 200 mM KCl (*Ec*, *Hs*).

3.3.2 Protein expression and purification

*Ph*BPL, *Ec*BPL and *Hs*BPL were recombinantly expressed and purified from *Escherichia coli* as previously described (31-32,89). The *E. coli* biotin acceptor substrate fragment *Ec*BCCP, which comprises the C-terminal 87 amino acids of the acetyl-CoA carboxylase BCCP subunit, was purified as in Nenortas et al. (28). All chromatographic steps were carried out on an AKTA prime FPLC platform at 4 °C (GE healthcare).

*Ph*BCCP corresponds to the 73 C-terminal amino acids of *P. horikoshii* BCCP domain of acetyl-CoA carboxylase and was expressed from a pet11-a plasmid derivative that was a generous gift from Riken (90). The plasmid was transformed into *E. coli* BL21(λDE3)-RIL strain by electroporation and selection was carried out on Luria-Bertani (LB) agar plates containing 50 µg/ml kanamycin. A 1 mL volume from a 5 mL overnight culture was diluted into 50 mL of LB media containing antibiotic and grown for 8 hours at 37°C with shaking at 250 rpm. A second 500 mL culture was started by addition of 10 mL of the previous growth and grown overnight. The final four 1 L cultures were inoculated with the previous culture at a dilution of 1:20. Protein expression was induced at an OD600 of 0.7 by addition of IPTG to 350 µM, and allowed to proceed for 2.5 hrs. Cells were harvested by centrifugation at 7000 rpm at 4 °C for 40 minutes, the pellet washed with 40 mL of lysis buffer per liter of culture, and the sample was centrifuged again for 20 minutes at 9000 rpm. The cell paste was re-suspended in twice its weight of lysis buffer (50 mM Tris, pH 7.5 at 4 °C, 500 mM NaCl, 5 % (v/v) glycerol, 0.1 mM DTT and 0.1 mM PMSF), and cells were disrupted by sonication using one minute bursts until the OD600 decreased to

less than 10 % of the original value. The lysate was diluted to 200 mL with lysis buffer and cleared of cell debris by centrifugation at 9000 rpm for 40 minutes. After adding $CaCl_2$, $MgCl_2$, DNase I and RNase, to 1mM, 2.5 mM and 0.03 mg/mL (both enzymes) final concentrations, respectively, the sample was stirred at room temperature for two hours. The solution was then heated to 90 °C for 15 minutes with stirring, cooled to room temperature, and the precipitated contaminating proteins were cleared by centrifuging at 9000 rpm for 30 minutes at 4 °C. In order to eliminate residual nucleic acid contamination PEI was added to the supernatant at a final concentration of 0.2 % (w/v), the sample was stirred at 4 °C for 15 minutes, and the precipitate was removed by centrifugation at 12000 rpm for 20 minutes. Solid ammonium sulfate was slowly stirred into the supernatant to 90 % (w/v) saturation, and precipitation was allowed to proceed overnight. The precipitate was collected by centrifugation at 12000 rpm for 1.5 hrs, and re-suspended in 30 mL of 50 mM Tris, pH 7.5 at 4 °C, 5 % (v/v) glycerol. This sample was dialyzed against 2 mM potassium phosphate buffer, pH 7.0, 5 % (v/v) glycerol and loaded on a hydroxyapatite column (Pall Lifesciences). The flow-through was collected, dialyzed against storage buffer (10 mM Tris, pH 7.5 at 4 °C, 200 mM KCl, 5 % (v/v) glycerol), and stored in aliquots at -70 °C. Since the *Ph*BCCP does not possess tryptophan or tyrosine residues, the stock concentration was determined by comparing the density of the bands from dilutions electrophoresed on a 20 % acrylamide-SDS-tricine gel against bands with known amounts of *Ph*BCCP (71). Lanes with known amounts of *Ph*BCCP were obtained by loading dilutions of a *Ph*BCCP desalted ‘standard’ solution, the concentration of which had been

determined in triplicate by quantitative amino acid analysis at the protein facility of the Iowa State University. Band density quantitation was performed using a Molecular Dynamics Laser Scanning Personal Densitometer (GE Healthcare) and ImageQuant software.

The *Hs*BCCP fragment corresponds to C-terminal 67 amino acids of the BCCP domain of propionyl-CoA carboxylase. In order to facilitate removal of the histidine tag and eliminate any exogenous residues originating from the vector, the p67 sequence from a pDEST17 derivative (a generous gift from Dr. Roy Gravel) was subcloned into pSUMO-pro (LifeSensors) (67). A tyrosine residue was added at the N-terminus to allow for concentration determination using uv absorption spectroscopy. The plasmid encoding the SUMO-*Hs*BCCP fusion was introduced into *E. coli* strain Rosetta (DE3) by electroporation, and transformants were selected by growth on LB agar containing 34 µg/ml chloramphenicol and 100 µg/ml ampicillin. A single colony was transferred to 5 mL of LB media supplemented with antibiotics and grown for 8 hrs with shaking at 37 °C. A 1:100 dilution was performed to initiate a 50 mL overnight culture and one liter cultures were inoculated with 20 mL of the overnight culture, grown at 37 °C, and protein expression was induced at an OD600 of 0.8 by addition of lactose to 0.5 % (w/v). Following overnight growth at 30 °C, cells were harvested by centrifugation at 4500 rpm at 4 °C, re-suspended in a volume of lysis buffer corresponding to five times the cell pellet weight, and lysed by sonication in *Hs*BCCP lysis buffer (50 mM sodium phosphate buffer, pH 8, 300 mM sodium chloride, 10 mM imidazole, 5 % (v/v) glycerol, 3 mM 2-mercaptoethanol, 1 mM PMSF). The crude lysate was cleared by centrifugation at 9000 rpm for 30

minutes at 4 °C, and the supernatant was subjected to chromatography on 8 mL Ni-NTA resin (Qiagen) packed in a 1.5 x 10 cm econo-column (BioRad) according to the manufacturer's instructions. The eluted protein was dialyzed against 10 mM sodium phosphate, pH 8.0, 60 mM NaCl, 5 % (v/v) glycerol, 5 mM 2-mercaptoethanol, and digested overnight at room temperature with SUMO-protease-1. In order to remove the protease, the his_6-SUMO tag and undigested protein, the sample was passed through Ni-NTA resin. The flow through was collected and dialyzed against 50 mM Tris pH 7.5 at 4 °C, 20 mM KCl, 1 mM 2-mercaptoethanol, 5 % (v/v) glycerol. The resulting sample was loaded onto a 8 ml DEAE anion exchange (GE Healthcare) column and eluted with a linear gradient of 20-400 mM KCl (VT=200 mL) at a flow rate of 2 ml/min. The pooled fractions (2 ml each) containing *Hs*BCCP were concentrated and loaded at 0.1 ml/min onto a 150 ml S-100 Sephacryl resin (GE Healthcare) packed in a 1.5 x 100 cm econo-column (BioRad) and equilibrated with 10 mM Tris, pH 7.5 at 4 °C, 0.8 M KCl, 5 mM 2-mercaptoethanol, 5 % (v/v) glycerol. The eluted sample was exchanged into 10 mM Tris-HCl, pH 8 at 4 °C, 200 mM KCl and 5 % (v/v) glycerol by dialysis and stored at –70 ^{o}C. The yield was 10 mg of protein per liter of bacterial culture and the concentration was determined spectrophotometrically using an extinction coefficient of 1450 M cm^{-1} at 276 nm (64).

3.3.3 Stopped flow measurements of biotin transfer

Biotin transfer was measured by monitoring the intrinsic fluorescence increase that occurs upon rapid mixing the enzyme.intermediate complex with the substrate biotin acceptor protein (28,32). A solution of 1-2 μM ligase was incubated with half

its concentration of biotin and 500 μM ATP for 20 minutes to allow for bio-5'-AMP synthesis. In order to avoid the complication from the large fluorescence change that accompanies ATP binding to the enzyme, *Ph*BPL catalyzed reactions were carried out using chemically synthesized bio-5'-AMP (31). Reactions catalyzed by the human and *E. coli* enzyme were carried out in standard reaction buffer, which contains 10 mM Tris, pH 7.5 at 20 °C, 200 mM KCl, 2.5 mM $MgCl_2$. In contrast, those reactions catalyzed by *Ph*BPL were performed at pH 7.5, 40 °C and a KCl concentration of 500 mM. The higher salt concentration and temperature are necessary to obtain complete activity of the thermophilic enzyme (31), a reflection of the fact that *P. horikoshii* intracellular salt concentration is about 500 mM, and the organism grows optimally at 98 °C (91). Each ligase-intermediate complex solution was rapidly mixed with varying concentrations of BCCP using a Kintek SF-2001 stopped flow instrument equipped with fluorescence detection. The excitation wavelength was 295 nm and fluorescence emission was monitored above 340 nm using a cutoff filter (Corion Corp.). At least six traces spanning 10 half-lives were collected at each BCCP concentration. The resulting transients were fit to an appropriate model (single or double exponential), and the apparent rates were plotted as a function of BCCP concentration. Further analysis and interpretation were performed as described in the Results section.

3.3.4 Quench flow measurements of biotin incorporation

Single turnover measurements of enzyme-catalyzed biotin transfer to the BCCP fragments was monitored as a function of time using a Kintek QF-3 quench flow apparatus. One syringe contained a solution of 1 μM ligase, 0.463 μM biotin, 37

nM ^{3}H-biotin, and 500 µM ATP that had been incubated for 30 minutes at the working temperature to allow for bio-5'-AMP synthesis. The second syringe contained variable concentrations of each BCCP fragment, ranging from 10 to 200 µM. All samples were prepared in the appropriate working buffer. Equal volumes of the two syringe solutions were mixed and the resulting reactions were allowed to age for a specific amount of time, after which they were quenched with a 2 M HCl solution. Free and BCCP incorporated biotin were separated using TCA precipitation (50). In reactions containing *Ph*BCCP, 0.02% (w/v) deoxycholate was included, in addition to BSA (0.1 mg/mL), to aid in precipitation. The samples were spotted on dried Whatman 3MM squares to which 200 µl of 800 µM unlabeled biotin had been added after soaking in 10 % TCA. After drying, the papers were washed twice in batch mode in 250 ml of ice cold 10 % TCA and once in 100 ml of cold ethanol. The radioactivity retained on the filters was quantified in a LS6500 Beckman counter using ReadyProtein^{+} (Beckman) scintillation fluid. Background corrections were performed with values obtained from control reactions that contained no BCCP. Correction for precipitation efficiency (typically above 80 %) and conversion from dpm to "µM biotin" were carried out using the relation between dpm and µM obtained from the precipitation of a reaction incubated for 30 minutes in order to allow for quantitative ^{3}H incorporation. Each discontinuous transient was fit to a single exponential equation and the resulting apparent rates as a function of BCCP concentration were subjected to linear least squares analysis. The slope of the line yielded the rate of biotin incorporation.

3.4 Results

3.4.1 Oligomeric states of the reacting species in biotin transfer

Interpretation of kinetic and binding data requires knowledge of the assembly states of all species participating in a reaction. The oligomerization properties of the three biotin protein ligases have previously been characterized using sedimentation equilibrium. The human ligase is monomeric in both its unliganded and liganded forms (32). By contrast, the *Pyrococcus horikoshii* ligase is a constitutive dimer (31). However, in the dimer the active sites for biotin transfer are available for interaction with the acceptor substrate (34). The *E. coli* enzyme can also form a homo-dimer, albeit in a reaction that depends on the intermediate in biotin transfer, bio-5'-AMP (70). Furthermore, the surface utilized for the homo-dimerization is identical to that used for hetero-dimerization with the biotin acceptor protein (92). The equilibrium dissociation constant governing homo-dimerization reaction in buffer conditions identical to those used in the present studies is approximately 10 μM (70). Consequently, in order to avoid any complication from this competing homo-dimerization reaction, all kinetic measurements in these studies were performed at a total enzyme concentration of 0.5 μM.

The assembly states of the three acceptor protein substrates employed in these studies were also characterized by sedimentation equilibrium. The *Ec*BCCP has previously been shown to be monomeric over a broad concentration range (28). For this work, sedimentation equilibrium measurements were performed on *Hs*BCCP and *Ph*BCCP (data not shown). Global analysis of the data obtained at three loading

concentrations and two speeds using a single species model yielded molecular weights for the proteins consistent with monomers

3.4.2 Single turnover assays of the second half reaction in biotin transfer

This work is focused on the interaction of the ligase with the biotin acceptor protein in post-translational biotinylation. Since the rate-determining step in the overall reaction is intermediate synthesis, steady state measurements provide limited information about this protein:protein interaction. However, the reaction proceeds through a double displacement mechanism that can be halted after formation of the kinetically stable ligase.bio-5'-AMP complex (Figure 14). Mixing of the preformed complex with BCCP allows monitoring of the second half reaction independent of the first.

3.4.3. Biotin transfer rates to cognate substrates are similar for the three Biotin Protein Ligases

In these experiments, BPL is pre-incubated with biotin at half of the enzyme concentration and excess ATP to allow for bio-5'-AMP synthesis. The BPL excess over biotin ensures that only one turnover of biotin transfer occurs in the stopped-flow measurement. Mixing of the pre-formed complex with BCCP yields a time-dependent increase in the intrinsic fluorescence (Figure 16A), that has been shown through measurements of the spectra of the two species to be consistent with conversion of the bio-5'-AMP-bound enzyme to the free enzyme (28,32).Transients acquired upon mixing the ligase-bio-5'-AMP complex at each BCCP concentration were fit to either a single or double exponential model to obtain apparent rates. For

example, the transient shown in Figure 16A, which was obtained by mixing *Hs*BCCP-bio-5'-AMP with 200 μM *Hs*BCCP, contains two well-separated exponential phases. While both the human and *E. coli*-catalyzed reactions displayed this biphasic behavior at higher BCCP concentrations, all *Ph*BCCP traces were monophasic.

Plots of the faster apparent rate versus biotin accepting substrate concentration for all three cognate ligase.substrate pairs were linear and showed no evidence of saturation (Figure 16B). Consequently, the slope of each line is interpreted as reporting on k_1, or BCCP association with the ligase-bio-5'-AMP complex, in the following mechanism:

$$\text{BPL·bio-5'-AMP + BCCP} \underset{k_{-1}}{\overset{k_1}{\rightleftharpoons}} \text{BPL·bio-5'-AMP·BCCP} \xrightarrow{k_2} \text{BPL + bio-BCCP + AMP}$$

The bimolecular association rates for the three BPLs with their cognate substrates (Table 4), obtained from linear regression of the apparent rate versus BCCP concentration profiles (Figure 16B), reveal that all three reactions are characterized by bimolecular association rates on the order of 10^4 $M^{-1}s^{-1}$. However, the human system displays the fastest rate.

For reactions that exhibited two exponentials, the rate of the slower phase exhibited no dependence on BCCP concentration, which supports its assignment to holo-BCCP dissociation from the ligase (28). The rates of *Hs*BPL and *Ec*BPL dissociation from their cognate holoBCCPs are both approximately 0.2 s^{-1} (Table 4).

Table 4: Biotin transfer rates for cognate ligase-BCCP pairs.

	Stopped-flow [a]	Quench-flow [b]
	($x10^4$ $M^{-1}s^{-1}$)	($x10^4$ $M^{-1}s^{-1}$)
*Hs*BPL	3.5 ± 0.3	3.1 ± 0.3
*Ec*BPL	1.15 ± 0.07	1.05 ± 0.08
*Ph*BPL	1.50 ± 0.06 [c]	1.5 ± 0.1 [c]

[a.] The errors represent the standard deviation of three independent stopped-flow experiments. [b.] The errors correspond to the standard deviation of results obtained in two independent quench flow experiments. [c.] Measurements with *Ph*BPL were carried out at 40 °C, in 10 mM Tris, pH 7.5, 500 mM KCL, 2.5 mM $MgCl_2$. All other experiments were performed at 20 °C, in 10 mM Tris, pH 7.5, 200 mM KCL, 2.5 mM $MgCl_2$

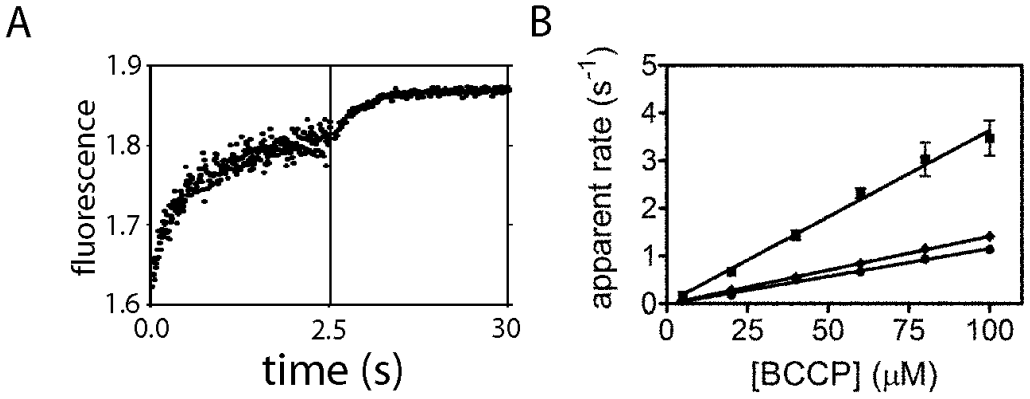

Figure 16. Stopped flow measurements of biotin transfer for cognate ligase-BCCP pairs. A. Stopped flow fluorescence trace obtained upon 1:1 (vol/vol) mixing 1 μM *Hs*BPL, 0.5 μM biotin, 0.5 μM ATP with 200 μM *Hs*BCCP. Data was collected with an equal number of points in two time windows in order to better capture the two exponential behavior. The solid line represents the best-fit of the data to a double exponential model. B. Plots of the dependence of the apparent rate of biotin transfer on BCCP concentration: (■) *Hs*BPL-*Hs*BCCP, (♦) *Ph*BPL-*Ph*BCCP, (·) *Ec*BPL-*Ec*BCCP. The data points represent the average of the apparent rate measured at each BCCP concentration in three independent experiments with standard deviations shown as error bars. The solid lines represent the best-fits of the rate versus concentration profiles to a linear equation.

3.4.4. Product formation is limited by bimolecular association of enzyme with substrate

The stopped flow assay reports on the disappearance of the ligase.bio-5'-AMP complex but provides no information on product accumulation in the second half reaction. Consequently, a quench flow assay was developed to quantify the production of biotinylated BCCP.

In the assay the reactants are prepared similarly to those used in the stopped flow experiments, with the exception that the cold biotin is spiked with tritium-labeled biotin. Once sufficient time has elapsed for bio-5'-AMP synthesis, an aliquot of the ligase-intermediate complex solution is rapidly mixed with BCCP. After aging for the appropriate time interval, the reaction is quenched by decreasing the pH. This low pH also destroys the non-covalent ligase-bio-5'-AMP complex while leaving the covalent amide linkage between biotin and BCCP intact. In contrast to the stopped-flow assay, the quench-flow assay of biotin transfer is discontinuous. Therefore, the transient acquired at each BCCP concentration (Figure 17A) results from multiple measurements in which reactions prepared at a given acceptor protein concentration are aged for variable amounts of time prior to quenching. Separation of free biotin from biotinylated BCCP is achieved using a modification of the TCA precipitation method previously used in steady state kinetic measurements performed on *Ec*BPL (50). The TCA precipitates BCCP and holo-BCCP, but not free biotin or bio-5'-AMP. Quantitation of the radioactivity in the acid insoluble material by scintillation counting yields information on the amount of biotin incorporated at a specific time, and ultimately a transient (Figure 17A). Transients for all cognate enzyme-substrate

pairs are well-described by a single exponential model, further supporting the assignment of the slow rate observed in the stopped flow traces with *Hs*BPL and *Ec*BPL to the enzyme-product dissociation rate. Plots of the apparent rates obtained from the transients versus BCCP concentration are linear and reveal no evidence of saturation (Figure 17B). Furthermore, for all three enzymes the rates obtained from the slopes of the lines are identical to the bimolecular association rates obtained from the stopped flow measurements (Table 4). Thus, for all cognate pairs, the rate of bimolecular association of enzyme with substrate limits accumulation of the biotinylated acceptor protein.

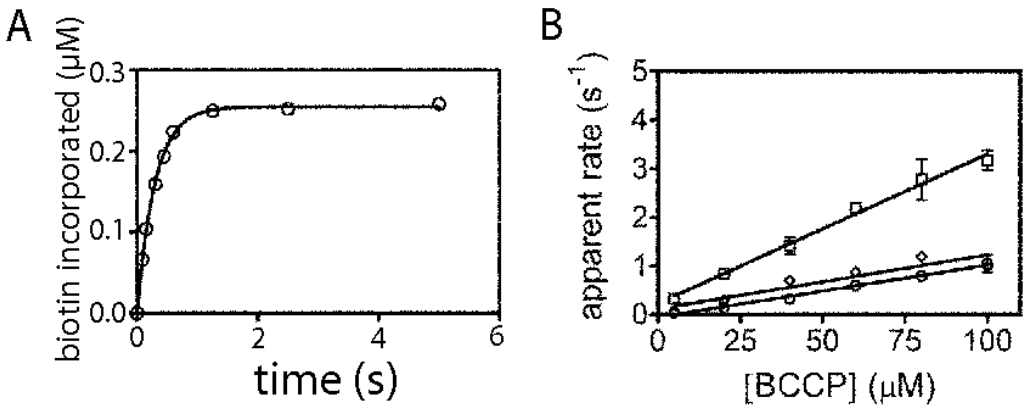

Figure 17. Quench flow measurements of biotin transfer for cognate ligase-BCCP pairs. A. Transient obtained upon mixing in equal parts 1 μM *Hs*BPL, 0.5 μM biotin, 0.5 μM ATP against 200 μM *Hs*BCCP. The solid line represents the best-fit of the data to a single exponential model. B. Plots of apparent rate versus substrate concentration for: (□) *Hs*BPL-*Hs*BCCP, (◊) *Ph*BPL-*Ph*BCCP, (○) *Ec*BPL-*Ec*BCCP. The data points represent the average of the apparent rate measured at each BCCP concentration in two independent experiments with standard deviations shown as error bars. The solid lines represent the best-fits of the rate versus concentration profiles to a linear equation.

3.4.5 Measurements of biotin transfer to noncognate acceptor proteins indicate substrate specificity

The specificity of biotin transfer was investigated by performing stopped-flow experiments with each BPL and non-cognate substrates (Table 5). Like the cognate reactions, noncognate biotin transfer yielded linear apparent rate versus substrate concentration profiles. The bimolecular association rates obtained from linear regression of the data span a large range, from undetectable to 43000 $M^{-1}s^{-1}$ with the fastest rate observed for *Ph*BPL-catalyzed biotin transfer to *Hs*BCCP, a non-cognate substrate. The only enzyme capable of biotinylating all three BCCP substrates is *Ph*BPL. No time-dependent change in the fluorescence signal is observed upon mixing either *Hs*BPL or *Ec*BPL with *Ph*BCCP, consistent with the absence of biotin transfer. This result was confirmed by MALDI-ToF MS analysis of reactions containing either the human or *E. coli* ligase and *Ph*BCCP (data not shown).

Table 5: Stopped-flow measurements of biotin transfer rates for cognate and non-cognate ligase-BCCP pairs.

	*Hs*BCCP[a]	*Ec*BCCP[a]	*Ph*BCCP[a]
	($x10^4 M^{-1}s^{-1}$)	($x10^4 M^{-1}s^{-1}$)	($x10^4 M^{-1}s^{-1}$)
*Hs*BPL	3.5 ± 0.3 (0.23 ± 0.02)[b]	0.027 ± 0.004	N.D. [c]
*Ec*BPL	3.2 ± 0.2 (0.33 ± 0.03)[b]	1.15 ± 0.07 (0.21 ± 0.02)[b]	N.D. [c]
*Ph*BPL	4.3 ± 0.5 [d]	0.42 ± 0.03 [d]	1.5 ± 0.6 [d]

[a.] The errors correspond to the standard deviation of three independent stopped flow experiments. [b.] BCCP dissociation rate, in s^{-1}. [c.] N.D., Not Detectable. [d.] Measurements with *Ph*BPL were carried out at 40 °C, in 10 mM Tris, pH 7.5, 500 mM KCL, 2.5 mM $MgCl_2$. All other experiments were performed at 20 °C, in 10 mM Tris, pH 7.5, 200 mM KCL, 2.5 mM $MgCl_2$

For all cognate BPL.BCCP pairs the stopped-flow and quench-flow assays of biotin transfer from bio-5'-AMP yield identical results. In order to determine if this is true for noncognate reactions, quench flow measurements of *Ph*BPL-catalyzed transfer to noncognate substrates were performed. The *Ph*BPL was chosen for this comparison because of its ability to catalyze biotin transfer to all three BCCP substrates. Results of quench flow measurements indicate holoBCCP accumulation rates identical to the rates of enzyme.intermediate depletion measured by stopped-flow (Figure 18, Table 6). Thus, even with non-cognate substrates, bimolecular enzyme-substrate association limits the rate of biotin transfer from the intermediate to the BCCP substrate.

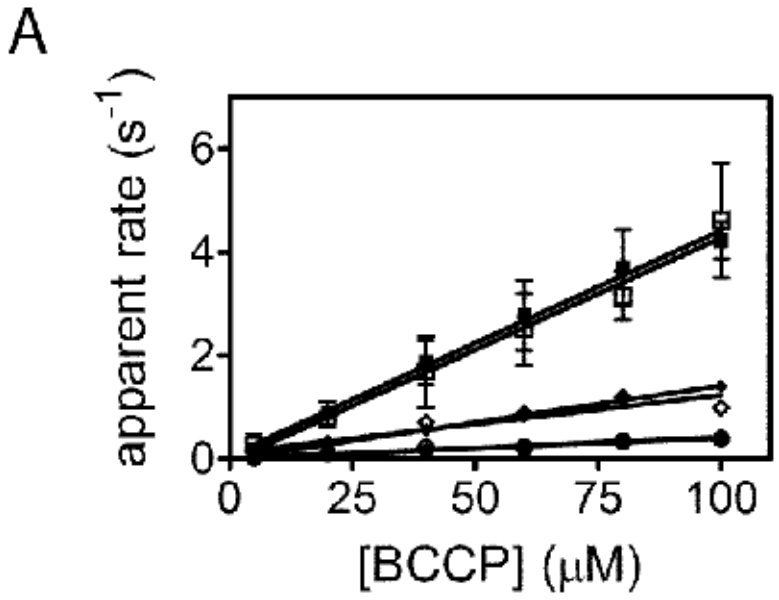

Figure 18. Stopped flow and quench-flow measurements of *Ph*BPL-catalyzed biotin transfer to cognate and non-cognate substrates. Rate versus concentration profiles obtained by stopped-flow for (■) *Hs*BCCP, (♦) *Ph*BCCP, and (·) *Ec*BCCP and quench-flow flow for (□) *Hs*BCCP, (◊) *Ph*BCCP and (○) *Ec*BCCP. The solid lines were obtained from linear regression of the data.

Table 6: Rates of *Ph*BPL-catalyzed biotin transfer

	Stopped-flow [a]	Quench-flow [b]
	($M^{-1}s^{-1}$)	($M^{-1}s^{-1}$)
*Hs*BCCP	4.3 ± 0.5	4.2 ± 0.7
*Ec*BCCP	0.420 ± 0.03	0.4 ± 0.1
*Ph*BCCP	1.50 ± 0.06[c]	1.5 ± 0.1[c]

[a.] The errors represent the standard deviation of three independent stopped-flow experiments. [b.] The errors correspond to the standard deviation of results obtained in two independent quench flow experiments. [c.] Measurements with *Ph*BPL were carried out at 40 °C, in 10 mM Tris, pH 7.5, 500 mM KCL, 2.5 mM $MgCl_2$. All other experiments were performed at 20 °C, in 10 mM Tris, pH 7.5, 200 mM KCL, 2.5 mM $MgCl_2$

3.5 Discussion

The structural and energetic basis of the specific enzyme-catalyzed post-translational biotin addition is not known. Previous steady-state measurements with *Hs*BPL indicated that the first step, bio-5'-AMP synthesis, is the rate limiting step in the two-step reaction (32). In this work the second half reaction in biotin transfer was measured independent of the first using single turnover stopped-flow and quench-flow assays. The measurements performed on ligases and substrates from three different organisms demonstrate that rate of bimolecular association of enzyme with substrate limits post-translational biotin addition. Furthermore, measurements on noncognate enzyme substrate pairs reveal specificity in post-translational biotin addition.

The stopped-flow measurements of biotin transfer from the bio-5'-AMP to BCCP, which monitors disappearance of the enzyme.intermediate complex, provides information about bimolecular association of enzyme with substrate for all ligase/BCCP pairs. This conclusion is based on the observed linear dependencies of the apparent rates on BCCP concentration. In order to obtain values for the rate of the chemistry of biotin transfer, a quench flow assay for the second half reaction, in which product holoBCCP formation is monitored, was applied to the three ligase-BCCP systems. The linear dependencies and resulting bimolecular rate constants obtained with this assay are identical those obtained using the stopped-flow assay. Therefore, for all three cognate BPL-BCCP pairs the chemistry of biotin transfer from the intermediate to acceptor protein is limited by the enzyme-substrate association

rate. As indicated by measurements performed using *Ph*BPL and the non-cognate BCCP substrates, this is also true for reactions involving non-cognate pairs.

The three enzymes display association rates with their cognate substrates of 1-5x104 $M^{-1}s^{-1}$, values that are well within range of the commonly observed association rates for protein-protein interactions (93). The rates also agree with previous measurements of the *Ec*BPL-*Ec*BCCP interaction performed in the same substrate concentration range (28). In addition, the results obtained with the human system are comparable to those previously obtained with p67, a biotin acceptor substrate that contains in addition to the *Hs*BCCP sequence some "extra" residues originating from the vector sequence (32). However, the measured association rate with p67 was only twofold slower than that measured for *Hs*BCCP.

Measurements performed with non-cognate substrates indicate that *Ph*BPL, which biotinylates the two non-cognate substrates at rates comparable to the cognate reaction, is the least discriminating of the three enzymes. By contrast, neither the *Hs*BPL nor *Ec*BPL can transfer biotin to *Ph*BCCP. The human enzyme, which fails to biotinylate *Ph*BCCP and reacts with the *E. coli* substrate with a slow rate of $3x10^2$ $M^{-1}s^{-1}$, is the most discriminating of the three ligases. Precedent for such slow bimolecular protein:protein association rates exist including a value of approximately 2 $M^{-1}s^{-1}$ measured for the binding of the p66 and p51 subunits of HIV reverse transcriptase (94).

Previous studies provide limited information on the structural features that are important for substrate recognition by biotin protein ligases. In the

*Ph*BPL.*Ph*BCCP complex structure the interface is characterized by multiple hydrogen bonds mediated by backbone residues as well as numerous van der Waals contacts. Functional studies of both *E. coli* BCCP and ligase variants have also been performed. Mutational studies on *E. coli* BCCP revealed that, in addition to the target lysine, a glutamic acid at position 119 is important for recognition (50). In the *E. coli* ligase several surface loops are proposed to function in BCCP recognition. Functional studies of *Ec*BPL variants at amino acids R116, R119, and A147 confirm the importance of three of these loop residues for the process (52). In addition to the catalytic domain, the human ligase is characterized by a ~450 amino acid N-terminal extension, which has been shown to both influence the association rate with p67 (32) and to directly interact the BCCP domain of Acetyl CoA carboxylase II (42). Additional studies to elucidate the structural origins of the range of bimolecular association rates exhibited by the BPL.BCCP pairs are in progress.

The control of biotin transfer by enzyme-BCCP association has potential biological consequences. First, consider any single organisms such as *H. sapiens* in which there are multiple biotin-dependent carboxylases. *In vivo* biotin concentrations are in the low nanomolar range (80) and, therefore, there is a limited amount of BPL.bio-5'-AMP. Therefore, the carboxylase that associates most rapidly with the enzyme-intermediate complex should acquire the greatest portion of the available biotin. The association rate should depend on both the intrinsic bimolecular rate constant for a ligase-carboxylase pair and on the carboxylase substrate concentration. Thus, the relative intracellular apo-carboxylase concentrations should be an important factor in determining biotin distribution in metabolism. The observed

collision-controlled reaction is also important for bifunctional ligases such as *Ec*BPL, which, in addition to forming the hetero-dimer with BCCP, homo-dimerizes to regulate transcription. Since a single surface on the ligase-intermediate complex is utilized for the both dimerization reactions (92), the two are mutually exclusive. However, homo-dimerization is governed by an association rate that is much slower than hetero-dimerization (27,29). This gives rise to a competition between hetero- and homo- dimerization in which kinetic preference is given to biotin transfer to BCCP. Only after the unbiotinylated BCCP pool has been depleted and metabolic demand for biotin is satisfied does the enzyme-intermediate complex linger sufficiently long to allow homo-dimerization and transcription repression.

This work quantitatively demonstrates specificity of post-translational biotin addition to BCCP substrates. This specificity exists in spite of the high degree of evolutionary conservation of sequence and structures in both ligases and BCCP substrates. In addition, the measurements indicate that the association of ligases with biotin acceptor substrate limits the biotinylation reaction rate. Together, the results highlight the importance of protein-protein interactions in post-translational biotinylation, and provide a mechanism for determining the distribution of biotin in carboxylases and, therefore, in metabolism.

Chapter 4: Biotin transfer to the five mammalian biotin dependent carboxylases

4.1 Abstract

Human Holocarboxylase Synthetase (HCS) catalyzes transfer of the vitamin biotin to the biotin carboxyl carrier protein (BCCP) domain of five biotin dependent carboxylases. The carboxylases comprise acetyl-CoA carboxylases 1 and 2 (ACC1 and ACC2), pyruvate carboxylase (PC), 3-methylcrotonyl-CoA carboxylase (MCC) and propionyl-CoA carboxylase (PCC). The reaction is catalyzed in two steps. First, an activated intermediate, bio-5'-AMP, is synthesized from biotin and ATP. The second step involves covalent linkage between the biotin moiety and a specific lysine residue on the carboxylase.

To address whether HCS displays selectivity among the BCCP domains of the five carboxylases, the biotin transfer reaction was investigated using single turnover stopped-flow and quench-flow assays. HCS catalyzed biotin transfer to minimal biotin acceptor BCCP fragments corresponding to the five carboxylases was measured. The results demonstrated that biotinylation of the BCCP fragments of the mitochondrial carboxylases PCC, PC, and MCC was fast and limited by the bimolecular association rate of the enzyme with the BCCP substrates. In contrast, biotinylation of the BCCP fragments of ACC1 and ACC2, to which HCS has continuous access from the cytoplasm, was slow and displayed a hyperbolic dependence on BCCP concentration. The correlation between HCS accessibility to

the biotin acceptor substrate and the rates of biotinylation suggests that mitochondrial carboxylase sequences have evolved to produce fast association rates with HCS in order to ensure biotinylation of the carboxylases before mitochondrial import. In addition, the results suggest an important role for the ligase specificity in dictating biotin distribution among carboxylases.

4.2 Introduction

Post-translational modifying enzymes must have specificity towards their intended targets, but at the same time be promiscuous enough to allow interaction with several partners. Biotin attachment is a post-translational modification essential for biotin-dependent carboxylase function. In mammalian cells, biotin linkage is catalyzed in a stepwise fashion by Human Holocarboxylase Synthetase (HCS):

$$\text{HCS} + \text{biotin} + \text{ATP} \longrightarrow \text{HCS} \cdot \text{bio-5'-AMP} + \text{PPi}$$

$$\text{HCS} \cdot \text{bio-5'-AMP} + \text{apo-carboxylase} \rightleftharpoons \text{HCS} + \text{holo-carboxylase} + \text{AMP}$$

In the first step an activated intermediate, bio-5'-AMP, is synthesized from biotin and ATP, with the release of pyrophosphate. The second step involves covalent attachment of the biotin moiety to a specific lysine residue on the biotin carboxyl carrier protein (BCCP) domain of a carboxylase(23). There are at least three HCS variants present in mammalian cells, but only two arise from differential splicing of the mRNA(38,40,57). The full length variant (FL-HCS) is comprised of 726 amino

acids and a shorter isoform corresponds to a protein that is lacking the first 57 amino acids (58-HCS).

In mammalian cells, there are five carboxylases that require post-translational biotin addition by HCS(11). Acetyl-CoA carboxylase 1 (ACC1) is a cytosolic enzyme that is involved in fatty acid synthesis by catalyzing the conversion of acetyl-CoA to malonyl-CoA. Acetyl-CoA carboxylase 2 (ACC2) catalyzes the same reaction as ACC1, but is the product of a different gene. It is involved in fatty acid oxidation, and localizes to the cytosolic side of the mitochondrial membrane. Propionyl-CoA carboxylase (PCC) synthesizes S-methylmalonyl CoA from propionyl-CoA. This mitochondrial enzyme is part of the odd fatty acid synthesis pathway, and is also involved in isoleucine, threonine, methionine and valine catabolism. Pyruvate carboxylase (PC) also localizes to the mitochondrial matrix and carboxylates pyruvate to produce oxaloacetate, a reaction necessary for gluconeogenesis. Finally, mitochondrial methylcrotonoyl-CoA carboxylase (MCC) converts 3-methylcrotonoyl-CoA to 3-methylglutaconyl-CoA, a reaction that is part of the leucine degradation pathway.

It has been demonstrated previously that FL-HCS discriminates among BCCP substrates from different species(95). In previous experiments, single turnover assays that monitored biotin transfer independently of bio-5'-AMP synthesis were used. This was necessary because comparison of steady state parameters for the overall reaction with the rate of bio-5'-AMP synthesis indicated the rate limiting step in the overall reaction was synthesis of the intermediate(28,32). HCS biotinylated the BCCP domain of PCC, did not biotinylate the BCCP domain from an archeal organism, and

it slowly biotinylated that from *E. coli(95)*. However, HCS selectivity of biotin transfer to the endogenous, biologically relevant substrates is unknown.

In order to investigate HCS substrate specificity among mammalian carboxylases, a single turnover assays were used to determine the rates of biotin transfer by FL- and 58-HCS to the BCCP domains of ACC1, ACC2, PC, PCC and MCC (Figure 19A). Biotin transfer rates to the BCCP domains of the mitochondrial carboxylases PC, PCC and MCC were faster than transfer to ACC1 and ACC2. In addition, the apparent rate vs concentration profiles were strikingly different. While the BCCP fragments of MCC, PC and PCC displayed a linear dependence of the apparent rate on substrate concentration, the BCCP fragments of ACC1 and ACC2 yielded a hyperbolic dependence, suggesting a difference in the identity of the rate limiting step for these two substrates. The different behavior correlated with the carboxylase localization, since ACC1 and ACC2 are continuously accessible to HCS in the cytoplasm, while the remaining carboxylases are transported into the mitochondria. A model consistent with these observations is proposed, whereby HCS biotinylates PC, PCC and MCC at a faster rate because these enzymes are only transiently present in the cytoplasm and they must be post-translationally modified before they reach their final destination. In addition, the data suggest a molecular mechanism for the establishment of a hierarchy that determines biotin distribution among carboxylases based on the rates of bimolecular association and carboxylase abundance.

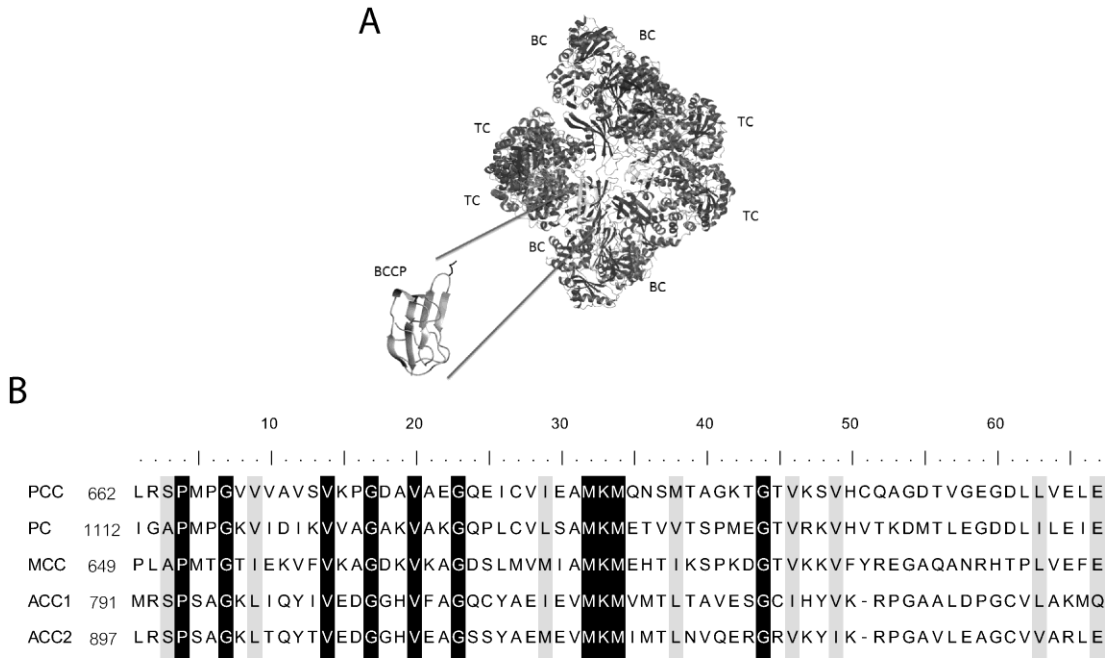

Figure 19. Mammalian biotin dependent carboxylases A. The PC BCCP fragments used for these studies are shown in the context of the whole biotin dependent carboxylase. All the carboxylases display complex assembly states and have multiple copies of the BCCP domains. The figure was generated using MolMol and the 3BG5 pdb file, which contains coordinates for *Staphylococcus aureus* PC carboxylase. B. ClustalW multiple sequence alignment of the minimal biotin acceptor domains of the five mammalian biotin-dependent carboxylases, highlighting residues that are similar (gray) or identical (black). The biotin acceptor lysine lies in the conserved MKM sequence.

4.3 Experimental procedures

4.3.1 Chemicals and biochemicals

All chemicals used were at least reagent grade. The concentration of the biotin stock was prepared by dissolving a carefully weighted amount of d-biotin (Sigma) powder in reaction buffer, adjusting the pH to 7.5, and bringing up the final desired volume in a volumetric flask. After filtering through 0.22 µm syringe filter units (Millipore), 1 ml aliquots were stored at -70 °C. In order to avoid problems

related to biotin solubility the concentrations of the prepared stocks were always lower than 850 µM. The d-Biotin (8,9-^{3}H(N)) (PerkinElmer) was aliquoted and stored under argon gas in sealed containers at -70 °C. The ATP stock was prepared by dissolving the ATP powder (sigma) in water and adjusting the pH to 7.5 with sodium hydroxide. The stock concentration was determined by UV absorbance using an extinction coefficient of 15400 $M^{-1}cm^{-1}$ at 259 nm, and stored in 0.5 ml aliquots at -70 °C. The concentrations of the enzymes and the biotin acceptor substrates were determined from their UV absorption spectra using extinction coefficients calculated according to the method of Gill and Von Hippel(64).

4.3.2 Sequence composition and cloning

The SUMO fusion plasmid used to purify the 67 amino-acid long C-terminal region of PCC carboxylase was described previously. This minimal biotin acceptor fragment corresponds to the 67 amino acids of the BCCP domain described by Leon del Rio (residues 662-728), preceded by an additional exogenous N-terminal tyrosine introduced to aid in protein concentration determination by UV spectroscopy(67,72,96). ClustalW multiple sequence alignment of the PCC BCCP minimal acceptor sequence with those of the remaining carboxylases aided in the selection of the corresponding regions of MCC, PC, and the ACC2 (Figure 19B). The coding regions for PC (residues 1112-1178), MCC (residues 649-715) and ACC2 (residues 897-962) BCCP fragments were cloned into the SUMOpro vector (LifeSensors) to yield constructs with a cleavable N-terminal $_{6}$his-SUMO tag. The fragment sequences were amplified using taq polymerase (Invitrogen) with PCR primers that introduced Eco31I (Fermentas) sites. In addition, in order to facilitate

concentration determination the amplification primers for PC BCCP were designed to introduce an exogenous tyrosine residue after the SUMO cleavage site. Because the SUMO protease does not cleave before a proline residue, an N-terminal glycine was introduced at the N-terminus of the MCC BCCP sequence. A pet28 plasmid coding for the full length PC carboxylase (Gift from Dr. Lain Tong) was used as the template to amplify PC BCCP. The cDNA sequence of the MCCA gene (Origene, Inc.) was used to amplify the MCC BCCP fragment. ACC2 BCCP was amplified from a pBSK plasmid containing the ACC2 BCCP coding sequence purchased from Epoch Biolabs Inc. After restriction enzyme digestion and agarose gel purification of the PCR products and the SUMO-pro vector, the fragments were ligated using T4 DNA ligase (Roche). The resulting ligation reactions were transformed by electroporation into *E. coli* Top10 cells and successful clones were selected for on LB-ampicillin media. Plasmid DNA from an antibiotic resistant clone was isolated and the correct sequence was verified by sequencing at the UMBI DNA sequencing facility.

The coding sequences for ACC2 (residues 891-965) and ACC1 (residues 785-859) BCCP fragments were cloned into a pet28 vector, introducing an uncleavable C-terminal hexahistidine tag. The primers used for PCR amplification contained NcoI and XhoI sites (NEB, Inc.). Template DNA plasmids containing the coding sequences for the two ACC BCCP domains were purchased from Epoch Biolabs Inc. After digestion, purification and ligation of the PCR products and the vector, the ligation mixtures were transformed into *E. coli* Top10 cells and clones were selected for on LB-kanamycin plates. Plasmids were extracted using a mini-prep plasmid extraction kit (Zymo Research). For ACC1 this plasmid DNA served as the template

for replacement of the three cysteine codons with serine codons using the QuikChange Multi Site Directed Mutagenesis Kit from Stratagene. In all cases DNA sequencing of the complete insert was used to verify the accuracy of each construct.

4.3.3 Protein expression and purification

FL-HCS, 58-HCS and the PCC BCCP domain were purified as previously described(32,95). ACC2, MCC and PC BCCP domains were also purified by affinity chromatography as his_6-SUMO fusions. Plasmids were transformed by elecroporation into Rosetta BL21λDE3, and clones were selected for with 100 ug/ml ampicillin and 34 ug/ml chlorampenicol. A single colony was used to inoculate 5 ml of LB media supplemented with antibiotics, and the culture was grown overnight at 37 °C with shaking at 250 rpm. After dilution into 50 mls of media and 8 hrs of growth, the culture was used to inoculate 1 L of media with antibiotics. When the OD_{600} reached 0.6, the temperature was lowered to 20 °C and expression was induced for 18-20 hrs by addition of 0.1 % (w/v) lactose. All subsequent steps were carried out at 4 °C. Cells were harvested by centrifugation at 4500 rpm. The resulting pellet was resuspended in 200 ml of lysis buffer (50 mM sodium phosphate, pH 8, 300 mM KCl, 10 mM imidazole, 5 % (vol/vol) glycerol, 1 mM PMSF, 3 mM 2-mercaptoethanol) and cells were pelleted by centrifugation at 6000 rpms. The pellet was resuspended in a volume corresponding to five times its weight of lysis buffer and cells were lysed by sonication until the OD_{600} was reduced to 10 % of its original value. The lysate was spun at 8000 rpm and the supernatant loaded on 10 ml of Ni-NTA resin (Qiagen) equilibrated with lysis buffer. After the column was washed with lysis buffer with 20 and then 50 mM imidazole until the absorbance returned to baseline after which the

protein was eluted with Ni-NTA elution buffer (50 mM sodium phosphate, pH 8, 300 mM KCl, 250 mM imidazole, 5 % (vol/vol) glycerol). Sumo protease-1, which was purified from a plasmid that was a generous gift from Dr. Christopher Lima(66), was added at a 1:100 (weight/weight) ratio, and the resulting sample dialyzed overnight into SUMO protease digestion buffer (10 mM sodium phosphate, pH 8.0, 60 mM NaCl, 5% vol/vol glycerol, 5 mM 2-mercaptoethanol). The SUMO tag and SUMO protease were removed by passing the sample through the Ni-NTA column equilibrated with lysis buffer. The MCC sample was concentrated down to 5 mls by dialysis against a viscous solution of PEG20000 in storage buffer (10 mM Tris, pH 8.0, 200 mM KCl, 5 % glycerol), and it was loaded at flow-rate of 0.1 mL/min on a 1.5 x 75 cm column containing 140 mls of Sephacryl S-100 resin equilibrated in storage buffer with 1 mM 2-mercaptoethanol for PC and MCC, or 1 mM DTT for ACC2. Before loading the PC BCCP sample onto the size exclusion column as described for MCC and ACC2, the sample was dialyzed against Q-sepharose starting buffer (10 mM Tris, pH 7.5 at 4 °C, 30 mM NaCl, 5 % (vol/vol) glycerol, 1 mM 2-mercaptoethanol) and loaded on a 10 ml of Q-sepharose resin (GE healthcare) in a 1.5 x 10 ml econo column (BioRad) at 0.5 ml/min. After washing until the absorbance returned to baseline, the protein was eluted at a flow rate of 0.5 ml/min with Q-sepharose elution buffer (10 mM Tris, pH 7.5 at 4 °C, 1 M NaCl, 5 % (vol/vol) glycerol, 1 mM 2-mercaptoethanol) using a linear NaCl gradient (30 mM to 1.0 M) of a total volume of 300 mL.

The longer ACC1 and ACC2 BCCP fragments were expressed as non-cleavable C- terminal his_6 tag. These fragments are referred to as ACC1-his_6 and

ACC2-his$_6$, and correspond to the ACC2 BCCP described by Lee *et al(42)*. Their expression was carried out in Rosetta *E. coli* cells using a similar protocol as the one described for PC and MCC, with the exception that expression was induced with 1.5 % (w/vol) lactose and selection was provided by 50 µg/ml kanamycin and 34 µg/ml chloramphenicol. After harvesting, washing and resuspending the cells in lysis buffer, the samples were loaded on Ni-NTA. The columns were washed with 20 and 50 mM imidazole in lysis buffer, and eluted with Ni-NTA elution buffer. The ACC1-his$_6$ sample was then dialyzed into Q-sepharose staring buffer, loaded on 10 ml of Q resin, and eluted with a gradient of Q-sepharose elution buffer as described for PC BCCP. The ACC2-his$_6$ sample did not require an ion exchange column. Both samples were concentrated down to 5 ml and chromatographed on Sephacryl S-100 columns as described above. The BCCP fragment preparations were determined to be more than 99 % pure, as judged by electrophoresis on 16.5 % polyacrylamide-SDS-tricine gels. In addition, all the BCCP preparations were tested using MALDI for lack of contamination with biotinylated BCCP, as well as for their ability to be quantitatively biotinylated by HCS. Samples were dialyzed into storage buffer and passed through 0.22 µm syringe filter units (Millipore). After UV spectrophotometric determination of their concentrations, the samples were aliquoted in 500 µL and stored at -70 °C.

4.3.4 Sedimentation equilibrium measurements

The molecular weights of PC, MCC, ACC1-his$_6$ and ACC2-his$_6$ were determined by equilibrium analytical ultracentrifugation. Measurements were performed in a Optima XL-I analytical ultracentrifuge (Beckman-Coulter) equipped with a four hole AnTi-60 rotor. Centrifugation was performed at 20 °C with samples

that had been extensively dialyzed against reaction buffer (10 mM Tris, pH 7.5 at 20 °C, 200 mM KCl, 2.5 mM $MgCl_2$). The BCCPs that contained cysteine residues were dialized against reaction buffer with 0.5 µM TCEP. Approximately 110 µL of sample at three different concentrations ranging from 40 to 400 µM were loaded into a cell assembled with a 12 mm six channel charcoal filled epon centerpiece. Samples were scanned at 276 nm through sapphire windows. Data were collected after a delay period of 8 hours at two different speeds (28000 and 32000 rpm) as an average of 5 scans with a 0.001 cm radial step. In each case a value for the reduced molecular weight, σ, was obtained by subjecting the data to global analysis using single species model in WinNonLin, which was converted to molecular weight using the following equation:

$$\sigma = \frac{M(1 - \bar{\upsilon}\rho)\omega^2}{RT}$$

in which M is the molecular mass, $\bar{\upsilon}$ is the partial specific volume of the protein, ρ is the buffer density, ω is the angular velocity, R is the gas constant and T is the temperature. The reaction buffer density was 1.017 g/ml. Partial specific volumes were calculated based on the protein sequences using the program SednTerp (http://www.rasmb.bbri.org), and had values of 0.7375 ml/g for PCC BCCP, 0.7593 ml/g for PC BCCP, 0.7485 ml/g for MCC BCCP, 0.7274 ml/g for ACC2-his_6 and 0.7311 ml/g for ACC1-his_6.

4.3.5 Stopped flow measurements of biotin transfer

Biotin transfer was measured using a Kintek SF-2001 instrument as described previously(28,32,95). The stopped flow instrument allows monitoring of the time dependent increase in intrinsic tryptophan florescence that accompanies the

disappearance of the enzyme-intermediate upon biotin transfer. In these experiments, one syringe contained a fixed concentration of enzyme-intermediate complex, while the second syringe contained varying concentrations of the BCCP substrates. The reactions were initiated by rapidly mixing equal volumes of the two solutions. The enzyme intermediate complex was pre-formed by incubating 1 µM HCS with 0.5 µM biotin and 500 µM ATP in reaction buffer at 20 ° for 20 minutes, thus allowing bio-5'-AMP synthesis to occur. The emitted fluorescence as a function of time was monitored using a 340 nm cutoff filter (Corion Corp.) and an excitation wavelength of 295 nm. At least 5 transients were collected at each BCCP concentration, and the apparent rates were obtained by individually fitting to an appropriate exponential model using the software provided with the Kintek instrument. Subsequent linear regression or non-linear least squares fitting to the Michaelis-menten equation were performed using PRISM 5 (GraphPad, Inc).

4.3.6 Quenched flow measurements of biotin transfer

The rate of HCS-catalyzed biotin incorporation into the BCCP fragments was monitored using a QF-3 quenched flow instrument as described previously. A single turnover of biotin transfer from HCS to BCCP was monitored by quantitating the amount of tritium labeled biotin incorporated into the BCCP fragments. Briefly, a solution of enzyme-intermediate, HCS·bio-5'-AMP was rapidly mixed with an equal volume of a BCCP solution. The enzyme-intermediate complex was pre-formed by incubating 1 µM ligase, 0.463 µM biotin, 37 nM ^{3}H-biotin, and 500 µM ATP in reaction buffer at 20 °C for 20 minutes. At each BCCP concentration, the biotin transfer reaction was repeatedly initiated and quenched with 2 M HCl, after aging for

an increasing amount of time. The reactions involving ACC1-his$_6$, ACC2-his$_6$ and ACC2 BCCP fragments were sufficiently slow to allow hand mixing of the enzyme and reactants in 280 µL total volume followed by quenching of 24 µL in 180 µL of 2 M HCL at different times. BSA was added to a final concentration of 0.1 mg/ml, and the sample was transferred to dried 3MM Whatman paper squares pre-spotted with 200 µl of 800 µM biotin in 10 % TCA. The papers were washed twice in 250 ml of cold 10 % TCA and rinsed once with ethanol. After drying, the radioactivity on the papers was counted on a LS6500 Beckman counter using 5 ml of ReadyProtein$^+$ (Beckman) scintillation fluid. After background correction, conversion from dpm to "µM biotin" was carried out using the relation between dpm and µM obtained from the precipitation of a reaction with quantitative ^{3}H incorporation. Apparent rates were obtained by fitting the transients to a single exponential model. The apparent rates vs concentration profiles were fit to either linear regression in the case of PCC, PC and MCC, or to non-linear least square regression to the Michaelis-Menten equation in the case of ACC1-his$_6$ and ACC2-his$_6$.

4.4 Results

4.4.1 Design and preparation of BCCP fragments

In order to investigate selectivity in HCS-catalyzed post-translational biotin addition to the five natural carboxylase targets appropriate substrates were first obtained in sufficient quantities for detailed kinetic measurements. Human carboxylases are large proteins with complex oligomeric structures (Figure 19A). Fortunately, it has previously been shown that a 67 amino acid fragment of the BCCP

domain of the human propionyl CoA carboxylase contains all the information necessary for HCS-catalyzed biotinylation (72) (Figure 19B). Moreover, this fragment can be readily overexpressed and purified in large quantity using the SUMO fusion protein strategy(95). A similar strategy was used to obtain BCCP fragments of the remaining carboxylases. Multiple sequence alignment of the PCC fragment with the sequences of the remaining carboxylases was used to identify the corresponding biotin acceptor regions of MCC, PC, ACC1 and ACC2. The BCCP domains of PC and MCC were successfully purified in quantities larger than 10 mg/L of bacterial culture using the strategy employed previously for the PCC fragment. By contrast, the ACC2 and ACC1 fragments presented a variety of problems. Yields of the ACC1 fragment were low (1 mg/L), and the SUMO-ACC1 fragment could not be cleaved, even when extended to include 7 additional endogenous residues before the tag. Consequently, following the ACC2 BCCP fragment design of Lee *et al.* (42) , the two acceptor domains were produced a his_6 fusion proteins. Relative to the MCC, PC and PCC acceptor domains, both ACC1 and ACC2 fragments contained 3 additional endogenous residues and the non cleavable -LEHHHHHH tag at the C-terminus, and 6 additional endogenous residues at the N-terminus. In addition, in order to prevent aggregation due to nonspecific disulfide bond formation the three cysteine residues of ACC1-his_6 were replaced by serine.

4.4.2 Oligomeric states of the BCCP fragments

Interpretation of the kinetic data was facilitated by determining the oligomeric states of all BCCP fragments using equilibrium analytical ultracentrifugation. Three different concentrations of each protein were allowed to reach equilibrium at two

different speeds. The resulting six scans were globally fit to a single species model to obtain values for sigma. The sigma values corresponded to molecular weights that were consistent with the monomeric BCCP species at the concentrations relevant to our studies (Table 7). The FL-HCS and 58-HCS have previously been determined to be monomers in both the unliganded form and when bound to bio-5'-AMP(32).

Table7. Assembly state of BCCP fragments

BCCP	*Analytical M.W.*	*Experimental M.W.*
PCC	7033	7200 ± 500 [a, b]
MCC	7462	7600 ± 700 [b]
PC	7254	8000 ± 1000 [b]
ACC1-his$_6$	9234	9400 ± 900 [b]
ACC2-his$_6$	9408	9700 ± 600 [b]

[a.] value obtained from Ingaramo and Beckett (95). [b.] molecular weights with 67% confidence limits obtained from global nonlinear least-squares analysis of equilibrium sedimentation data using WinNonLin.

4.4.3 *Biotin transfer assays*

HCS specificity in post-translational biotin addition was measured using stopped-flow and quench-flow kinetic assays. The rate-determining step in the overall two-step biotinylation reaction catalyzed by HCS is bio-5'-AMP synthesis. Therefore, information about the selectivity in the second step in which biotin is transferred from the adenylate to the acceptor protein is lacking in steady state measurements. Two single turnover assays were used to monitor the biotin transfer reaction independent of bio-5'-AMP synthesis(28,32,95). In both assays the enzyme, biotin and ATP are pre-incubated to allow for complete bio-5'-AMP synthesis. Only

then is the enzyme-intermediate complex rapidly mixed with BCCP, and the biotin transfer reaction progress monitored. Thus, the reaction monitored in these assays is:

$$\text{HCS·bio-5'-AMP + BCCP} \underset{k_{-1}}{\overset{k_1}{\rightleftharpoons}} \text{HCS·bio-5'-AMP·BCCP} \xrightarrow{k_2} \text{HCS + bio-BCCP + AMP}$$

The stopped flow assay allows observation of the time dependent increase in HCS intrinsic fluorescence that accompanies biotinylation (Figure 20A). Transients obtained upon mixing equal volumes of a constant concentration of enzyme-bio-5'-AMP with different concentrations of BCCP fit to a single exponential model, except in the case of the PCC fragment. For this substrate the stopped flow traces display a second slow phase, the rate of which is independent of BCCP concentration and is, therefore, interpreted as reporting on product dissociation (k_2) . The second assay, which employs a quench-flow system, follows the product, bio-BCCP, accumulation and is based on the quantitation of the amount of radioactive biotin incorporated into BCCP. Each transient is obtained after repeatedly initiating the biotinylation reaction by mixing pre-formed enzyme intermediate complex with BCCP, and quenching it at different times (Figure 20B). Quenching of the reaction is accomplished by adding 2M HCl, which both abolishes enzymatic activity and destroys the enzyme-intermediate complex. After protein precipitation with TCA, the acid insoluble radioactivity is quantified to measure biotin incorporation. All transients obtained from this analysis are well-described by a single exponential model.

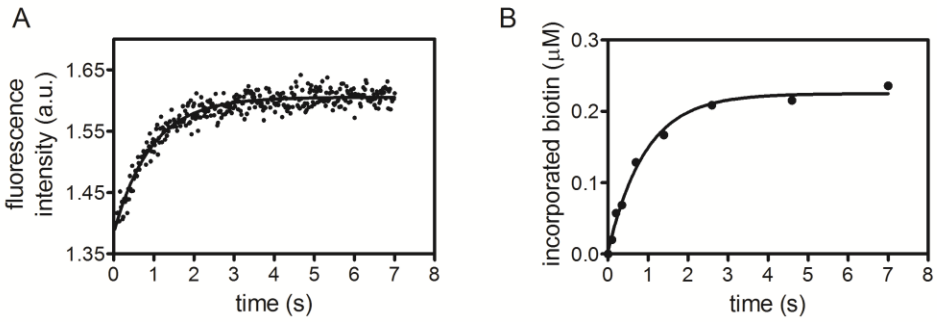

Figure 20: single turnover assays of biotin transfer. A. Stopped flow fluorescence (arbitrary units) trace obtained upon 1:1 (vol/vol) mixing of 0.5 μM FL-HCS.bio-5'-AMP with 120 μM MCC BCCP. The solid line represents the best-fit of the data to a single exponential model. B. Transient obtained by quantifying the amount of 3H-biotin incorporation after mixing equal volumes 0.5 μM FL-HCS.bio-5'-AMP and 120 μM MCC BCCP for different times before quenching. The solid line represents the best-fit of the data to a single exponential model.

4.4.4 Biotin transfer to MCC, PC and PCC BCCPs is fast

Three of the BCCP fragments, including those of PC, MCC, and PCC, exhibited similar kinetic behavior in HCS-catalyzed biotin transfer. The dependence of the apparent rates of transfer measured by stopped-flow fluorescence as a function of BCCP concentration was linear for all (Figure 21A and 21B) with no leveling off of the rate at high substrate concentration. For the PCC fragment, which was characterized by biphasic transients, the linear dependence was obtained for the faster kinetic phase. This same behavior has previously been observed for the same reaction catalyzed by the human, an archaeal and a bacterial ligase(28,32,95). The simplest interpretation of the linear dependence is that it reports on the bimolecular association of the enzyme-bio-5'-AMP intermediate with the BCCP substrate, with the slope providing the bimolecular rate constant, k_1. The magnitudes of the bimolecular rate constants obtained for the three carboxylase substrates reveals moderate selectivity in

the process. The rate constants span a 3.5 fold range and the order of the rates for the fragments is PCC>MC>PC (Table 8).

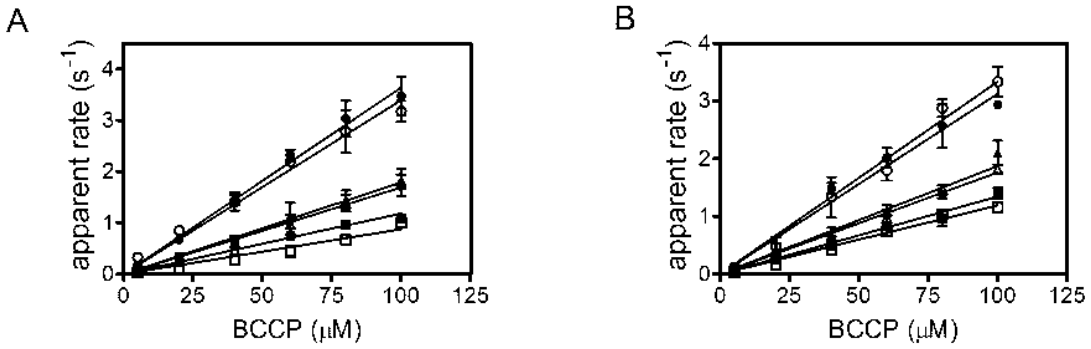

Figure 21: Dependence of the apparent rate of biotin transfer on BCCP concentration measured by stopped flow (*filled* symbols) and quench flow (*open* symbols). A. Rate versus concentration profiles obtained by stopped-flow for FL-HCS with PCC(●), MCC (▲) and PC (■) BCCPs, and those obtained by quench flow for PCC (○), MCC (Δ) and PC(□) BCCPs. B. Rate versus concentration profiles obtained by stopped-flow for 58-HCS with PCC(●), MCC (▲) and PC (■) BCCPs, and by quench flow for PCC (○), MCC (Δ) and PC(□) BCCPs. The data points represent the average of the apparent rate measured at each BCCP concentration in three independent experiments in the stopped flow, or two independent experiments in the quench flow, with standard deviations shown as error bars. The solid lines were obtained from linear regression of the data.

Table 8. FL- and 58-HCS biotin transfer rates to PCC, MCC and PC BCCP

HCS variant	*BCCP*	*Stopped Flow*[a] ($x10^4$ $M^{-1}s^{-1}$)	*Quench Flow*[d] ($x10^4$ $M^{-1}s^{-1}$)
FL-HCS	*PCC*	3.5 ± 0.3[b] (0.23 ± 0.03)[b,c]	3.1 ± 0.3[b]
	MCC	1.9 ± 0.2	1.9 ± 0.2
	PC	1.00 ± 0.07	1.00 ± 0.05
58-HCS	*PCC*	3.2 ± 0.2 (0.21 ± 0.02)[c]	3.5 ± 0.3
	MCC	2.03 ± 0.05	1.81 ± 0.07
	PC	1.2 ±0.1	1.28 ± 0.05

[a.] The errors represent the standard deviation of the rates obtained in three independent stopped-flow experiments. [b.] values from Ingaramo and Beckett. [c.] PCC BCCP dissociation rate, in s^{-1}, obtained from the concentration independent phase. [d.] The errors correspond to the standard deviation of results obtained in two independent quench flow experiments.

The results obtained using the quench flow assay were similar to those obtained in the stopped flow measurements. Transients were well-described by a single exponential model at all the BCCP concentrations. Moreover, the same linear dependence of the apparent rates on substrate protein concentration that was observed in the stopped flow analysis was also obtained using the quench flow assay (Figure 21A and 21B). Additionally, for each enzyme-substrate pair the best-fit lines obtained from linear regression are nearly superimposable for the two assays. This behavior was also previously observed with the human, archaeal and bacterial ligases. The linear dependence and similarity of the quench flow and stopped flow results indicates that collision between HCS and the mitochondrial BCCPs is rate limiting and that the rate of biotin transfer to these substrates is not affected by the rate of the chemistry of biotin attachment to the acceptor lysine residue. Consistent with the

stopped flow results, HCS displays selectivity among the three BCCP domains by displaying biotin transfer rates that are 3.5 fold different. In addition, the linear dependencies of the rates of FL and 58-HCS-catalyzed reactions for any single BCCP substrate were similar.

4.4.5 Biotin transfer to ACC1-his$_6$ and ACC2-his$_6$ displays a different kinetic behavior

The kinetic behavior of the two ACC BCCP fragments in HCS-catalyzed biotin transfer is distinct from that observed for the mitochondrial substrates. For simplicity the results obtained with the ACC2 fragment are first presented followed by those obtained for the ACC1 fragment. Like the PC and MCC fragments, transients obtained upon mixing of the enzyme·intermediate complex with ACC2-his$_6$ BCCPs were well described by a single exponential model. However, at any single substrate concentration the measured rate was significantly slower than the rates obtained for the mitochondrial BCCP fragments. For example, the apparent rate obtained at a final concentration of 80 µM ACC2-his$_6$ is approximately 40 fold slower than the apparent rate at the same concentration of PC BCCP, the slowest of the mitochondrial substrates. In contrast to the linear behavior exhibited by the mitochondrial BCCPs, ACC2-his$_6$ displayed a hyperbolic dependence of the apparent biotinylation rate on BCCP concentration (Figure 22A and 22B). Nonlinear least squares analysis of the data using the Michaelis-Menten formalism yielded a K_M of approximately 65 µM and a k_{cat} of 0.04 s^{-1} (Table 9). The saturable behavior indicates that, in contrast to the three BCCP fragment discussed above, the rate-limiting step in the second half reaction for the ACC2 substrate is limited by the chemistry of biotin

attachment. In turn, bio-5'-AMP synthesis, which is associated with a rate of 0.1 s^{-1}, is not the rate limiting step in the overall two-step biotinylation reaction for this substrate.

Measurements of product incorporation into ACC2-his_6 BCCP yielded results similar to those obtained in the stopped-flow measurements (Figure 22A and 22B, table 9). The slow reaction rates observed for this substrate obviated use of the quench-flow, and manual mixing and quenching of ^{3}H-biotin spiked reactions was used to construct the transients, which were all well-described by a single-exponential model. The rates obtained from the analysis are, like those obtained using the stopped-flow assay, slow. One source of concern associated with the slow measured rates of biotin transfer to the ACC2-his_6 is the potential influence of the tag on the reaction rate. Although the untagged version of the fragment could not be obtained in sufficient quantity to determine full rate versus concentration profiles, sufficient material was available to compare its kinetic behavior to that of the tagged protein. Comparison of the transients obtained at a final concentration of 20 μM ACC2 BCCP with the corresponding transients for 20 μM ACC2-his_6 showed that FL and 58-HCS catalyze the biotin transfer reaction to both BCCP constructs with similarly slow rates that are within error identical (data not shown). Furthermore, the results show that both tagged and untagged ACC2 BCCPs are similarly slow. Plots of the measured rates versus substrate concentration displayed a hyperbolic dependence on ACC2-his_6 concentration and non-linear least squares of the data to the Michaelis-Menten model yielded parameters values that agree with those obtained in the stopped flow measurements (Table 9).

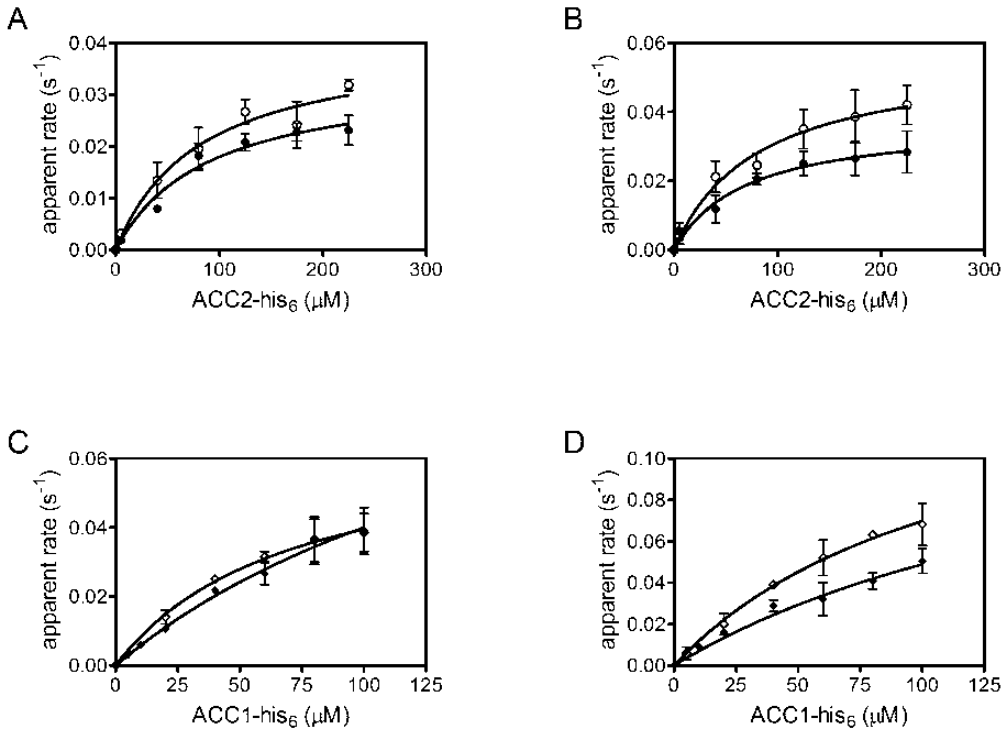

Figure 22: biotin transfer to the BCCP fragments of acetyl-CoA carboxylases. Panels A and B: rate vs concentration profiles for FL-HCS (A) or 58-HCS (B) biotin transfer to his$_6$-ACC2 obtained by stopped flow (●) and quench flow (○).The data points represent the average of the apparent rate measured at each BCCP concentration in three independent experiments in the stopped flow, or two independent experiments in the quench flow, with standard deviations shown as error bars. The solid lines represent the best-fits of the rate versus concentration profiles to the Michaelis-Menten equation. Panels C and D: Apparent rates for biotin transfer to ACC1-his$_6$ obtained by stopped flow (♦) or quench flow (◊) with FL-HCS (C) and 58-HCS (D). The quench flow data points represent the average of the apparent rate measured at each BCCP concentration in two independent experiments, with standard deviations shown as error bars. The stopped flow data points for the three higher ACC1-his$_6$ concentrations are the average of at least 10 traces each, while the data points at the lower concentrations represent the average of three independent experiments, with error bars indicating their standard deviation.

Table 9: FL- and 58-HCS catalyzed biotin transfer to ACC2-his$_6$ BCCP

	Stopped Flow[a]		*^{3}H-biotin incorporation assay*[b]	
	K_M (μM)	k_{cat} (s^{-1})	K_M (μM)	k_{cat} (s^{-1})
FL-HCS	80 ± 20	0.032 ± 0.005	60 ± 20	0.037 ± 0.004
58-HCS	70 ± 30	0.038 ± 0.007	90 ± 20	0.058 ± 0.006

[a.] The errors represent the standard deviation of the rates obtained in three independent stopped-flow experiments, or the propagated 68% confidence interval obtained from the individual fits, whichever was larger. [b.] The errors correspond to the standard deviation of results obtained in two independent experiments, or the propagated 68% confidence interval obtained from the individual fits, whichever was larger.

HCS-catalyzed biotin transfer to ACC1-his$_6$ was similar to transfer to ACC2-his$_6$. Stopped flow traces displayed apparent rates that were very slow compared to those measured for the mitochondrial carboxylases (Figure 22C and 22D). In addition, as observed for ACC2-his$_6$, the apparent rates displayed a hyperbolic dependence on ACC1-his$_6$ concentration. Non-linear least square regression of the apparent rate dependence on BCCP fragment concentration to the Michaelis-Menten provided k_{cat} and K_M values of (Table 10). The large errors associated with the stopped flow derived K_M values for ACC1-his$_6$ are likely due the limited concentration range over which the measurements could be performed because of the fragment's low solubility. The ^{3}H-incorporation experiments provided K_M values comparable to those obtained for ACC2-his$_6$ (Table 10), and k_{cat} values that were approximately 2-fold larger than those for ACC2-his$_6$. Moreover, this k_{cat} value is similar in magnitude to that obtained for bio-5'-AMP synthesis.

Table 10. FL- and 58-HCS catalyzed biotin transfer to ACC1-his$_6$ BCCP

	Stopped Flow[a]		*^{3}H-biotin incorporation assay*[b]	
	K_M (μM)	k_{cat} (s^{-1})	K_M (μM)	k_{cat} (s^{-1})
FL-HCS	190 ± 90	0.12 ± 0.04	70 ± 30	0.06 ± 0.02
58-HCS	200 ± 90	0.15 ± 0.05	80 ± 30	0.12 ± 0.03

[a.] The errors represent the propagated 68% confidence limits obtained from globally fitting the data, which comprised three independent datasets for the three lower concentrations, and at least 10 traces for the three largest concentrations. [b.] The errors correspond to the standard deviation of results obtained in two independent experiments, or the propagated 68% confidence interval obtained from the individual fits, whichever was larger.

4.5 Discussion

Holocarboxylase synthetase is known to display preference for its cognate human biotin acceptor (BCCP) domain over those of other species (95). However, prior to these studies it was not known if the enzyme shows any specificity in biotin addition to the five endogenous human BCCPs. It was also not known if the HCS N-terminus affects the interaction with these BCCP fragments. In this work the application of two single turnover assays allowed measurements of specificity in HCS-catalyzed biotin transfer to the five endogenous human acceptor substrates (28,32,95) that revealed a kinetic preference for mitochondrial over cytosolic substrates.

The BCCP fragments of the mitochondrial carboxylases, PC, PCC and MCC, displayed similar kinetic properties in biotin transfer. All exhibited a linear dependence of the apparent transfer rate on BCCP concentration when monitored by either stopped flow or quench flow. This behavior indicates that transfer to these

substrates is limited by the rate of collision of the enzyme-intermediate with BCCP, and provides a measure of the bi-molecular association rate constant formation of the ternary complex. The slowest rate constant, 10,000 $M^{-1}s^{-1}$, was measured for the PC substrate and the fastest, 33,000 $M^{-1}s^{-1}$, for the PCC fragment. This 3-fold difference in transfer supports the notion that HCS shows modest discrimination in biotin transfer to the three mitochondrial carboxylases. However, for all substrates the full length and the N-terminal truncated enzymes showed identical rates of biotin transfer.

The properties of ACC1 and ACC2 BCCP fragments in HCS-catalyzed biotin transfer are both qualitatively and quantitatively distinct from those of the three mitochondrial substrates. Although, like the mitochondrial substrates, transients for the cytosolic substrates were well-described by a single exponential model, the apparent rates at comparable acceptor protein concentrations were significantly slower (approximately 100-fold). The identical rates measured for the untagged and tagged versions of the ACC2 substrate indicate that the slow rates cannot be attributed to the presence of the his_6 tag. Furthermore, in contrast to the linear dependence observed for the mitochondrial substrates, the apparent rates of biotin transfer to the ACC substrates displayed a hyperbolic dependence on BCCP concentration. This saturable behavior and slow biotin transfer rates indicate that the rate-limiting step in the second step of biotin transfer to the ACC substrates differs from that for the PCC, PC and MCC substrates and corresponds to either the chemistry of biotin attachment or the dissociation rate. Additionally, the slow rates measured for HCS-catalyzed biotin addition to the ACC substrates indicates that, in contrast to the mitochondrial substrates for which bio-5'-AMP synthesis is rate-

limiting, it is the second step of biotin transfer from the adenylate to the acceptor protein that is rate-limiting in the overall two step biotinylation reaction. The k_{cat} in the second step of the transfer reaction for the ACC2 BCCP fragment is approximately 0.04 s^{-1}, and that of ACC1 is twice as large. Comparison of these rates to the bio-5'-AMP synthesis rate of 0.1 s^{-1} indicates that for the ACC substrates the overall reaction rate for the two-step biotin transfer reaction is influenced by the second step of biotin transfer from the adenylate to the lysine residue on BCCP(32).

The two-fold larger k_{cat} observed for 58- vs FL-HCS biotinylation of the BCCP fragment of ACC2 was the largest difference observed for the two enzyme isoforms. This suggests that the N-terminus of HCS affects biotin acceptor substrate recognition mainly for ACC2 and perhaps for ACC1 and are consistent with results of NMR measurements performed on the ACC2-his_6 construct. Lee *et al.* monitored the chemical shift perturbations that occur in ACC2-his_6 spectra upon addition of FL-HCS and the initial 160 amino-acids of HCS (160-HCS)(42). Signals for several ACC2-his_6 side chains were shown to undergo chemical shift perturbations upon addition of either HCS partner, which led to the proposal that the N-terminus might be involved in recruitment of the BCCP substrate. In addition, chemical shift perturbations on the N-terminal HCS fragment indicated that this domain undergoes conformational rearrangements upon binding ACC2-his_6. While these NMR studies provided valuable structural information, only the ACC2-his_6 BCCP has been subjected to them.

The magnitudes of the rates of BCCP biotinylation correlate with the cellular localization of the corresponding carboxylases. Biotinylation of the BCCP fragments

of PC, PCC and MCC displayed faster apparent rates than those of ACC1 and ACC2. While the latter two are present in the cytoplasm, the other carboxylases are transported into the mitochondria matrix. It is tempting to speculate that HCS biotinylates PC, PCC and MCC enzymes faster because mitochondrial enzymes are only transiently present in the cytoplasm and must be biotinylated prior to mitochondrial import. Conversely, HCS has continuous access to ACC1 and ACC2, so there is no biological pressure to increase the biotinylation reaction speed.

Previous studies provide some support for a model that rationalizes faster biotinylation rates of substrates destined for the mitochondria based on lack of access once transported. First, even though ACC2 is associated with the mitochondria, it localizes to the cytosolic side of the mitochondrial membrane (19). Thus, HCS has continuous access to ACC2 as well as ACC1 and a fast biotinylation rate would not need to evolve. Second, carboxylases are imported into mitochondria whether biotinylated or not (97). If indeed there is no mechanism to prevent unbiotinylated carboxylase transport into the mitochondria, then it is even more pressing that biotinylation of mitochondrial carboxylases display a fast rate.

The above model assumes that HCS localizes to the cytoplasm, with no HCS found in the mitochondria. Subcellular localization of HCS has been a matter of debate. Its presence in the cytoplasm is well established through fluorescence microscopy localization studies and western blots of fractionated cells (44). While no mitochondrial localization of HCS was evidenced in microscopy studies of intact cells in which the N- and C- terminally GFP tagged enzyme was expressed, western blots of mitochondrial fractions were inconclusive and showed a 60 kDa band that is

not consistent with the sizes expected for HCS splice variants (40). The identity of this band remains to be confirmed, but suggests the presence of a processed form of HCS in the mitochondria. In addition, an independent study involving pulse-chase ^{35}S labeling of PC provided evidence supporting the presence of biotinylating activity in the mitochondria(97). The possibility of HCS mitochondrial localization poses a problem for our explanation for HCS faster biotin transfer rates to mitochondrial carboxylases. However, confirming the presence of biotinylating activity in the mitochondria and the identity of the 60 kDa species would reveal new mechanistic possibilities, and does not negate the fact that HCS displays specificity among its natural biotinylation targets.

The observed HCS selectivity suggest a mechanism for biotin distribution among carboxylases that is controlled kinetically at two levels. First, HCS displays a marked distinction between cytosolic and mitochondrial substrates, favoring biotin transfer to those carboxylases to which it has only transient access. Second, HCS will display selectivity among the mitochondrial carboxylases. The intracellular biotin supply is low and, accordingly, the HCS·adenylate complex is limiting. Kinetically, the carboxylase that associates most rapidly with this complex will be favored in biotinylation. However, the significance of the relative intrinsic rates of biotinylation can be overridden by altering relative carboxylase concentrations. Carboxylases will compete for the biotin, and those that have the fastest kinetics of association, which is dependent on substrate concentration and inherent association rate, will be preferentially modified. As a result of these preferences, the cell can establish a

hierarchy among the carboxylases that determines metabolic use of biotin based on the rates of bimolecular association and carboxylase abundance.

Chapter 5: Conclusions and future directions

The initial biochemical studies presented yielded valuable insight into the mechanism of the biotinylation reaction, allowed for the investigation of HCS specificity, and suggested a model for the control of biotin distribution among carboxylases. Biochemical characterization of the two HCS isoforms demonstrated that both variants are monomers in the unliganded form and when bound to bio-5'-AMP. Steady state analysis of the overall reaction, as well as pre-steady state kinetic measurements of bio-5'-AMP synthesis indicated that FL- and 58-HCS synthesize bio-5'-AMP at a rate of 0.1 s^{-1}. Single turnover measurements of the biotin transfer reaction alone indicated that BCCPs from mitochondrial carboxylases were biotinylated much faster than the BCCP fragments of cytosolic carboxylases. In the case of the two cytosolic carboxylases the second step, biotin transfer, is the slowest step observed, likely becoming the rate limiting step. However, in the biotinylation of the three mitochondrial BCCP fragments, the HCS catalyzed reaction is limited by the rate of bio-5'-AMP synthesis.

Comparison of the results obtained from the single turnover stopped flow with those of quench flow measurements of the biotin transfer reaction to the mitochondrial minimal biotin acceptor substrates revealed that the rate of biotin transfer to mitochondrial carboxylases is limited by the rate of enzyme-BCCP association. These results were used to propose a model to explain biotin distribution among carboxylase substrates based on HCS specificity and the concentration of substrate protein. Inside the cell, HCS binds biotin and converts it to bio-5'-AMP. Since this is the rate limiting step in most cases, an accumulation of enzyme-

intermediate complex occurs. This holo-enzyme then transfers the biotin moiety to the carboxylase with the largest apparent association rate, leading to an effective competition among the mitochondrial carboxylases. The apparent association rate depends on carboxylase concentration and on the intrinsic association rate, which gives the cell a chance to override biotin distribution by controlling carboxylase expression.

The *E. coli* and an archaeal ligase catalyzed biotin transfer reactions were also found to be limited by the rate of enzyme-intermediate complex collision with the biotin acceptor substrate, indicating that this mechanistic aspect of the reaction is ubiquitous. In the mammalian system, this behavior highlights the importance of protein:protein recognition in determining the fate of biotin among the various substrates, and mitochondrial ligases likely have evolved sequences that provide faster association rates. In the *E.coli* system, association rates have an equally central role. The bacterial ligase acts like a switch in which the ligase can transfer biotin to the carboxylase substrate, or homodimerize to repress transcription of biotin biosynthetic genes. Since the two interactions are isoenergetic, it is the competition of the association rates that controls the switch.

This work has laid the foundation for several future studies. The structural basis of HCS specificity is still vague, and it remains to be determined which residues play critical roles in modulating the recognition both on HCS and on the biotin acceptor substrate. This is due, in part, to the lack of an X-ray crystallography model of HCS. Identifying which residues cause the dramatic difference between the BCCP domains of ACC1 and 2 vs those of PC, PCC, and MCC, can potentially provide

insight on the involvement of those residues in catalysis vs binding. The effect of mutating residues that affect binding will have larger effects on the apparent rate vs BCCP concentration profiles for the mitochondrial carboxylases, while those residues that affect catalysis might have larger effects on the cytosolic carboxylases. This work would require a combination of mutational and crystallographic studies of enzyme substrate complex. The *Ph*BPL/*Ph*BCCP crystallographic structure stands as precedent for this type of work, although the human complex might prove more difficult to crystallize.

The previous mutational studies can then be expanded to include those naturally occurring variants of HCS and BCCP that are linked to MCD. Most of the defects are expected to relate to compromised catalytic activity or biotin affinity. However, it would be of interest to characterize those mutations that cause low biotin responsiveness, since this phenotype may be caused by an increased K_M for biotin acceptor substrate. This is important because it would yield information on interacting residues, and moreover, it would allow prediction of biotin responsiveness. The assays that we developed allow us to assign the defective reaction as either bio-5'-AMP synthesis or biotin transfer, and to evaluate HCS response to pharmacological doses of biotin.

Studies with the whole carboxylases would be very relevant to the understanding of HCS specificity. Human PC (98) and PCC (99) carboxylases have been recombinantly expressed and purified in *E. coli* , and MCC (100) and ACC1 in baculovirus systems. ACC2(101) has also been purified from a baculovirus system, but is missing 146 amino-acids (102). The single turnover quenched flow experiment

could be easily applied to investigate the effect of the complete carboxylase structure on biotin transfer. After this characterization is complete, the model that we proposed regarding distribution of biotin based on HCS association rate and the concentration of carboxylase could be tested in human cells by careful measurement of the carboxylases amounts and their relative biotinylation state as a function of biotin concentration.

The key role that phosphorylation plays in regulation of cellular processes renders HCS phosphorylation an issue that should not be overlooked. HCS activity could be regulated by this phosphorylation. However, cell biology studies to validate the relevance of phosphorylation to HCS regulation are lacking. It is possible that HCS phosphorylation is unrelated to its regulation in, for example, a cell cycle dependant manner. It is necessary to determine HCS phosphorylation status as a function of biotin concentration before any conclusions can be drawn regarding its biological significance. The observation that biotin activates guanylate cyclase suggests a mechanism by which a cGMP dependent kinase would phosphorylate transcription factors to upregulate gene expression, or maybe, phosphorylate and regulate HCS. Identifying HCS possible interaction partners and the players of the signaling cascade that leads to biotin regulation of gene expression in mammalian cells is a field advancement to look forward to.

HCS biochemical characterization is not complete. Thermodynamic characterization of small molecule binding is important because it provides assays that aid in the design of inhibitors to either target or avoid the human ligase. Rational drug design has traditionally used thermodynamics as a guide in binding affinity

optimization. Bacterial ligases have been proposed as targets for antibiotics (59), and for this purpose, avoiding binding to the human ligase would be desirable. In addition, it has been demonstrated that a variety of cancer cells display upregulation of ACC, in line with their high growth rate and higher need for lipogenesis, and that ACC is a potential anti-cancer target. Moreover, inhibition of ACC1 has shown, in some cases, to be selective for cancer cells (103). Given this information, and the importance of ACC for metabolism, the idea of ACC as a plausible anti-cancer drug is not so farfetched.

In conclusion, the biochemical studies presented here provided insight into HCS mechanism and specificity. Furthermore, the results led to the development of models for HCS function that relate to cellular regulation and are of direct biological relevance. We hope to have provided the framework for future HCS studies and elucidation of the role of HCS in biotin sensing.

Bibliography

1. Rodionov, D. A., Mironov, A. A., and Gelfand, M. S. (2002) *Genome Res* **12**, 1507-1516
2. Hall, C., and Dietrich, F. S. (2007) *Genetics* **177**, 2293-2307
3. Said, H. M., Ortiz, A., McCloud, E., Dyer, D., Moyer, M. P., and Rubin, S. (1998) *Am J Physiol* **275**, 1365-1371
4. Boas, M. A. (1927) *Biochem J* **21**, 712-724
5. Gyorgy, P., Melville, D. B., Burk, D., and Du Vigneaud, V. (1940) *Science* **91**, 243-245
6. du Vigneaud, V. (1942) *Science* **96**, 455-461
7. Bentley, R. (1985) *Trends in Biochemical Sciences* **10**, 51-56
8. Knowles, J. R. (1989) *Annu Rev Biochem* **58**, 195-221
9. St. Maurice, M., Reinhardt, L., Surinya, K. H., Attwood, P. V., Wallace, J. C., Cleland, W. W., and Rayment, I. (2007) *Science* **317**, 1076-1079
10. Attwood, P. V., and Wallace, J. C. (202) *Acc Chem Res* **35**, 113-120
11. Jitrapakdee, S., and Wallace, J. C. (2003) *Curr Protein Pept Sci* **4**, 217-229
12. Cronan, J. E., and Waldrop, G. L. (2002) *Prog Lipid Res* **41**, 407
13. Castle, J. C., Hara, Y., Raymond, C. K., Garret-Engele, P., Ohwaki, K., Kan, Z., Kusunoki, J., and Johnson, J. M. (2009) *PLoS ONE* **4**
14. Brownsey, R. W., Boone, A. N., Elliot, J. E., Kulpa, J. E., and Lee, W. M. (2006) *Biochem Soc Trans* **34**, 223-227
15. Kim, C. W., Moon, Y. A., Park, S. W., Cheng, D., Kwon, H. J., and Horton, J. D. (2010) *Proc Natl Acad Sci* **107**, 9626-9631

16. Abu-Elheiga, L., Matzuk, M. M., Kodari, P., Oh, W., Shaikenov, T., Gu, Z., and Wakil, S. J. (2005) *Proc Natl Acad Sci* **102**, 12011-12016

17. Olson, D. P., Pulinilkunnil, T., Cline, G. W., Shulman, G. I., and Lowell, B. B. (2010) *Proc Natl Acad Sci* **107**, 7598-7603

18. Choi, C. S., Savage, D. B., Abu-Elheiga, L., Liu, Z. X., Kim, S., Kulkarni, A., Distefano, A., Hwang, Y. J., Reznick, R. M., Codella, R., Zhang, D., Cline, G. W., Wakil, S. J., and Shulman, G. I. (2007) *Proc Natl Acad Sci* **104**, 16480-16485

19. Abu-Elheiga, L., Brinkley, W. R., Zhong, L., Chirala, S. S., Woldegiorgis, G., and Wakil, S. J. (2000) *Proc Natl Acad Sci* **97**, 1444-1449

20. Miyazaki, T., Ohura, T., Kobayashi, M., Shigematsu, Y., Yamaguchi, S., Suzuki, Y., Hata, I., Aoki, Y., Yang, X., Minjares, C., Harauta, I., Uoto, H., Ito, Y., and Muller, U. (2001) *J Biol Chem* **276**, 35995-35999

21. Jitrapakdee, S., Walker, M. E., and Wallace, I. C. (1996) *Biochem Biophys Res Comm* **223**

22. Wang, X., Wurtele, E. S., and Nicolau, B. J. (1995) *Plant Physiol* **108**, 1133-1139

23. Lane, M. D., Rominger, K. L., Young, D. L., and Lynen, F. (1964) *J Biol Chem* **239**, 2865-2871

24. Wilson, K. P., Shewchuk, L. M., Brennan, R. G., Otsuka, A. J., and Matthews, B. W. (1992) *Proc Natl Acad Sci U S A* **89**, 9257-9261

25. Barker, D. F., and Campbell, A. M. (1981) *J Mol Biol* **146**, 451-467

26. Lin, K. C., Cambell, A., and Shiuan, D. (1991) *Biochim Biophys Acta* **1090**, 317-325

27. Streaker, E. D., and Beckett, D. (2006) *Biochemistry* **45**, 6417-6425

28. Nenortas, E., and Beckett, D. (1996) *J Biol Chem* **271**, 7559-7567

29. Zhao, H., and Beckett, D. (2008) *J. Mol. Biol* **380**, 223-236

30. Beckett, D. (2007) *Annu Rev Genet* **41**, 443-464

31. Daniels, K. G., and Beckett, D. (2010) *Biochemistry* **49**, 5358-5365

32. Ingaramo, M., and Beckett, D. (2009) *J Biol Chem* **284**, 30862-30870

33. Purushothaman, S., Gupta, G., Srivastava, R., Ramu, V. G., and Surolia. (2008) *PloS One* **3**, 2320

34. Bagautdinov, B., Matsuura, Y., Bagautdinova, S., and Kunishima, N. (2008) *J Biol Chem* **283**, 14739-14750

35. Solorzano-Vargas, R. S., Pacheco-Alvarez, D., and Leon-Del-Rio, A. (2002) *Proc Natl Acad Sci U S A* **99**, 5325-5330

36. Zempleni, J. (2005) *Annu Rev Nutr* **25**, 175-196

37. Bailey, L. M., Ivanov, R. A., Wallace, J. C., and Polyak, S. W. (2008) *Anal Biochem* **373**, 71-77

38. Leon del Rio, A., Leclerc, D., Akerman, B., Wakamatsu, N., and Gravel, R. A. (1995) *Proc Natl Acad Sci U S A* **92**, 4626-4630

39. Yang, X., Aoki, Y., Li, X., Sakamoto, O., Hiratsuka, M., Kure, S., Taheri, S., Christensen, E., Inui, K., Kubota, M., Ohira, M., Ohki, M., Kudoh, J., Kawasaki, K., Shibuya, K., Shintani, A., Asakawa, S., Minoshima, S., Shimizu, N., Narisawa, K., Matsubara, Y., and Suzuki, Y. (2001) *Hum Genet* **109**, 526-534

40. Hiratsuka, M., Sakamoto, O., Li, X., Suzuki, Y., Aoki, Y., and Narisawa, K. (1998) *Biochim Biophys Acta* **1385**, 165-171

41. Campeau, E., and Gravel, R. A. (2001) *J Biol Chem* **276**, 12310-12316

42. Lee, C. K., Cheong, C., and Y.H., J. (2010) *FEBS lett* **584**, 675-680

43. Narang, M. A., Dumas, R., Ayer, L. M., and Gravel, R. A. (2004) *Hum Mol Genet* **13**, 15-23

44. Bailey, L. M., Wallace, J. C., and Polyak, S. W. (2010) *Arch Biochem Biophys* **496**, 45-52

45. Rodriguez-Melendez, R., Cano, S., Mendez, S. T., and Velazquez, A. (2001) *J Nutr* **131**, 1909-1913

46. Pacheco-Alvarez, D., Solorzano-Vargas, R. S., Gonzalez-Noriega, A., Michalak, C., Zempleni, J., and Leon-Del-Rio, A. (2005) *Mol Genet Metab* **85**, 301-307

47. Villen, J., Beausoleil, S. A., Gerber, S. A., and Gygi, S. P. (2007) *Proc Natl Acad Sci* **104**, 1488-1493

48. Dakashinamurti, K., and Cheah-Tan, C. (1968) *Arch Biochem Biophys* **127**, 17-21

49. Beckett, D., Kovaleva, E., and Schatz, P. J. (1999) *Protein Sci* **8**, 921-929

50. Chapman-Smith, A., Morris, T. W., Wallace, J. C., and Cronan, J. E. (1999) *J Biol Chem* **247**, 1449-1457

51. Reche, P., Fuller, C., Eichhorn, K., and Perham, N. (1998) *Biochem J* **329**, 589-596

52. Zhao, H., Naganathan, S., and Beckett, D. (2009) *J Mol Biol* **389**, 336-348

53. Leon del Rio, A. (2005) *J Nutr Biochem* **16**, 432-434

54. Pacheco-Alvarez, D., Solorzano-Vargas, R. S., and Leon del Rio, A. (2002) *Arch Med Res* **33**, 439-427

55. Dupuis, L., Campeau, E., Leclerc, D., and Gravel, R. A. (1999) *Mol Genet Metab* **66**, 80-90

56. Dupuis, L., Leon-Del-Rio, A., Leclerc, D., Campeau, E., Sweetman, L., Saudubray, J. M., Herman, G., Gibson, K. M., and Gravel, R. A. (1996) *Hum Mol Genet* **5**, 1011-1016

57. Suzuki, Y., Aoki, Y., Ishida, Y., Chiba, Y., Iwamatsu, A., Kishino, T., Niikawa, N., Matsubara, Y., and Narisawa, K. (1994) *Nat Genet* **8**, 122-128

58. Suzuki, Y., Yang, X., Aoki, Y., Kure, S., and Matsubara, Y. (2005) *Hum Mutat* **26**, 285-290

59. Pendini, N. R., Bailey, L. M., Booker, G. W., Wilce, M. C., Wallace, J. C., and Polyak, S. W. (2008) *Biochim Biophys Acta* **1784**, 973-982

60. Sherwood, W. G., Saunders, M., Robinson, B. H., Brewster, T., and Gravel, R. A. (1982) *J Pediatr* **101**, 546-550

61. Sweetman, L., Burri, B. J., and Nyhan, W. L. (1985) *Ann N Y Acad Sci* **447**, 288-296

62. Chauhan, J., and Dakshinamurti, K. (1991) *J Biol Chem* **266**, 10035-10038

63. Abbott, J., and Beckett, D. (1993) *Biochemistry* **32**, 9649-9656

64. Gill, S. C., and von Hippel, P. H. (1989) *Anal Biochem* **182**, 319-326

65. Marblestone, J. G., Edavettal, S. C., Lim, Y., Lim, P., Zuo, X., and Butt, T. R. (2006) *Protein Sci* **15**, 182-189

66. Mossessova, E., and Lima, C. D. (2000) *Mol Cell* **5**, 865-876

67. Healy, S., Heightman T. D., Hohmann, L., Schriemer, D., and Gravel, R. A. (2009) *Protein Sci* **18**, 314-328

68. Roark, D. E. (1976) *Biophys Chem* **5**, 185-196

69. Johnson, M. L., Correia, J. J., Yphantis, D. A., and Halvorson, H. R. (1981) *Biophys J* **36**, 575-588

70. Eisenstein, E., and Beckett, D. (1999) *Biochemistry* **38**, 13077-13084

71. Schagger, H., and von Jagow, G. (1987) *Anal Biochem* **166**, 368-379

72. Leon del Rio, A., and Gravel, R. A. (1994) *J Biol Chem* **269**, 22964-22968

73. Tissot, G., Pepin, R., Job, D., Douce, R., and Alban, C. (1998) *Eur J Biochem* **258**, 586-596

74. Burri, B. J., Sweetman, L., and Nyhan, W. L. (1985) *Am J Hum Genet* **37**, 326-337

75. Burri, B. J., Sweetman, L., and Nyhan, W. L. (1981) *J Clin Invest* **68**, 1491-1495

76. Sakamoto, O., Suzuki, Y., Li, X., Aoki, Y., Hiratsuka, M., Suormala, T., Baumgartner, E. R., Gibson, K. M., and Narisawa, K. (1999) *Pediatr Res* **46**, 671-676

77. Aoki, Y., Suzuki, Y., Li, X., Sakamoto, O., Chikaoka, H., Takita, S., and Narisawa, K. (1997) *Pediatr Res* **42**, 849-854

78. Johnson, K. A. (1998) *Curr Opin Biotechnol* **9**, 87-89

79. Mock, D. M., deLorimer, A. A., Liebman, W. M., Sweetman, L., and Baker, H. (1981) *N Engl J Med* **304**, 820-823

80. Baker, H., Frank, O., Matovitch, V. B., Pasher, I., Aaronson, S., Hunter, S. H., and Sobotka, H. (1962) *Anal Biochem* **3**, 31-39

81. Polyak, S. W., Chapman-Smith, A., Brautigan, P. J., and Wallace, J. C. (1999) *J Biol Chem* **274**, 32847-32854

82. Cronan, J. E. (1990) *J Biol Chem* **265**, 10327-10323

83. Marini, P., Li, S. J., Gardiol, D., Cronan, J. E., and de Mendoza, D. (1995) *J Bacteriol* **188**, 7003-7006

84. Slavoff, S. A., Chen, I., Choi, Y., and Ting, A. Y. (2008) *J Am Chem Soc* **130**, 1160-1162

85. Rice, P., Longden, I., and Bleasby, A. (2000) *Trends Genet* **16**, 276-277

86. Bagautdinov, B., Kuroisgi, C., Sugahara, M., and Kunishima, N. (2005) *J Mol Biol* **353**, 322-333

87. Larkin, M. A., Blackshields, G., Brown, N. P., Chenna, R., McGettigan, P. A., McWilliam, H., Valentin, F., Wallace, I. M., Wilm, A., Lopez, R., Thompson, J. D., Gibson, T. J., and Higgins, D. G. (2007) *Bioinformatics* **23**, 2947-2948

88. Waterhouse, A. M., Procter, J. B., Martin, D. M. A., Clamp, M., and Barton, G. J. (2009) *Bioinformatics* **25**, 1189-1191

89. Brown, P. H., Cronan, J. E., Grotli, M., and Beckett, D. (2004) *J Mol Biol* **337**, 857-869

90. Bagautdinov, B., Matsuura, Y., Bagautdinova, S., and Kunishima, N. (2007) *Acta Crystallogr Sect F Struct Biol Cryst Commun* **63**, 334-337

91. Gonzalez, J. M., Masuchi, Y., J.W., A., Maeder, D. L., Yanagibayashi, M., Tamaoka, J., and Kato, C. (1988) *Extremophiles* **2**, 123-130

92. Weaver, L. H., Kwon, K., Beckett, D., and Matthews, B. W. (2001) *Protein Sci* **10**, 2618-2622

93. Koren, R., and Hammes, G. G. (1976) *Biochemistry* **15**, 1165-1171

94. Venezia, C. F., Meany, B. J., Braz, V. A., and Barkley, M. D. (2009) *Biochemistry* **48**, 9084-9093

95. Ingaramo, M., and Beckett, D. (2011) *J Biol Chem* **286**, 13071-13078

96. Healy, S., Heightman T. D., Hohmann, L., Schriemer, D., and Gravel, R. A., McDonald, M. K., Wu, X., Yue, W. W., Kochan, G., Oppermann, U., and Gravel, R. A. (2010) *Biochemistry* **49**, 4687-4694

97. Taroni, F., and Rosenberg, L. E. (1991) *J Biol Chem* **266**, 13267-13271

98. Xiang, S., and Tong, L. (2008) *Nature Struct Mol Biol* **15**, 259-302

99. Chloupkova, M., Maclean, K. N., Alkhateeb, A., and Kraus, J. P. (2002) *Hum Mutat* **19**, 629-640

100. Chu, C. H., and Cheng, D. (2007) *Protein Expr Purif* **53**, 421-427

101. Locke, G. A., Cheng, D., Witmer, M. R., Tamura, J. K., Haque, T., Carney, R. F., Rendina, A. R., and Marconkeviciene, J. (2008) *Arch Biochem Biophys* **475**, 72-79

102. Kim, K. W., Yamane, H., Zondlo, J., Busby, J., and Wang, M. (2007) *Protein Expr Purif* **53**, 16-23

103. Beckers, A., Organe, S., Timmermans, L., Scheys, K., Peeters, A., Brusselmans, K., Verhoeven, G., and Swinnen, J. V. (2007) *Cancer Res* **67**, 8180-8187